Micro Injection Moulding: Tooling and Process Factors

A thesis submitted to the University of Wales, Cardiff

for the degree of

Doctor of Philosophy

by

Christian Andrew Griffiths

Manufacturing Engineering Centre

School of Engineering

University of Wales, Cardiff

United Kingdom

2008

ProQuest LLC
789 East Eisenhower Parkway
P.O. Box 1346
Ann Arbor, MI 48106-1346

ABSTRACT

The development of new micro devices is highly dependent on manufacturing systems that can reliably and economically produce micro components in large quantities. Micro-injection moulding is one of the key technologies for micro-manufacture and is considered as a cost effective replication method for mass production. The capabilities of this replication technology have to be studied systematically in order to determine the process constraints.

The present work concerns the tooling and process factors that influence micro injection moulding. The requirements of this manufacturing process are identified, and a review of the current state of the art in the field, Chapter 2, is used to assess the potential of this technology. To analyse further the manufacturing capabilities of this technology against the requirements, an investigation of the pre-filling, filling and part removal stages of the process cycle is conducted.

In particular, in Chapter 3 the pre-filling capabilities of multi cavity micro tools with the use of a runner system is explored. The filling performance of spiral-like micro cavities was studied as a function of runner size in combination with selected process factors. Then, in Chapter 4 the filling of micro mould cavities with controlled tool surface finishes is investigated. Factors affecting the flow behaviour are discussed and a special attention is paid to the interaction between the melt flow and the tool surface roughness.

Using the same part design as that of the tool surface finish investigation, in Chapter 5 a Finite Element Analysis (FEA) is used to verify the effects of process parameters, particularly the factors affecting shear rate, pressure and temperature. The results of this investigation were then compared with those reported in the experimental study. Finally, in Chapter 6 the application of micro mould surface treatments is analysed. The effects of different surface treatments on the de-moulding of parts with micro features are investigated to identify the best processing conditions in regards to de-moulding behaviour.

To validate the process effects for these three process stages micro injection moulding experimental set-ups were specially designed and implemented. These experiments apply various part designs, tool-making techniques, process factors, part inspection and condition monitoring techniques, and FEA. To further understand the importance of process characteristics at the micro scale, an in depth analysis of the experimental results for each of the selected investigations was carried out.

Finally, in Chapter 7 the results from each of the investigations are summarised, and the main research findings identified, in particular the influence of runner size on the process performance, tool surface finish effects on the filling process, the accuracy and sensitivity of the proposed FEA model, and the effects of tool surface treatment on part de-moulding.

ACKNOWLEDGMENTS

I wish to express sincere thanks to the University of Wales Cardiff, in particular I gratefully acknowledge the acceptance of my application for pursuing postgraduate education and the support of this investigation obtained via the Manufacturing Engineering Centre.

I am privileged to have Professor S.S Dimov and Professor D.T Pham as my supervisors. My personal inspiration for research is derived from their high standards in both work principles, and scientific expertise. I am deeply grateful for their consistent advice, support and above all encouragement in making several of my ambitions a reality.

Thanks are also due to all the members of staff of the Manufacturing Engineering Centre, in particular special thanks go to my fellow team members A. Rees, A. Thomas, R. Barton and E. Brousseau for their friendship and technical advice.

My most sincere gratitude goes to my dear wife Cathrin, her advice and encouragement has supported my endeavours over the years. And thanks also go to my wonderful son Evan who gives me enormous pride.

I am deeply indebted to my loving parents, brother and sisters for the support they provide throughout life. Together with my closest friends, they provide me with a deep appreciation of daily life.

DECLARATION

This work has not previously been accepted in substance for any degree and is not concurrently submitted in candidature for any degree

Signed..... (Candidate)
Date 03/09/08

Statement 1

This thesis is the result of my own investigation, exception where otherwise stated. Other sources are acknowledged by footnotes giving explicit references. A bibliography is appended.

Signed..... (Candidate)
Date 03/09/08

Statement 2

I hereby give consent for my thesis, if accepted, to be available for photocopying and for inter-library loan, and for the title and summary to be made available to outside organisations.

Signed..... (Candidate)
Date 03/09/08

CONTENTS

LIST OF FIGURES

LIST OF TABLES

NOTATION

ABS	Acrylonitrile butadiene styrene
A_C	Part core surface area
ANOVA	Analysis of variance
COC	Cycloolefin copolymer
c_P	Specific heat capacity
CrN	Chromium nitride
CVD	Chemical vapour deposition
D	Runner diameter
DLC	Diamond like carbon
DOE	Design of experiment
E_f	Force sensitivity
E_p	Pressure sensitivity
E_R	Efficiency ratio
FCC	Faced central composite
FDM	Finite difference method
F_E	Ejection forces
FEA	Finite element analysis
FEM	Finite element method
F_R	Release force
GPC	Gel permeatation chromatography
GT	Global thickness multiplier
HMDSO	Hexamethyldisiloxane

IM	Micro injection moulding
L	Runner length
LCP	Liquid crystal polymer
LF	Low frequency
LFPECVD	Low frequency plasma enhanced chemical vapour deposition reactor
MEMS	Micro electro mechanical systems
MFI	Melt flow index
M_i	Molecular weight
MMT	Micro machine technology
MST	Micro system technology
M_w	Average molecular weight
N_i	Number of molecules
OA	Orthogonal array
OMCTSO	Octamethylcyclotetrasiloxane
PA	Polyamide (nylon)
P_A	Determination of moulding contact pressure
PBT	Polybutylene terephthalate
PC	Polycarbonate
PECVD	Plasma Enhanced Chemical Vapour Deposition
PEI	Polyetherimide
PDMS	Polydimethylsiloxane
P^h	Holding pressure
P_i	Injection pressure
PLD	Pulsed laser deposition

P_{max}	Maximum cavity pressure
POM	Polyoxymethylene (acetal)
PP	Polypropylene
PPE	Polyphenylene ether
PSU	Polysulfone
PTFE	Polytetrafluoroethylene
PVD	Physical vapour deposition
Ra	Roughness average
RP	Rapid prototyping
RSM	Response surface methodology
SF	Surface finish
Si	Silicon
SL	Stereolithography
S_{max}	Maximum part thickness
SV_R	Surface to volume ratio
T*	Reference temperature
T_b	Melt temperature
t	Time
t_c	Cooling time
t_e	Ejection time delay
TEOS	Tetraethoxysilane
T_{ff}	Flow front temperature
T_g	Glass transition temperature
t_h	Holding pressure time

TiN	Titanium nitride
T_m	Tool temperature
TMS	Tetramethylsilane
V	Velocity vector
VI	Moldflow viscosity index
V_i	Injection speed
VOF	Volume of fluid method
W	Part weight
WEDM	Wire electro discharge machining
WLF	Williams-Landel-Ferry
ρ	Density
η	Viscosity
τ	Shear stress
γ	Shear rate
μ	Coefficient of friction
μ_k	Kinetic coefficient of friction
μm	Micrometer
λ	Slip length
μ_s	Static coefficient of friction
μTAS	Micrometer scale total analysis systems
υ	Velocity
υ_s	Fluid velocity or slip velocity

CHAPTER 1

INTRODUCTION

1.1 Motivation

The motivation for undertaking the work presented in this thesis stems from humanistic and economic reasons. In relation to the humanistic reasoning, it can be seen that humans have an ability or inability to perceive physical conditions beyond their intellect. The evolutionary biologist and Professor of public understanding of science at the University of Oxford Richard Dawkins goes further by describing a middle world where the understanding of sizes, times and speeds is limited to a level importance relative to survival. One area outside of the middle world is that of the micro world, and only in recent times has there been a need and capability to venture into this discipline (Dawkins, 2006). Clearly in this context the term micro is not a direct reference to the prefix used in the metric system denoting one millionth, and 10^{-6} metre or 1 micrometre (μm) (2005). However the point is relevant, and it is clear that as the need for technology progresses, the concerns, interests, needs, and welfare of humans, related to the micro world presents a challenge to the species. And through scientific endeavour, this relatively new area of research can provide a vastness of knowledge that as Dawkins would say 'was previously unimagined'.

The economic reason for conducting this work comes from a need for industrial competence. The Confederation of British Industry has stated that the European Union (EU) should focus resources and create a critical mass of activity in core themes to

compete on the international stage. One such area for European research is the scientific potential for product miniaturisation (Potocnik, 2007). There is a clear trend for both research institutions and companies to dedicate significant resources on developing the operational capabilities for a range of micro-system technology (MST) based products.

With consumer awareness of a new industrial market, micro products developed and sourced from the EU offer great economic potential. However, to capitalise on and develop this potential, it is paramount that production platforms underpinning the design and serial manufacture of MST-based products are created and characterised to reduce uncertainties associated with the "translation" of micro-engineering ideas into commercial opportunities. Downscaling of designs for the production of MST products is one way for broadening the functionality for existing products and at the same time to develop the new products. With a decrease of size, cost reductions can be achieved through the use of less material, energy, storage space, and transport. There are also environmental incentives with the potential for reduction in carbon emissions. However, there are many challenges associated with such downscaling. One of them is the larger surface area per unit of mass that affects the physical properties of the parts produced and also introduces specific requirements in regards to the equipment used for their manufacture. The behavioural effects of speed, temperature and time on micro size designs allows some of the traditional design concepts to be re-considered and/or new ones developed.

One important development in micro engineering is the micro tooling industry that has emerged to underpin the product miniaturisation. This industry benefits from traditional and rapidly emerging manufacturing processes for both batch production, and tool-

making that are necessary for serial micro manufacture. For the latter the market demands the development of micro tooling technologies as a platform for production of parts in high volumes. In particular, mass production requires the capabilities and limitations of viable replication techniques, e.g. micro-injection moulding and thermal imprinting, to be studied in order to broaden their commercial impact.

Injection moulding is a complex process with a large number of factors determining its capabilities, these constraints have to be investigated systematically in order to establish it as a viable platform for the production of miniaturised parts in volume. In particular, this necessitates significant advances in our knowledge in micro tooling, machine capabilities and polymer flow behaviour in micro cavities. The process designers have to be equipped with this knowledge in order to reduce the uncertainties at the product development stage when it is required to select the most appropriate production route for a given product by "mapping" product technical requirements with capabilities of the available replication and tool-making techniques.

The engineering challenge tackled in this research are centred on broadening our understanding of micro injection moulding technology and also in developing it further to address specific requirements for replication of functional micro features in existing and new emerging products. This PhD thesis is an attempt to identify the limitations of this technology and thus reduce uncertainties in applying it for serial manufacture of miniaturised products.

In this research empirical knowledge is used to improve the design process, both of the products and the manufacturing processes, by quantifying the technical requirements and

limitations, and developing new processing solutions. Particularly, the aim is to reduce uncertainties in developing manufacturing platforms for high throughput replication of polymer micro components and products such as micro pumps, micro valves, micro fluidic mixers, lenses and gears.

In order to keep the investigation focused the investigation of the micro injection moulding process is extensively supported by a state-of-the-art survey of latest research and developments in the field.

1.2 Research Objectives

The overall aim of this research was to investigate the factors affecting the performance of micro injection moulding technology. Due to their large number only a selected facet of them was investigated applying empirical and analytical methods and tools with the objective to reduce the process uncertainty. To carry out the empirical part of this research test parts and tools were developed employing various micro tool-making methods in order to investigate the following micro-injection moulding process concerns:

- The influence of runner size on the process performance;
- Tool surface finish effects on the process;
- Tool surface treatment effects on part de-moulding;
- Factors affecting the polymer flow length in micro cavities.

After identifying the fundamental issues related to each of the above, a selection of process conditions were used to evaluate the impact of both the tool and the machine influences on the production of micro-injection moulded parts. Further to this, FEA

models were developed to conduct simulation studies of the process. In addition, condition monitoring techniques were applied innovatively to quantify some moulding conditions that were deemed vital in understanding the technology. To achieve the overall aims of the research the following objectives were set:

- To investigate the pre filling capabilities of multi cavity micro tools incorporating a runner system. Also, to assess the relationship between runner cross section areas and the achievable flow length, and runner temperature and pressure.

- To perform a detailed analysis of the filling of micro cavities with varying surface finish. This includes also an assessment of the influence of process factors on melt flow behaviour of polymers with a particular emphasis on the relationship between the mould, and the achievable flow length and part quality.

- To develop FEA models for simulating the filling of micro mould cavities, and thus to conduct analytical studies of the same process factors as those investigated in the physical experiments. In particular, to assess the process by comparing the Physical Field Data (PFD) with the simulation results.

- To investigate both the filling and the de-moulding of parts from micro mould cavities by conducting experimental studies. A particular emphasis to be paid on the process factors and the de-mounding performance when using different surface treatments.

To achieve the objectives of this research an analytical investigation of the micro injection moulding process is carried out employing FEA and simulation experiments in

parallel to the empirical studies. Results from each of the experimental trials are quantified, and the influence of different factors affecting the process performance is analysed and compared. Furthermore recommendations are made how to improve the process performance based on the identified effects of these factors and thus to address the micro-injection moulding concerns outlined in this section.

1.3 Thesis Organisation

The research is presented in seven chapters, of which Chapters 3 to 6 encompass the main investigations, where as Chapters 2 and 7 are a literature review and a summary of the main contributions of this work, respectively.

In Chapter 2, the context of this investigation is set by making provision of background knowledge for Chapters 3 to 6. This chapter includes three sections. In the first section the available micro tool manufacturing and micro injection moulding processes are reviewed and their capabilities are analysed. Then, the main characteristics and fundamental principles of micro-injection moulding are presented and critically analysed. The third section describes the specific focus of this research including the main concepts that are investigated. Also, the research methods that were employed are reviewed and scrutinised against the principal purpose of better understanding of this micro fabrication process.

Chapter 3 takes a close look at the pre filling capabilities of multi cavity micro tools, and especially on the effects of runner systems on polymer flow behaviour. In particular, the focus is on the scaling effects of the runner cross sectional area in order to understand the effects of runner function/design in micro injection moulding. The chapter starts with a

discussion of important characteristics of runner systems in the context of the micro injection moulding process. Then, the experimental set-up used to measure Cavity Temperature, Cavity Pressure and Polymer Flow Length together with the research method employed to investigate the runner system effects are described. Finally, the empirical results are analysed and conclusions made about the relationship between the runner design and process factors.

Chapter 4 investigates the melt flow behaviour of the polymers during the filling of the mould cavity, with a particular focus on the relationship between the tool surface finish, part flow length and part quality. First, the chapter discusses the effects of surface finish of runners and cavities on the melt flow behaviour together with their manufacture tool-making constraints. Next, the experimental set-up and the research method applied in investigating surface finish effects on polymer flow behaviour are described. The chapter finishes with a systematic analysis of the interrelationship between surface finish and process factors, and their impact on part and tool manufacturability.

In Chapter 5, by deploying and building upon the findings of Chapter 4, the conditions used to perform the empirical study are applied to investigate analytically the melt flow behaviour, with a particular focus on shear effects and temperature effects on part quality. The chapter starts with the description of the FEA method used to simulate the process. Then, the model that is used to simulate the micro injection moulding process is validated and the simulation study conducted employing it is presented. Conclusions are made about shear and flow temperature effects on the process performance.

Chapter 6 is dedicated to an investigation of the de-moulding stage of the micro-injection

moulding process. De-moulding is a complex issue in micro-injection moulding that requires a special attention due to the high surface to volume ratio (SV_R) of micro cavities and respectively the parts moulded in them. Thus, in this chapter first the factors affecting the de-moulding process are discussed and a condition monitoring technique is proposed to quantify the de-moulding forces. Then, an experiment design to investigate the influence of different surface treatments on de-moulding forces is described and the results of the study presented. Finally conlusions are made about the limitations of the studied surfaces treatments and the influence of the process factors on the resulting de-moulding forces.

In Chapter 7 the main contributions and conclusions of the research are summarised. Some possible directions for further investigations are also suggested.

CHAPTER 2

LITERATURE REVIEW

In this chapter a review of the micro replication process is presented. In the first section a discussion of the available micro tool manufacturing and micro injection moulding processes is carried out together with an analysis of their capabilities. In the second section the chapter continues with a description of the state of the art, where the main characteristics and fundamental principles of micro-injection moulding are presented and critically analysed. The third section concludes the chapter with a summary of the concepts identified for examination in this study.

2.1 Micro manufacturing

As early as 1960 Feynman (1960) discussed the potential for miniturisation, he described a field in which little has been done but an enormous amount can be done in principle. With reference to the issues of control and manipulation of components on a small scale, he even mentions the manufacture of multiple plastic parts from a metal master tool as a replication technique. Prior to the interest of eminent physicists the mechanical miniaturisation of components can be seen as far back as 1929, where J. Le Coultre held a record for the smallest calibre watch (4.8mm by 14mm by 3.4mm thickness). The trend in this industry continued as demonstrated by A. Beyner producing a watch 0.98mm thick, with a 7000 turn coil of 10μmm diameter wire in 1981 (Nicoud, 1995). Following Feynman's speculations, the main driver for the use of micro technology were the silicon integrated circuit (IC) industries. Vast progress was made possible by the continuous

reduction in transistor size and the trend in the number of transistors placed on an IC as observed by Intel co-founder G. Moore (http://en.wikipedia.org/wiki/Moores_law). As a result of the mastery of semiconductor technology, micromachining technologies developed the microminiaturisation of mechanical structures for the fields commonly referred to as micro electro mechanical systems (MEMS)(terminology in the USA), micro system technology (MST)(terminology in Europe) and micro machine technology (MMT)(terminology in Japan) was realised (Kussul et al., 1996).

In recent years there has been an interest in micro manufacturing research and development (Ehmann, 2007). In 2006 under the U.S. National Science Foundation (NSF) the World Technology Evaluation Centre (WTEC) initiated a study on advanced manufacturing. One of the outcomes was that micro manufacturing technologies might play an important factor in the change in the manufacturing landscape. The opportunities associated with micro manufacturing were identified in the following three categories:

- Scientific challenges and needs.
- Technological challenges and needs.
- Environmental and social challenges and needs.

The Multi-Material Micro Manufacture (4M) network of excellence that was setup as an instrument for integration of European research recognised that whilst the late 20th century has seen a silicon based micro electronics revolution, the 21st century looks forward to the adoption of micro and nano manufacturing technologies (MNT) (Dimov, 2005). It was recognised that for miniaturisation to have applications to product platforms such as micro fluidics, micro-optics and micro sensors, each constituent part had to have

the potential to be manufactured at serial production volumes. Business needs are the driving force behind product recognition and any subsequent consumerism. For this to happen, high standards of manufacturing capability and product performance must exist, or be evident for any potential development and investment. When investigating market expectations particularly micro-fluidic, micro-optic, and micro-sensor & actuator applications, with an identified map of technologies (Figure 2.1) the industrial community of the 4M network perceived the most significant market sectors in order of importance to be: medical/surgical, automotive and transport, biotechnology, consumer products, information and communication, energy/chemical, scientific/academic community, and pharmaceutical (Dimov et al., 2006). In order for these industry sectors to utilise micro products, the requirement for low cost / volume production is paramount.

Dimension capabilities	1D Processing 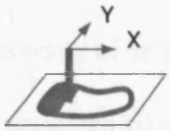	Multiple 1D Processing 	2D Processing 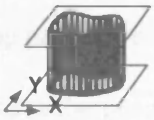	3D Processing (Surface) 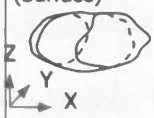	3D Processing (Volume) 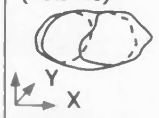
Metals	LH, EDM, ECM, Grinding	MF, Grinding	Lap, Pol, MF	Lap, Pol, ECP, EF, EP	EDM, MF
Polymers	3DL	3DP	EBL, IBL, LL, PUL, XL		HUE, NIL, NI, R2RE, IM
Ceramics	3DL, Grinding	3DP	IBL, LL,	Lap, Pol	NIL, NI, R2RE
Any material	EBM, FIB, LA, PM, AWJ, Drilling, Milling, Turning, SLS		Etch, PMLP, SP	PVD, CVD, SC, SA	Casting, MCIM, PIM (1)

Key:

3DL	3D Lithography	Lap	Lapping
3DP	3D Printing	LH	Laser hardening
AWJ	Abrasive water jet	LL	Laser lithography
Casting	Casting	MCIM	Multi-component injection moulding
CVD	Chemical vapour deposition	MF	Metal Forming
DL	Direct LIGA	Milling	Milling
Drilling	Drilling	NI	Nano-imprinting
EBM	Electron beam machining	NIL	Nano-imprint lithography
EBL	Electron beam lithography	PIM	Powder injection moulding
ECM	Electrochemical machining	PUL	Photo / UV lithography
EDM	Electrical discharge machining	PM	Plasma machining
EF	Electroforming	PMLP	Projection mask-less nanopatterning
ECP	Electro-chemical polishing	Pol	Polishing
EP	Electroplating	PVD	Physical vapour deposition
Etch	Etching	R2RE	Reel to reel embossing
FIB	Focused ion beam	SA	Self assembly
Grinding	Grinding	SC	Spin coating
HUE	Hot/UV embossing	SLS	Selective laser sintering
IBL	Ion beam lithography	SP	Screen printing
IM	Injection moulding	Turning	Turning / Diamond turning
LA	Laser ablation	XL	X-ray lithography

Figure 2.1 Map of technologies

2.2 Micro machining

Tooling applications in micro manufacturing require recognition of the technologies available. The diversity of existing manufacturing processes is large, and the use of such equipment on downscaled sizes creates challenges to the process capability. To simplify the application route. (Masuzawa, 2000)) classified micromachining processes methods according to material interaction with working principles of: mechanical force, melting/vaporisation (thermal), ablation, dissolution, solidification, recomposition, polymerisation and sintering. Table 2.1 further identifies the different processes in relation to the 2d, 2 and a half and 3d dimensional capabilities and material type.

The manufacture of moulds for replication requires that though the machined material will be predominantly metal, the dimensions will vary dependent on the part design. For this reason it has been found that micro machining processes currently employed for the manufacturing of micro moulds show limitations (Uriarte et al., 2006). Of particular importance to the production of moulds is the feature size and achievable tolerance that the process can work to. Part designs can adopt features with wide range variations thus affecting the machining strategy. Also the material being machined is a factor for both the process capability and the material removal rate. Particularly important to machine time costs, the removal rate presents an economic consideration, this can be demonstrated with a comparison of the time required to machine 1 mm^3 where the laser ablation methods range from 2.77-21.37 hours, the micro milling would take 26.71 hours and the FIB 385 days.

The increase in miniaturization and the integration of different micro features requires that a combination of processes must be used. Capable of providing solutions for mould

manufacture (Tosello et al., 2007), hybrid tooling can be defined as "the capability of producing a mould insert combining two or more processes in sequence" (Azcarate et al., 2006). Processes with exclusivity to micromachining usually have equipment specifications based on technology development and specialised functions. For mould manufacture, laser technology can provide machining capabilities for features below that of micro milling and the use of laser technology in processing materials has been reported over the last decade (Gower, 2000, Meijer et al., 2002, Pham et al., 2002); (Pham et al., 2004, Knowles et al., 2007). Additionally focused ion beam (FIB), is a technique that can be used for the deposition, and ablation of materials. (Ochiai et al., 1999, Loeschner et al., 2003); (Platzgummer et al., 2006). The following processes are an overview of technologies currently used in the manufacture of moulds for this thesis.

2.2.1 Micro milling

There are several micro cutting processes such as grinding and ultrasonic machining, but the main one used for tooling purposes is micro milling. Micro milling is characterised by the mechanical interaction of a sharp tool with the workpiece. With controlled and dedicated tool paths, the tool in interference to the workpiece removes the unwanted material. Mechanically this is only possible when the tool material is sufficiently harder than the material being cut. (Dimov et al., 2004) found that the step over movements, the depth of cut, feed-rates per tooth, cutting speeds, cutting tool wear, and the use of cutting fluid/air/oil mist are important for their influence on the cutting behaviour. (Popov et al., 2006) also found that interfacial interaction between the cutter and the workpiece material work was important, in particular it was found that the microstructure of the workpiece can play a fundamental role in the cutting process. For tool life expectancy mechanical loading and thermal diffusion between the materials should be at a minimum. Tool

fabrication is another important issue, the cut depth must take into account the tool having a sufficiently small edge radius. Currently sintered carbide end mill tools and drills of 100μm are commercially available. These tools have the capability to machine plastic, metal and composite materials but hard or very brittle materials are difficult to machine. Unpredictable tool life and premature tool failure are major problems in micro-machining, and research has been carried out in the development of new systems for detecting tool breakage during micro-milling and drilling to overcome tool related problems (Gandarias et al., 2006). Another condition for this micro cutting process is the availability of an ultra precision machine. One commercial available piece of equipment is the Kern micro-milling centre. With a part model and a generated NC program the machine has a wide range of possibilities for the machining of micro 3D structures with high aspect ratio and high geometrical complexity. With such a dedicated process there are foreseeable drawbacks such as a need for temperature control, with every 0.1° change the Kern can expect an additional 1μm (or more) enlargement error. The Z Axis direction also experiences errors such as the potential for dust on the tool holder, and chips of cut material (up to 25 μm size) present on the tool during calibration and measurement. Setups and tool changeovers also require a controlled procedure that includes a 15 minute temperature run in of the machine spindle. With such influences known and controlled to a minimum, the machine is adept to producing tool inserts for moulding purposes.

2.2.2 Micro electro discharge machining

Micro electrode discharge machining (μEDM) is one technology widely used for the manufacture of microstructures and tooling inserts for micro-injection moulding. With the workpiece and electrode submerged in a dielectric fluid, material is removed by melting and vaporization by high frequency electrical sparks generated by high voltage

pulses between the cathode tool and a workpiece anode (Madou, 2001). Originally μEDM was applied for producing small holes in metal foils. Due to the flexibility of the EDM process and its capability to produce complex 3D structures, currently the technology is employed in a number of applications including micro parts for watches, keyhole surgery, housings for micro-engines, tooling inserts for fabrication of micro-filters and micro fluidics devices (Rees et al., 2007). However, for this technology a number of constraints remain most notably volumetric wear. The electrodes are usually made from copper, graphite or tungsten carbide, and during use the ratio of wear between electrode and workpiece is considered high and non negligible (S. Bigot, 2005). Thus, to manufacture microstructures there is often a need to compensate the wear by applying machining strategies like the uniform wear method (Zuyuan et al., 1998), and the multiple electrode strategy (Meeusen, 2003). The electrode generation and re-generation is considered a key enabling technology for improving the performance of the μEDM process (Masuzawa, 2001). And with techniques for electrode generation such as the technology called Wire Electro-Discharge Grinding (WEDG) (Masuzawa et al., 1985), the accuracy and repeatability the μEDM process is still relevant for micromachining. Typical μEDM technologies include Wire EDM (WEDM), Die sinking (SEDM), EDM Drilling, EDM milling and Wire Electro-Discharge Grinding (WEDG).

Table 2.1 Process capabilities

Technology/Feature & geometry	Min. feature size/ feature tolerance	Material removal rate	Materials
Focused Ion Beam (FIB) / 2D & 3D	200 nm/20 nm	20-30 μm3/sec	Any
Micro-milling or -turning/2D or 3D	25 μm/2 μm	10,400 μm3/sec	PMMA, aluminium, brass, mild steel
Excimer laser/2D or 3D	6 μm/ submicron	40,000 μm3/sec	Polymer, ceramics, metals
Fempto laser/2D or 3D	2-4 μm/ submicron	13,000 μm3/sec	Any
Micro-EDM/2D or 3D	25 μm / 3 μm	25 millions μm3/sec	Conductive materials
Pico laser/2D or 3D	4-6 μm / submicron	100,000 μm3/sec	Any
PROFIB/2D & 3D	100 nm/10 nm	1,000 μm3/ sec	Any

2.3 Replication

From the development and validation of prototype micro components, replication provides the requirements for manufacturing products at a low cost and at high volume. With the identification of a replication process it is possible to use the manufacturing knowledge to reliably produce parts to a quality standard. It can be seen from the conducted road mapping study that seven technology areas are identified (Dimov et al., 2006). Regarding importance, both research and industry are in agreement that replication is a technology of both current and future importance. Of thirty eight manufacturing technologies identified as important for future technologies in sixth position it can be seen that both research, and industry organisations consistently regard the process of injection moulding as important. Furthermore with the prospect of batch-manufacture of micro products, the process of multi-component injection moulding was positioned in eighth place, solely by industrial organisations.

Injection moulding is one of the most common replication methods available, and like other replication processes each part design exclusively requires a tool or mould to produce parts. With added cost factors, this addition requires a very specialised set of engineering requirements.

2.4 Injection moulding

One of the unique features of the chemistry of carbon is its ability to form long chains of atoms, this property is the basis of industrial chemistry concerned with the manufacture of polymetric material. Polymers are man made or man altered organic materials, they are a substance composed of molecules of repeating structural units, or monomers. The

properties of these natural and synthetic materials are developed for purpose through plastics processing, in particular conversion processes allow for a varying range of uses for the various polymers (Muccio, 1994). Using an efficiency ratio based on applied material and end product, there are many significant plastics processing methods, and the British plastics federation (BPF) claims that UK plastics industry represents 80% of industrial turnover with the steel industry at 15%. And with origins that date back as far as 1872, the largest process for making discrete objects from plastic is injection moulding (Johannaber, 1994). Capable of operating with a wide range of polymers and unit weights between 5g to 85 kg, a wide range of parts can be processed (Throne, 1979 , Belofsky, 1995). The procedure for the injection moulding of thermoplastic parts involves the heating of polymer granules with in a machine barrel, typical melting temperatures are about 180 °C but depending on the polymer being moulded this figure varies. Using an injection unit the polymer is then injected into a mould, during this part of the process very high pressures on the order of 70,000 kPa can be expected. With the polymer transition into the mould, cooling and solidification takes place, resulting in the plastic taking the final shape of the tool. Finally the mould opens and the part together with runners is removed. The complete cycle takes around 45 seconds but this figure can vary depending on the material of size of the part being moulded (Bralla, 1999).

2.4.1 Micro injection moulding

A general definition of micro injection moulding is that of the production of polymetric parts with structure dimensions in the micron or sub-micron range (Kemmann and Weber, 2001, Piotter et al., 2002). (Yao and Kim, 2004) further proposed that components manufactured by micro injection moulding fall into one of the following two categories. Type A are components with overall sizes of less than 1 mm while Type B

have larger overall dimensions but incorporate micro features with sizes typically smaller than 200 μm. (Kukla et al., 1998) suggested that micro moulding could also cover parts of any dimension including a mass of the order of a few milligrams, but the feature tolerances are required to be in the μm range. For an injection moulding machine to perform at such sizes the reality is that there are two important factors to be considered when comparing standard injection moulding machines and micro-injection moulding machines, and that is the amount of deliverable volume and the control of the deliverable volume.

Conventional machines use hydraulic power from central and sub distribution points, from these areas of the machine, energy transfer to a variation of hydro mechanical movements is controlled by electro hydraulic valves. With filling times for micro injection moulding measured below 1 second, standard valves are not suitable to the increased requirements, and subsequent time delays and deceleration behaviour cause unacceptable quality defects in micro components. Also with part volumes so low, the injection process becomes difficult particularly as a standard injection screw holds a specific volumes of material within the screw flutes and a controlled volume in front of the screw. The controlled volume would be so small that the theoretical stroke of the screw movement to fill the cavity could be below that of 1mm. This is far below the design intent or capability of the machine. Another consideration is that of accuracy of movement. Designs that require injection mould tool alignment accuracies of 10-20μm have to use machines that can provide movements such as the machine platens to a high standard of positional accuracy. The same requirement applies to the linear and rotational position accuracy of the machine screw.

When moulding parts below a weight of the weight of 100 mg production on conventional injection moulding machines reaches its physical limits. Machine developments require that the delivery of material volumes for micro parts requires specific additions such as high-speed control of valves and measurement functions, positional accuracy, and high tolerance alignment of moving parts. For this an alternative approach to standard injection moulding equipment must be appraised.

2.4.2 Development of a micro injection moulding machine/process

Professor Helmut Detter of the Department of Precision Mechanics the Technical University of Vienna predicted the integration of micro parts and micro components into existing products. He also believed that the micro injection moulding process would have a faster growth into different market applications than the IC (http://www.devicelink .com/emdm/archive/99/03/report.html). Together with a consortium of companies and organizations dedicated to developing complete microsystem production solutions, Professor Detter managed the original project that resulted in the development of Battenfeld's micromoulding system. With a focus on reliable production output, increased productivity from reduced cycle times and material reduction. The result was that Battenfeld was one of the first companies to develop a micro injection moulding machine (http://www.immnet.com/articles?article=665)

Launched at K 98 in Düsseldorf, Germany the all electric Battenfeld Microsystem 50 is made up of several modules. The unilog B4 control module is designed for compatibility with the drive systems, where the servo drives provide movements of all machine axes with a positional accuracy of 0.01mm. The injection module as shown in Figure 2.2 uses a plasticising method that differs to standard screw type machines. Here the screw

plasticizes the polymer material to a metering unit and via a valve mechanism, the material is diverted to a delivery nozzle where it is possible for a 5-mm plunger to move forward. The polymer can then be delivered into the runner and cavity and a combination of fast servo drives and mechanical parts ensures extremely short switchover times of 2.5 ms at an injection speed of 800 mm/s. The clamp module can produce up to 5 tonne clamp force, and the platen rotation and handling module enables parallel functions with one station for injection moulding and a second for part ejection. Not normally associated with injection moulding, the machine also take into consideration high standards of air purity control. With provisions that meets all clean room requirements the machine forms a closed cleanroom within itself, to class 100, which means a particle count of fewer than 100 particles < 0.5 m per cubic foot. With suitable machine specifications (Table 2.2) all micro moulding products discussed in this thesis were moulded using a Battenfeld Microsystem50 machine.

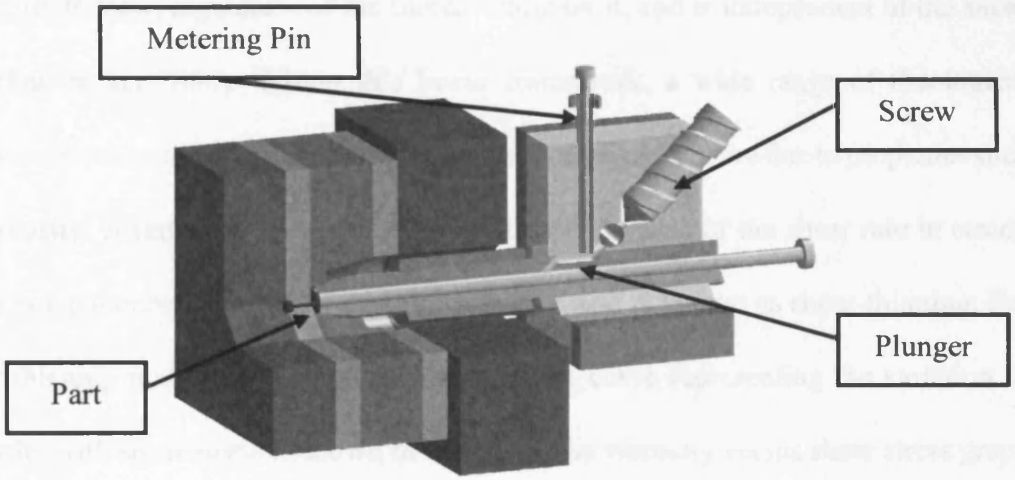

Figure 2.2 Battenfeld Microsystem 50 Injection unit

Table 2.2 Battenfeld Microsystem 50 specifications

Clamp unit Specifications		Injection unit Specifications	
Clamp force	50kN	International size designation	3
Opening force	10kN	Extruder screw	14mm
Max mould size	196 x 156mm	Injection piston diameter	5mm
Min mould height	100mm	Specific injection pressure limited to	2500 bar
Opening stroke	200mm	Theoretical shot volume	1.1 cm3
Max daylight	300mm	Nozzle stroke manual	165mm
Ejector force	1.2kN	Max screw speed	300rpm
Ejector stroke	30mm	Screw torque	54Nm
Dry cycle rate	40mm	Injection rate into air	25 cm^3/s

2. 5 Polymer Rheology

In the study of the flow of liquids Newtonian fluids assume a linear law of direct proportionality between stress and strain. In common terms, this means the fluid continues to flow, regardless of the forces acting on it, and is independent of the shear rate (Fan et al., 2006). Within this linear framework, a wide range of rheological behaviours can be accommodated; however they can be restrictive due to properties such as viscosity. A reduction of the viscosity with the increase of the shear rate in steady flows is a common example of this non-linearity, and is known as shear-thinning. For shear-thinning materials, the general shape of the curve representing the variation of viscosity with shear stress is shown in Figure 2. The viscosity versus shear stress graph (Fig 2.3(a)) shows that the viscosity change can be seen in the middle region, and at both low (lower Newtonian region) and high (upper Newtonian region) shear rates the viscosity is constant. For the shear stress versus shear rate graph (Fig 2.3(B)) with the increase in the rate the stress increases, too. The viscosity versus shear rate graph (Fig 2.3(c)) highlights the shear rate range that affects viscosity. (Barnes et al., 1989). The study of polymer rheology is very important in understanding the behaviour of the injection moulding process, in particular by correctly characterising the materials' behaviour part quality can be controlled.

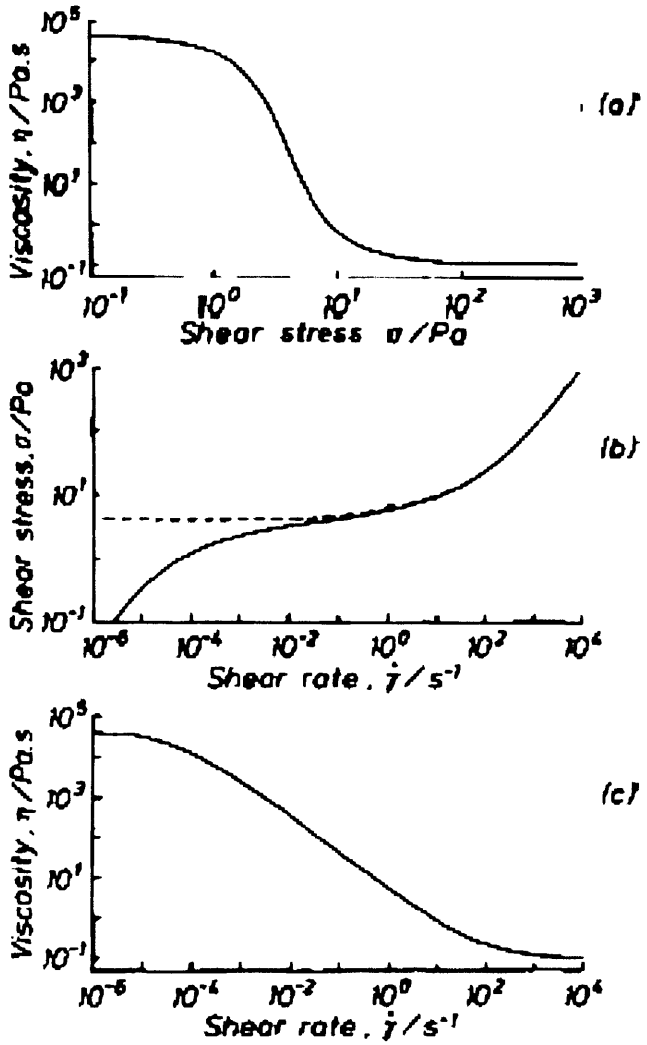

Figure 2.3 Graphs showing (a) shear stress against viscosity (b) shear rate against shear stress and (c) shear rate against viscosity

2.5.1 The Power-law viscosity model

Viscosity is the most widely used material parameter when determining the behaviour of polymers during processing. Polymer viscosity can be defined as a fluid property that represents the material internal resistance to deform. During shear deformation the polymer molecules are stretched out, enabling them to slide past each other with more ease, thus the reduction of viscosity is both shear and temperature dependent. A viscosity model is an idealised relationship of rheological behaviour expressible in mathematical

terms. Mathematically, viscosity η is defined as the ratio of shear stress τ and shear rate γ. The most important requirement for a viscosity model is that it should represent the behaviour of polymer melts, fundamentally the viscosity should decrease with the increase of shear rate and with the increase of temperature (Greene, 1997). The Power-law model is a simple model that accurately represents the shear thinning region in the viscosity versus strain rate curve, but neglects the Newtonian plateau present at small strain rates. The power law model can be expressed as follows:

$$\eta = m\gamma^{n-1} \tag{1}$$

where: m is referred to as the consistency index and n - the power law index. The consistency index (consistency coefficient) describes the viscosity range across the flow curve and may include the temperature dependence of the viscosity. The exponent n is known as the power law index and represents the shear thinning behaviour of the polymer melt. The 0 - 1 rate index is the slope of the viscosity shear rate curve. The closer n is to zero the more shear-thinning is present. The Power-law model is a basic representation of the way in which viscosity changes with shear rate (Figure 2.4). The model is limited at low shear and high shear rates and it should be noted that there are restrictions to the model. In particular, the infinite viscosity at zero strain rates leads to an erroneous result in problems where there is a region of zero shear rate (η_0), such as at the center of a channel (Osswald and Menges, 2003).

$$\eta = 0 \; as \; \gamma = \infty \tag{2}$$

$$\eta = \infty \; as \; \gamma = 0 \tag{3}$$

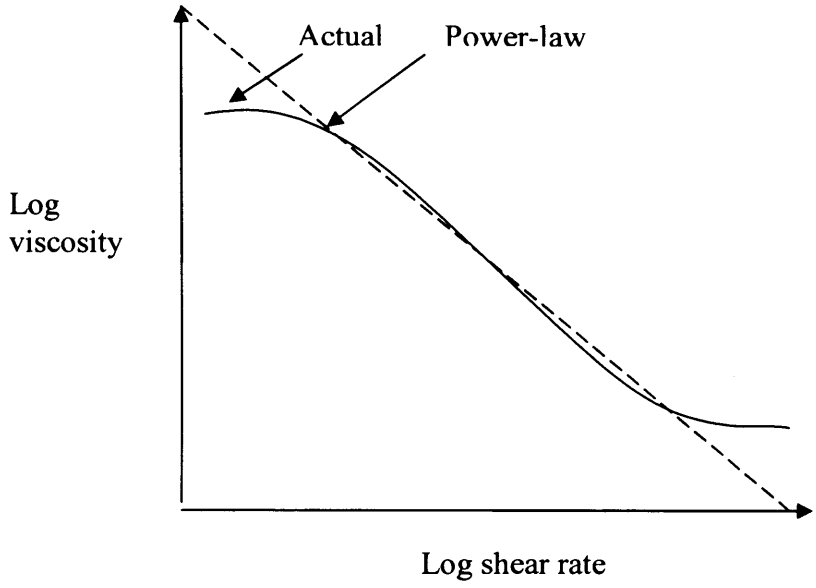

Figure 2.4 Power-law fluids: viscosity decrease lineally with the increase of the shear rate in the log-log scale

2.5.2 The cross viscosity model

A model that fits a wider range of strain rates is the Cross viscosity model with the Williams-Landel-Ferry (WLF) temperature and pressure dependence factor. The Cross WLF viscosity model is a mathematical expression that describes the shear thinning behaviour of polymers and is widely used for numerical simulations. The mathematical expression of the model is (Theilade, 2004):

$$\eta = \frac{\eta_0}{1 + \left(\frac{\eta_0 \gamma}{Tau}\right)^{(1-n)}} \tag{4}$$

where: η_0 represents the zero shear viscosity with pressure and temperature dependence on the viscosity by the following exponential law (Poslinski, 2001):

$$\eta_0 = D1\exp\left(\frac{-A1\left(T-T^*\right)}{A2+\left(T-T^*\right)}\right) \quad (5)$$

T - the melt temperature, T* - the reference temperature which can be based on glass transition temperature (T_g), and n, Tau, D1, A1, A2 are data fitted coefficients. n represents the shear rate sensitivity where 1 - n characterises the slope of the line over the pseudo plastic region in the logarithmic plot of η and γ (Helleloid, 2001). The Cross WLF model uses the zero shear viscosity region (η_0) as a function of temperature and pressure. Also known as interfacial viscosity region, η_0 is η with a low strain rate and is particularly important for modelling viscosity and is considered to be more effective at high and low γ in comparison to the Power-law model (Tadmor and Gogos, 1973, Young, 2005).

Material choice selection in relation to viscosity would traditionally result in research from Melt Flow Rate (MFI) (ISO1133) information. The use of direct comparisons of polymer viscosity curves (Appendix A) can provide vital information on the polymer viscosity at different shear rates and temperatures.

2.5.3 Molecular weight

The most important material structural variables for polymer flow properties are molecular weight (M_w) and chain length (Billmayer, 1971). Polymer molecules vary in size and chain length, thus resulting in varying levels of chain entanglement (Fig 2.5). The molecular distributions can be defined with two averages. The number-average molecular weight, M_n,

$$M_n = \frac{\Sigma_i N_i M_i}{\Sigma_i N_i} \tag{6}$$

where: N_i is the number of molecules of molecular weight M_i, while the weight average molecular weight M_w is defined as

$$M_w = \frac{\Sigma_i N_i M_i^2}{\Sigma_i N_i M_i} \tag{7}$$

The weight average molecular weight is always larger than the number average, and for simple distributions, M_w may be 1.5 to 2.0 times M_n. To assess the distribution of molecular weights in a sample, a ratio sometimes called the Polydispersity Index (PDI) provides a simple definition of the molecular weight distribution. PDI can be calculated based on M_w *and* M_n, (Sperling, 2006, Teramachi et al., 1978).

$$PDI = \frac{M_w}{M_n} \tag{8}$$

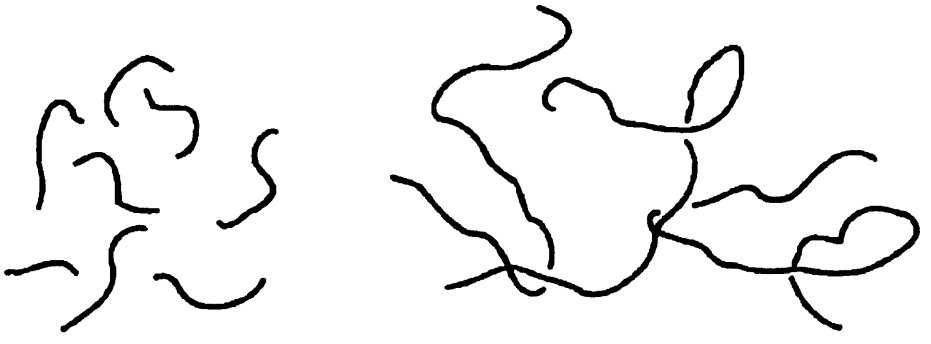

(a) (b)

Figure 2.5 Entanglement of polymer chains (a) low M_w limited entanglement (b) high M_w increased entanglement (Sperling, 2006).

2.5.4 Molecular weight influence on rheology

The rheological behaviour of polymetric systems is influenced by molecular weight and molecular weight distribution. As a polymer melt moves the chains orient along the lines of flow, and this reduction in the number of chain entanglements results in a viscosity reduction. The power law and cross models have no dependence on molecular parameters but previous studies have reported a relationship between η_0 and molecular weight. In particular, η and γ are shown to be especially sensitive to polydispersity at a high shear rate (Nichetti and Manas-Zloczower, 1998). A polymer melt in relation to η_0 can exceed a critical molecular dependence (M_c) and a plot of the log shear rate viscosity and the log molecular weight identifies two different power laws for:

$$\eta_0 = \mathrm{K}\,(M_w)^{\mathrm{p}} \tag{9}$$

In particular, at low M_w, p is equal to 1.0 and thus $\eta_0 = \mathrm{K}\,M_w$. At the same time, at high M_w, p is equal to 3.4 and $\eta_0 = \mathrm{K}\,M_w^{\,3.4}$ (K is a constant for the degree of polymerisation). The power dependence represents the simple increase in viscosity, η_0 of the melt increases as p = 1.0, the viscosity increases with a further increase in M_w. At 3.4, the change in the slope of the curve is sudden and above this M_c the polymer melt is highly elastic. With downscaling and the possibility of increasing molecular influences, material factors such as PDI may be an additional requirement in polymer selection for micro parts.

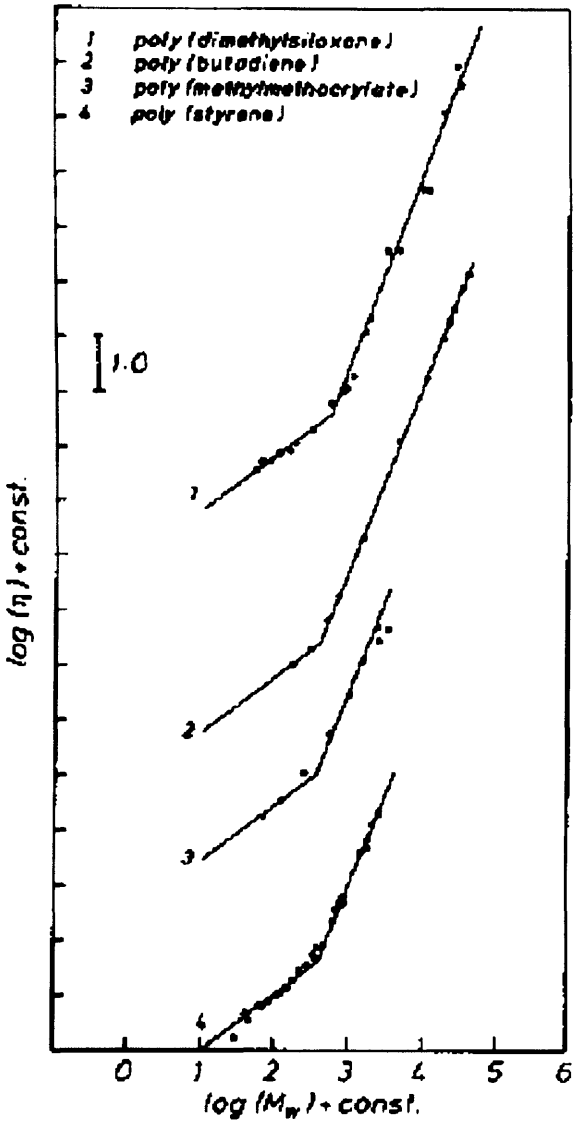

Figure 2.6 Variation of zero shear melt viscosity with molecular weight (Ferry 1980)

2.5.5 Polymers used in micro injection moulding

In micro injection moulding the small size of the parts affects the selection of polymers to be used. One of the properties required is that the material should have a viscosity low enough to allow the melt to fill the cavity. For micro injection moulding LCP,COC, PC, PA, POM, PBT, PEI, PPE and PSU material have been investigated (Bourdon and Schneider, 2002, Chang and Yang W, 2001, Kemmann and Weber, 2001, Kim et al., 2004, Lee, 1997, Madou et al., 2001, Mönkkönen et al., 2002, Saito et al., 2002, Shen and Wu, 2002, Shen et al., 2004, Su, 2004, Yoshii and Kuramoto, 1994, Yu et al., 2004, Zhao et al., 2003). (Mönkkönen et al., 2002) found that different polymers have different responses to flow directions in small spaces, and also (Yao and Kim, 2004) concluded that previously used materials have to be researched again because of the complexity of the melt flow in micro cavities. In this research three commonly used materials in injection moulding, Polypropylene (PP), Acrylonitrile Butadiene Styrene (ABS) and Polycorbonate (PC), were selected to conduct the planned experiments. The viscosity data and molecular weight distributions for each of the selected materials can be found in Appendix A.

2.6 Factors affecting replication capabilities in micro injection moulding.

One of the most important problems in micro injection moulding is the incomplete filling of the cavity, many researchers have focused their attention on the filling stage of the process, and it is clear from the process that the main factors are Melt temperature (T_b), Mould temperature (T_m), Injection Speed (V_i) and Injection Pressure (P_i).

In recent years many researchers have investigated the effects of these factors, (Masaki et al., 1994) used polycarbonate (PC) to replicate 0.55μm grooves to investigate the relationship between the mentioned process factors and replication. The experiments found that an increase of temperature (T) and V_i improved results. (Wimberger-Friedl, 2001) found that T_m was of major importance to the replication results. For the relationship between V_i and the cavity pressure conventional part thicknesses generally result in a pressure increase with an increase in V_i however research by (Yao and Kim, 2004) found that injection pressure was lower at higher V_i.

The specific volume (V) of polymers varies with pressure (P) and temperature (T), in particular V increases with the decrease of P and the increase of T (Appendix B) The relationship with polymer volume as a function of temperature and pressure can be represented with Pressure–volume- temperature (PVT) data (Binet et al., 2005). The modified 2-domain Tait PVT model is a model that represents material compressibility during flow simulation, and is given by the following formula:

$$V(T,P) = V_0(T)\left[1 - C\ln(1 + \frac{P}{B(T)})\right] + V_t(T,P) \qquad (10)$$

Where $V(T,P)$ is the specific volume at temperature T and pressure P, V_0 is the specific volume at zero gauge pressure, T is the temperature, P is the pressure, C is a constant, and B accounts for the pressure sensitivity of the material. The compressibility of a material affects the volume of plastic required. (Chang et al., 1996) found that cooling rates influenced PVT behaviour, therefore high cooling rates as associated with micro injection moulding could influence the prediction the melt fill. In addition the T_b, T_m and V_i process factors that influence the micro moulding could directly impact on the temperature influence on compressibility.

The results from literature indicate high process parameters can be used to overcome the short freezing time of polymer melts, however such increases lead to negative effects such as melt degradation. Thus it possible that the factors that improve the filling of micro cavities also increase the negative effects. With the downscaling of part sizes, it is important to consider that factors that are considered negligible for macro parts have a more direct impact on the micro scale. Therefore it is important to consider such factors together with the known influences on micro injection moulding process.

2.6.1 Runner influence on flow behaviour

The runner system is one of the most important basic elements of thermoplastic injection moulds (Javierre et al., 2006). Its main function is to facilitate the flow of molten material from the injection nozzle into the mould cavity. To increase productivity and thus reduce the unit cost, often moulding tools incorporate multiple cavities and runner systems that are designed for producing many components from a single shot volume. One of the most important conditions for consistent replication is ability of the runner to deliver a polymer melt to all cavities at same time and with as small as possible variations of pressure and

temperature. Therefore, these are important design considerations in deciding which runner configuration to be adopted (Li and Shen, 1995).

In addition, during the filling stage, a frozen layer is formed along the walls of the mould that affects the flow behaviour. In particular, a thicker frozen layer results in a lower flow of polymer melt, and as the flow reduces, the heat loss increases and thus the frozen volume, too. The resulting flow resistance can then lead to excessive pressure in order to fill the multiple cavities (Spina, 2004). To avoid this, it is necessary to employ monitoring techniques such as the measurement of maximum cavity pressure (P_{max}) during the filling stage (Coates et al., 2006).

There are two main types of runner systems, in particular standard and hot runners. In the case of a standard runner system the melt is fed through a sprue and delivered to the part cavity via a gate. Polymer solidification at the walls can be controlled by monitoring the tool temperature. In this way the temperature of the runner system can be the same as T_m, with the exception of some localised heating from the cyclic iso-thermal temperature changes occurring when the melt enters the cavity within each injection cycle.

The design of a runner system for macro-size components considers the relationship between their size and weight. In particular, the cross section diameter of the runner system was considered as the main variable in controlling the heat loss (Yen et al., 2006). Three main types of runner cross sections are typically used: round, trapezoidal and parabolic. Square runners are also possible but they are rarely used due to the required draft angle on the side walls for an easier part removal. The injection moulding machine, mould design and part design influence runner selection, in addition, for micro moulding

surface to volume ratio (SV_R) of the runner should be considered, too. In particular, high SV_R that is typical for micro components has a significant effect on the filling behaviour (S.Yuan et al., 2003). SV_R and its corresponding efficiency ratio (E_R) can be expressed as follows:

$$E_R = {}^{A}/_{C} \quad \ldots (11)$$

$$SV_R = {}^{S}/_{V} \quad (12)$$

Where A and C are the area and circumference of the runner cross section respectively, and S and V - the surface area and the volume of the runner system.

The cross section also has an impact on the thermal losses in the runner system, and thus on ensuring that an optimum viscosity is maintained for each specific material. Although previous research has found that the runner type has no significant effect on warpage of parts with lower SV_R (Ozcelik and Erzurumlu, 2006), a round cross section is considered optimum in regards to temperature losses. However, the disadvantage of using such cross sectional profiles is that they require machining of both halves of the tool together with an accurate alignment. Machining on only one side of the mould can be obtained with the trapezoid and parabolic forms. However, both shapes have more heat loss and increased material volume compared with circular cross sections (Menges and Mohren, 1993, Tang et al., 2006b).

In multi cavity moulds, there is a need for controlled and simultaneous filling while relatively high T_b and T_m are maintained in order to replicate micro features (Sha et al., 2007). Even though a high temperature also means that the runner requires more time to cool down to the desired ejection temperature (Zhao et al., 2005). Therefore, to ensure the

selection of the most suitable moulding temperature for optimum filling and cooling cycles the size of the runner cross-sections must be chosen very carefully. Material effects such as viscosity (η), shear stress (τ) and rate (γ), and process effects like T_m, T_b and V_i all relate to the part design. Thus, a good understanding of process, material and part design interactions coupled with an experimental knowledge about their combined effects is necessary in order to optimise the runner performance. In addition, because of the complex nature of polymers, it is difficult to estimate what will be the optimum diameter (D) size of the runner based on the existing empirical knowledge. For example, the existing literature on injection moulding suggests two different equations for calculating the runner dimensions (Menges and Mohren, 1993, http://www.dsm.com/en_US /html/dep/ coldrunnersystems.htm) :

$$D = S_{max} + 1.5 \tag{13}$$

$$D = \frac{W^{0.5} \times L^{0.75}}{3.7} \tag{14}$$

Where: S_{max} is the maximum thickness of the part, W - part weight and L -runner length.

The Equation 13 is used as a general rule for the tool design and manufacture in which S_{max} is taken into account and material rheological data, part weight and runner length are ignored. It is not difficult to see that the ultimate goal is a runner system with a minimum volume (Alam and Kamal, 2005) while the 1.5 mm constant in this equation means that in spite of the reduction of part dimensions, D should be always above this figure. This could result in a runner volume much higher than that of the parts produced, and therefore

the application of this equation in micro injection moulding is limited. On the contrary, equation 14 ignores S_{max} and takes into account only W and L. Both equations are applicable for estimating the optimal dimensions of the runner system when designing macro moulds however different factors dominate with the reduction of part size, especially when the parts incorporate micro features. Therefore, the effects of the runner cross section on the behaviour of the micro injection moulding process should be investigated by taking into account material and process related factors.

The micro injection filling process depends on the optimum design of runner systems and this is an important pre-requisite for the production of quality parts. Therefore, it is paramount to investigate the flow behaviour of the polymer melt in micro cavities with a particular focus on the relationship between the filling of micro parts and runner designs.

2.7 The influence of tool surface quality in micro injection moulding

There are several alternative methods of manufacturing cavities for micro-injection moulding. By applying each of these methods a different surface finish could be achieved. Thus, the surface finish specified at the design stage in respect to the parts and the tool cavities should take into account the manufacturing constraints introduced by these tool-making processes.

In micro tooling applications, the quality and topography of the machined surface could have a significant impact on their replication capabilities (Dobrev et al., 2005). The surface finish of the cavities should reflect the part design requirements, and may differ from that specified for the runner system. The high part to runner volume ratio means that a high percentage of the total shot volume that travels through the tool melt flow path

does not require a surface finish dictated by components technical requirements. Therefore, the runner system is usually manufactured using the most cost-effective method. This is in spite of the fact that its surface finish could have a significant impact on the tool filling behaviour and part quality.

2.7.1 Slip at liquid-solid interfaces

To investigate the flow of polymers in micro cavities it is important to understand interfacial interactions. The no-slip boundary condition or the phenomenon of slip refers to any conditions in the dynamics of fluids where the value of the tangential component of the velocity is different from that of the solid surface in contact with it. Controlled experiments have demonstrated an apparent violation of the no-slip boundary condition for the flow of Newtonian liquids, and De Gennes (1979) suggested that non-Newtonian fluids would also exhibit a non-zero tangential velocity at the liquid - solid interface. Subsequent research has shown that polymer solutions have significant apparent slip in a variety of conditions, some of which can lead to slip-induced instabilities (Lauga et al., 2005).

2.7.2 Slip and shear rate

When the surface velocity of a fluid is equal to zero this is called the no slip boundary condition. Navier (1827) first suggested that the slip velocity at the liquid-solid interface varies linearly with γ. Zhao and Macosko (2002) considered the interfacial slip to be a result of the low viscosity of the polymer flow. Slip results from the interaction between the polymer flow and the tool surface. Figure 2.7 represents the velocity and melt front profiles during the flow, which indicate that the temperature and velocity are not the same throughout the channel. The difference in velocity results in a change of γ of the outer

layer in regards to the bulk material. The change of γ results in a variation in the molecular entanglement within the boundary area of the bulk melt. Figure 2.8 identifies three velocity profiles with their respective different behaviours at the liquid-solid interface. Figure 2.8 (a) is the stick state in which the slip length (λ) equals 0 while Figure 2.8 (b) is a velocity field which identifies a partial slip. A slip state in which λ increases and there is fluid velocity or slip velocity (υ_s) at the tool surface is shown in Figure 2.8 (c).

A possible dependence of γ on the tool surface finish, is particularly important for polymers with sensitive flow characteristics. Leger et al., (1997) observed that when a polymer melt was sheared against a surface on which polymer chains were strongly attached, three friction regimes existed.

1. *Low shear rates.* A weak slip at the wall exists and the friction coefficient is independent from the slip velocity due to entanglements between the surface-anchored chains and the bulk polymer.
2. *Above the critical slip velocity.* When the critical slip velocity for a given material is reached a non-linear friction regime appears. In particular, the friction coefficient decreases with the increase of γ, due to a progressive dynamic decoupling of the surface and bulk chains.
3. *High shear rates.* The surface chains are totally disentangled from the melt flow, and a linear friction regime is in place similar to that expected along an ideal surface.

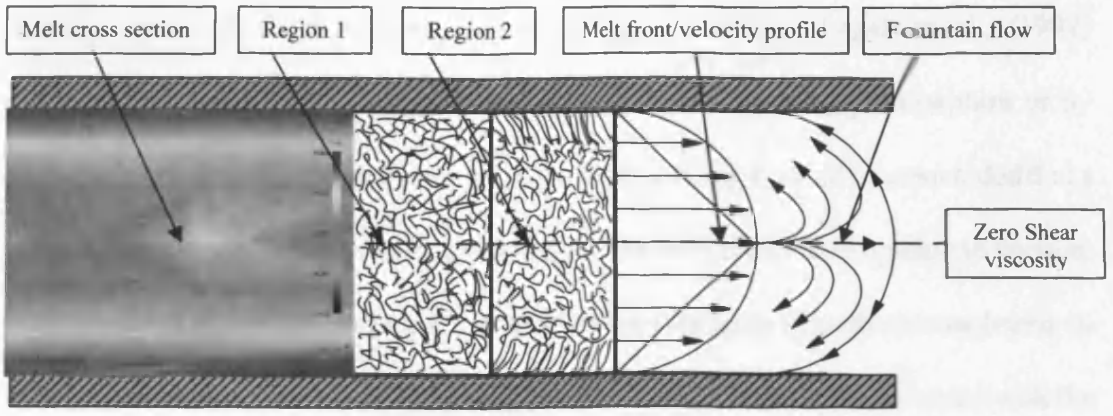

Figure 2.7 Velocity and melt front profiles

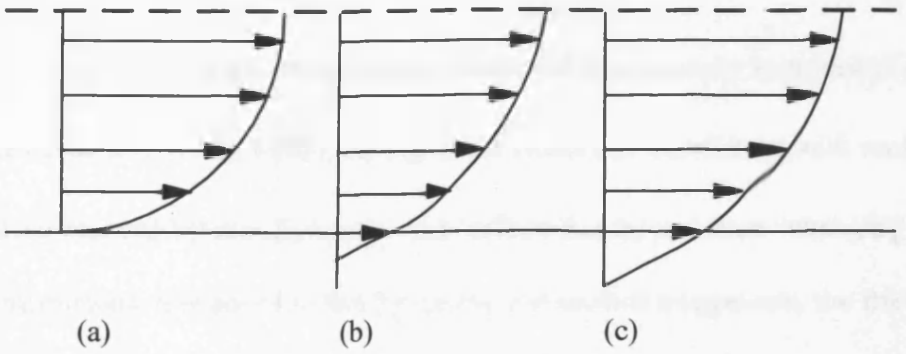

Figure 2.8 Velocity profiles of no-slip (a) partial slip (b) and slip (c) states

2.7.3 Slip and tool surface roughness

Roughness and surface structures have been observed to influence the flow behaviour at liquid-solid interfaces, in particular surface features cause flows to resist motion due to the dissipation of the mechanical energy. The tool surface can increase or decrease friction in fluid flows, and a strong friction at the walls can influence the chain entanglements within the polymer. Thus, the origin of λ is at the tool surface (Lauga et al., 2005, Brochard-Wyart et al., 1992). Investigations into the flow behaviour of polymer melts and interfacial slips occurring at the tool surfaces have provided an insight into the effects of polymer molecule anchoring to solid surfaces and the tool surface finish

hindering polymer chain motion (Harmandaris et al., 2003). Leger et al., (1997) demonstrated that such anchoring could be caused either by strong absorption or by chemical grafting, resulting in a strong friction at low γ. Thus, it could be concluded that a shear threshold exists above which a strong slip at the wall could develop due to friction. Bonaccurso et al., (2003) were the first to study the influence of surface roughness on melt flow behaviour, and made the conclusion that the slip effect had increased with the increase of the surface roughness.

If the slip stick originates from a strong dynamic structural discontinuity introduced by a solid surface (Drda and Wang, 1995), the high shear stress (τ) associated with such an effect could be reduced by modifying the tool surface finish, and thus changing the interfacial interactions. It is possible that by varying the surface roughness, the friction forces could be changed, in particular this could result in:

- A state of no-slip, partial slip or slip at the polymer tool interface.
- The outer skin layer not breaking loose but remaining at the wall thus reducing the layers and instability effects in the bulk material.
- Sufficient turbulence is introduced to the melt flow to facilitate the mixing of the polymer and thus to reduce the discontinuity in the bulk and the skin material phases.

By controlling the tool surface finish, for example by using tools with surface roughness higher than Ra 0.1 μm, the changes in surface properties can affect friction levels and the conditions that influence the slip at the liquid-solid interfaces. It should be said that the published research on the impact of the surface roughness on the flow behaviour is not

conclusive (Neto et al., 2005), and the scale effect of surface features in micro flows could be difficult to predict.

2.7.4 Molecular influence on the slip effect

Another important factor affecting flow behaviour is the molecular weight (M_w) of polymers. Inn and Wang (1996) found that the slip at the liquid-solid interface depended on M_w, and the existence of a relationship between η and M_w was evident from the occurrence of polymer disentanglement at high γ. Leger (2003) also observed that interfacial slips as a result of polymer surface anchoring could vary depending on M_w of the polymer. The flow profile of high M_w polymers is dependant on interfacial interactions especially for those with sensitive flow characteristics, and in addition due to the relatively high γ in micro moulding these effects could be considerable.

The factors that contribute to interfacial interactions between the polymer and the tool have been identified in polymer replication processes (Savvas., 1994). It is expected that micro injection moulding with its wide range of process factors, and the use of moulds with varying surface finish will have a significant influence on the flow behaviour. A lack of understanding of the effects of these factors could result in processing conditions leading to critical shear, degradation and interfacial instability.

2.7.5 Melt fracture

Viscosity is a function of γ, and shear-thinning is a result of polymer molecules moving more easily past one another as they line up parallel to the flow. As the shear increases the progressive thinning can lead to instabilities. The following regimes are typical in

melt extrusions:

- At low flow rates, the extruded polymer is smooth and regular.
- An increase in the flow rate results in a surface texture that is distorted. Termed; sharkskin or tiger stripes, the extruded polymer at this rate develops a sawtooth texture (Shore et al., 1996)
- A further increase in the flow rate results in gross melt fracture, and at this extreme conditions the extruded polymer is highly irregular.

The regimes of slip-stick through to melt fracture can be attributed to high shear stresses between the polymer and the tool wall. In particular, it is possible to extrude polymers at such high speeds that an intermittent separation of melt and inner wall develops. De Gennes (1979) suggested that the slip and stick behaviour could be a result of the stretching and uncoiling of some polymers attached to the wall, while a further increase of γ could lead to the polymers sticking and then breaking loose from the tool surface. The pressure change as a result of this alternating stress and relaxation conditions can cause pulsations to transmit through the melt as it exits the die. Also, such an increase in the pulsation rate can cause the outer skin layers to rupture. Another explanation for these oscillatory conditions is that when the stress at the wall becomes too high, the polymer molecules along the walls orientate themselves and slip. This, in turn, results in a decrease of the stress at the walls which eventually causes the polymers to reorient themselves again and thus back to the stick conditions. (Shore et al.,(1997) Osswald and Menges(2003)).

2.7.6 Part quality

Each polymer material has a corresponding critical γ, which if exceeded results in changes

to its visual appearance. Other negative effects relate to mechanical properties. By exceeding the critical γ instabilities can occur when two polymer layers with a different viscosity are formed, resulting in a variance of τ when they join together in the cavity. If the shear force overcomes the friction between the tool surface and the skin layer of already frozen polymer, the frozen polymer can be separated from the walls (Smialek and Simpson, 2001). This slip-stick effect results in a solidified or semi solidified melt joining the bulk of material in the cavity, and leads to defects and variations of the part's mechanical properties.

In plastic melt extrusion, instabilities within the die can translate to texturing of the extrudate resulting in observed defects on the skin of the produced polymer parts (Shore et al., (1997), Tao and Huang, (2002)). In the case of injection moulding medium to large parts, strong slippage in such large flow domains will have a little influence on the overall flow (McFarland and Colton, 2004). However in micro injection moulding, shear values are considerably higher than those observed in classical injection moulding (Zhao et al., 2004), and instabilities such as slippage at liquid – polymer interfaces can be strongly influenced by the behaviour of micro scale flows, in particular γ, tool surface roughness and M_w (Priezjev and Troian, 2004). Therefore, experimental investigations into the flow behaviour of the polymer melt in micro cavities with varying surface roughness levels are essential to further understand the relationship between the melt fill and tool surface.

2.8 The finite element analysis of melt flow behaviour in micro injection moulding.

The melt behaviour of pressurised polymer materials in contact with tool surfaces particularly micro channels, is reliant on process factors. The process settings used in injection moulding can influence temperature and shear related conditions that affect part quality (Taylor et al., 2005, Drda, 1995, Inn and Wang, 1996, Lauga et al., 2005). Various mould filling factors can be simulated using existing Finite Element Analysis (FEA) systems. In particular, to simulate polymer flow of generalised Newtonian fluids these FEA systems employ flow and viscosity models. However, although these simulation models are viscosity based and take into account such process parameters as shear rate, pressure and temperature, they are considered not sufficiently sensitive to determine the scale effects when filling micro channels, and do not account for cavities with varying surface finish.

2.8.1 Numerical model

A model is a hypothesis that can provide quantitative predictions, and then these predictions can be tested against experimental data and ultimately provide more information than what can physically measured. Thus, the model does not replace experiments but extends the previous understanding of the experimental evidences (Tucker., 1989).

The first law of thermodynamics says that the total inflow of energy into a system must equal the total outflow of energy from the system, plus the change in the energy contained within the system. For theoretical simulation the basic mathematical model can be written in different forms (Anderson, 1995, Shames, 1992, Welty et al., 1984). The equations of continuity, momentum and energy that describe fluid flow can be simplified for

application in injection moulding (Kennedy, 1993). Theoretical flow models' approximations based on a boundary condition of the three governing equations can be defined as:

- Conservation of mass. Conservation of mass means that the mass contained within a volume of fluid does not change in relation to a given time rate of change of mass. The compressibility application of the injection moulding process to the conservation of mass in a given volume provides the integral form of the continuity equation.
- Conservation of momentum. The momentum equation is a motion equation where momentum forces are transported onto a volume of material.
- Conservation of energy. The energy equation is the work done to increase the total energy of a material boundary and volume, involving rate of change of energy and rate of work done factors.

A mathematical model that is widely used for the simulation of injection moulding of polymers is the generalized Hele-Shaw approximation (Su, 2004, Hieber and Shen, 1995). The Hele-Shaw approximation assumes that the flow is pressure driven and takes place between parallel plates. If the flow takes place in x-y plane, pressure variation is assumed to be negligible in the thickness direction z. Taking into account non-isothermal, non-Newtonian and inelastic flows, simplification for filling mould cavities expressed by the Chain rule of differentiation for a Cartesian co-ordinate system (derivatives of xyz) results in.

Cavity Continuity equation $$\frac{\partial \upsilon_x}{\partial x} + \frac{\partial \upsilon_y}{\partial y} + \frac{\partial \upsilon_z}{\partial z} = 0 \qquad (15)$$

Where υ is the velocity component.

Cavity Momentum equation

$$\frac{\partial P}{\partial x} = \frac{\partial}{\partial z}\left(\eta \frac{\partial \upsilon_x}{\partial z}\right) \tag{16}$$

$$\frac{\partial P}{\partial y} = \frac{\partial}{\partial z}\left(\eta \frac{\partial \upsilon_y}{\partial z}\right)$$

$$\frac{\partial P}{\partial z} = 0$$

Where P is the pressure and η is the viscosity.

The Hele-Shaw approximation allows further simplification of the governing equations. For the two dimensional flow in the x – y plane the energy equation can be reduced to

Cavity Energy equation

$$\rho c_P \left(\frac{\partial T}{\partial t} + V_x \frac{\partial T}{\partial x} + V_y \frac{\partial T}{\partial y}\right) = \eta\gamma^2 + \mathrm{k} \frac{\partial^2 T}{\partial z^2} \tag{17}$$

Shear rate γ is calculated as:

$$\gamma = \sqrt{\left(\frac{\partial v_x}{\partial z}\right)^2 + \left(\frac{\partial v_y}{\partial z}\right)^2} \tag{18}$$

Where the density (ρ) and specific heat capacity (c_P) determines the amount of heat required to melt the material and is used to calculate the heat lost due to conduction, t is time, V_x and V_y are the components of velocity vector V in the directions x and y, respectively and viscosity η is a function of shear rate (γ) and temperature (T) (Kennedy, 1993). Further simplification by integrating the momentum and continuity equation results in a single governing equation for polymer flow in a cavity under pressure:

$$\frac{\partial}{\partial x}\left(S_2\frac{\partial P}{\partial x}\right)+\frac{\partial}{\partial y}\left(S_2\frac{\partial P}{\partial y}\right)=0 \qquad (19)$$

Where S_2 is the fluidity of cavity and P is Pressure.

The Hele-Shaw approximation is a standard method used to simulate injection moulding of polymers (Su et al,. 2004). In particular, when solving the mass, momentum and energy equations used to simulate the injection moulding process the model considers:

- No pressure in the thickness direction, so pressure is a function of x and y only.
- Pressure and temperature are calculated at each node, and the velocity is derived from the pressure gradient.
- The flow regions are considered to be fully developed flows in which inertia and gravitational forces are ignored.
- The flow is shear dominated and the shear viscosity is taken to be both temperature and shear rate dependent.
- Heat loss from the edges is ignored.

The model dramatically simplifies the governing equations for the flow of a viscous fluid in a narrow gap. However, the Hele-Shaw approximation cannot capture physical phenomena at the edges of the mould and at the flow front.

2.8.2 Finite Difference Method

Finite difference method (FDM) is used to solve the temperature across the thickness. FDM is the finite difference (discretization) method, it is the method for solving the differential temperature conduction equation through the thickness direction of the part. By defining laminae through the thickness of the part the FDM solves the conduction

equation through the thickness direction, thus describing how the polymer melt cools over time due to the mould temperature being lower than the polymer temperature. For numerical analysis the number of laminae can be specified in the Solver, in particular 0.0 can be set as the centre plane of the thickness, 1.0 is at the positive mould wall, and -1.0 is at the negative mould wall.

In Moldflow dual-domain analysis the temperature variation across the thickness is calculated with a heat transfer coefficient boundary condition on the outermost laminate. Added into this equation is the shear heating term (which uses the viscosity and shear rate) and also the convection term which describes how the hot polymer melt is carried forward by the moving polymer (velocity). For convenience, the discretization points are chosen to be the same as the laminae used for shear rate and viscosity calculations, thus giving the temperature solution on those laminae also.

Regarding the flow front, the fountain flow effect is solved using the filled elements. When an element is filled by the advancing flow front, the temperatures at all laminates through the thickness in the newly filled element are initialized to the temperature of the centre laminate. This represents the material of the fast flowing centre of the flow spreading out to fill the thickness in a fountain effect.

2.8.3 Tracking of free surface

The simulation of a mould filling is defined by mould boundaries and the instantaneous change in the flow fronts with time. The flow front is advanced using a volume of fluid method (VOF). In this scheme each node is assigned a volume. These control volumes are defined by the polygonal region formed by linking the half way point of a triangular

element to its centroid by straight line segments. The control volumes associated with their nodes are shown in Figure 2.9. After the pressure and velocity distributions are solved, the flow rates into each node on the flow front can be calculated. Since the time step is known, the node can be tested to see if it is filled. Once the node is filled, the flow front is advanced by incorporating all nodes connected to the last node to fill. A new instantaneous flow domain is then defined and a new pressure and velocity distribution is found.

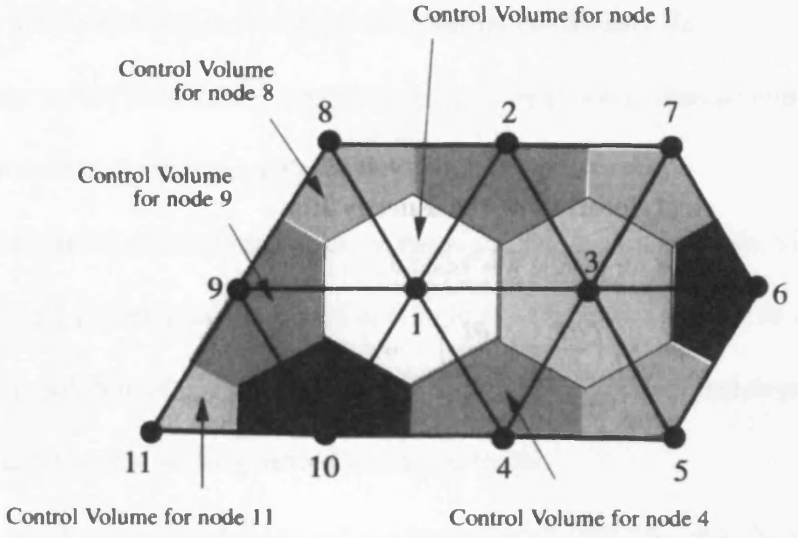

Figure 2.9 Control volumes (Kennedy, 1993)

2.8.4 Numerical solution

The governing equations are solved using numerical techniques. The most common ones are FEM and FDM. To find a numerical solution the governing differential equations are replaced by a system of algebraic equations (Bilovol., 2003). Based on the Hele-Shaw approximation the following three steps describe the procedure of finding a basic numerical solution.

1. Calculate the fluidity S2. If this step is the start of an analysis, a nominal value of viscosity at the melt temperature is used. If it is not, shear rate and temperature data from a previous step may be used.

- With S2 known, pressure can then be solved using Equation (19).
- After calculating the pressure field, it is possible to determine the velocity.
- A new value of shear rate may then be calculated using the expression in Equation (18), and assuming constant temperature, the viscosity is updated using the shear rate value.
- This viscosity value is then used to calculate the fluidity S2.
- Equation (19) is now solved again and the entire process repeated until the change in pressure is less than a defined tolerance.

2. After the pressure calculation has converged, the value of shear rate, viscosity and velocities V_x and V_y, are used in Equation (17) to calculate the convective and viscous heating terms. Solution of the equation is therefore reduced to a conduction problem with convection and viscous heating treated as source terms.

- The conduction calculations are performed with FDM to give the temperature field.
- With temperature now known, an updated viscosity value is calculated.
- This is then used to calculate the flow into each control volume on the flow front.

3. Knowing the flow rate into each control volume it is possible to predict which of them will be filled in the next time increment. The flow front is then advanced accordingly. Thereafter steps 1, 2 and 3 are repeated until the mould is filled (Kennedy, 1993).

2.8.5 3D Flow Analysis

3D flow analysis uses the Navier-Stokes model. The task of this solver is to find a more accurate solution to the equations of momentum and continuity, the Navier-Stokes solver differs from the Hele-Shaw approximation in that it makes no assumptions as to the relationship of the velocity field and the pressure gradient. Based on a generalized Newtonian fluid model, the polymer shear stress (τ) is expressed explicitly as a function of the shear rate ($\dot{\gamma}$) and conduction of heat in the material is assumed to obey Fourier's law, in particular, heat transfer due to conduction is linearly proportional to the temperature gradient (Bird et al., 1987). The algorithm used is an equal order velocity-pressure formulation adapted from the technique of Rice and Schnipke (1986). Due to the highly coupled nature of the equation set the computation is very intensive and therefore takes up most of the time required to solve the set.

When solving the mass, momentum and energy equations used to simulate the injection moulding process the 3D model:

- solves pressure, temperature X, Y, Z velocity components, at each node;
- considers heat conduction in all directions;
- provides inertia and gravity effects;
- does not use a FDM mesh .

FDM is generally complicated and impractical for complex three-dimensional geometries (Chang and Yang., 2001) and is not used to carry out a 3D analysis. Instead, the Moldflow 3D mesh function uses an automatic/manual mesh refinement scheme to calculate the temperature variation across the part thickness. This tool ensures that at least

6 layers of elements are present in the direction of the part thickness. The solution time for the 3D analysis is higher than that of mid-plane or dual-domain analysis but the benefits that it brings are a more accurate calculation of temperature and shear rate gradients through the thickness.

2.8.6 FEA of micro parts

It is well known that FEA models are widely used to simulate replication processes at macro scale and in the last two decades significant advances in this field was reported. Also, some attempts were made to apply such models for simulating injection moulding of micro parts and features (Su, 2004, Shen et al., 2004), and a good correlation between actual process behaviour and simulation results was reported (Yuan et al., 2003). The CAD model once imported and meshed by applying a hybrid FEM-FDM approach, is used for a dual domain analysis of laminar flow in generalised Newtonian fluids utilising the Hele-Shaw flow model. An alternative 3D flow model based on the Navier Stokes equation has been used by (Shen et al., 2002, Chang and Yang, 2001). Both flow models can be used to carry out temperature and pressure related simulation studies of micro parts but to assess their variations and accuracy require to validate them against physical field data.

Though, it should be stated that currently investigated models do not allow some phenomena to be simulated, e.g. surface finish (SF) effects or the melt slip, it is possible to investigate flow length and possible flow instabilities that can lead to surface defects (Grillet et al., 2002). Previous research has found that the simulation accuracy can be improved by comparing the results with actual values (McFarland. and Colton., 2004). Therefore, one important objective of this research is to compare the simulation results

with those obtained in experimental studies (Griffiths et al., 2006) and thus find ways to improve the accuracy of FEA models. In particular, by carrying out series of simulation runs the effects of a range of process variables on the filling behaviour can be analysed and the results compared with the experimental findings. Then, conclusions can be drawn about the accuracy and sensitivity of simulation models.

2.9 Surface treatment effects on part demoulding

An important step in micro injection moulding which can affect the mechanical properties of the produced components is part demoulding. During the solidification process of the moulding cycle, the polymer melt shrinks onto the mould cavity walls and features. The part-mould forces that develop at this stage have to be overcome for subsequent part removal. To avoid yielding when breaking the bond between the polymer and the tool cavity, the maximum equivalent stress applied for part removal should not exceed the tensile yield stress of the material (Navabpour et al., 2006). Thus, the factors that influence the demoulding process have to be studied carefully to avoid destroying parts and features and/or introducing further internal stress to a component through plastic deformation.

2.9.1 Part mould forces

Part-mould forces are a result of an interaction between the polymer and the mould cavities. They are a combination of contact pressure mainly due to the effect of shrinkage of the moulded material and the coefficient of friction of both materials (Menges and Mohren, 1993). An ejector system that can comprise of a number of ejector pins is used to apply a release force to overcome the friction force. The requirement for each pin is to overcome the local friction force without introducing defects to the removed part. In

particular, during demoulding, ejector pins can cause high local stresses and strains that lead to part deformation and damage, particularly for brittle materials and micro parts. Previous studies have shown that part deformation is affected by the number of pins and their positions within the cavity (Kwak et al., 2003). This problem is exacerbated in micro injection moulding due to the limited space for optimum positioning of ejectors and the reduced surface area of the pins resulting from their downsizing. In addition to the coefficient of friction properties of the polymer and tool surfaces, the design of the ejection system should also take into account factors such as draft angles, surface finish, and ejection temperature.

During the demoulding stage, part-mould forces can cause a variety of defects to the produced parts, these including stress marks, deformation, fracture and stretching of the polymer structures (Heyderman et al., 2000). The reduced mechanical properties and higher SV_R of micro parts makes them particularly susceptible to damage during demoulding.

In polymer injection moulding, predicting the adhesion forces between the part and the tool is a complex task due to its dependence on part geometry and on process parameters such as the temperature and the pressure used during the process. The force that resists the motion of one surface relative to another is defined as friction (2005). In injection moulding literature, two types of ejection forces (F_E), also called release forces (F_R), have been identified (Hopkinson and Dickens, 1999). The first applies when the tool contains simple geometrical features. In this case, a total friction between the tool and the polymer interface was investigated by (Menges and Mohren, 1993). Based on the part core surface area (A_C), the coefficient of friction of the moulded polymer (μ) (ISO 8295) and the

determination of moulding contact pressure (P_A) (ISO 294-4), F_R could be calculated as follows (Kwak et al., 2003):

$$F_R=\mu P_A A_C \tag{20}$$

F_R can be also characterised by the existence of imbalanced and localised part-mould forces that result from geometric and feature variations within a given part. In injection moulding, a known process factor that has a direct impact on friction is the level to which the part is filled. A complete and packed volume of polymer in a cavity with the optimum holding pressure (P^h) and holding time (t_h) will allow a complete fill of surface irregularities that are dependent on surface finish characteristics and surface to volume ratio of features. Alternatively, short shots or unpacked polymer volumes will lead to voids and sinks that retreat from the tool surface and thus reduce F_E.

Two friction coefficients, static (μ_s) and sliding or kinetic (μ_k), are important factors determining part-mould forces. μ_s is defined as the ratio of tangential force required to produce sliding and the normal force between the surfaces, best describes initial or breakaway motion stage during ejection (Pouzada et al., 2006). The subsequent motion to remove the part is then described by μ_k.

Previous research studies on IM forces and demoulding behaviour found that there are instances in which the friction effects can be difficult to explain. In particular, (Sasaki et al., 2000) showed that injection pressure did not affect F_E noticeably and that during processing μ is different to published data. (Bataineh and Klamecki, 2005) observed that the number of ejector pins affects the part-mould forces. More specifically, an increase in

the number of ejector pins resulted in a reduced stress distribution in the moulded part. In another study, F_E was found to increase with the increase of the tool surface roughness but also with highly polished surfaces (Pouzada et al., 2006). (Pontes and Pouzada, 2004, Pontes et al., 2005), found that the holding pressure (P^h) and surface temperature of the cavity substantially influence F_E. The reported results showed force measurements increasing with lower P^h and surface temperatures. Temperature factors are of particular importance in micro injection moulding. In particular, the increase of melt flow temperature results in a reduction of its modulus of elasticity (R.J.Crawford, 1987) and a better replication of micro features. However, without a reduction of the temperature during the cooling part of the cycle, the overall surface finish of the polymer can deteriorate during demoulding (Namseok et al., 2004).

The study of F_E is also very important when brittle injection moulds are employed such as those produced through rapid prototyping (RP) techniques. Tools manufactured by stereolithography (SL) can produce 50 to 500 parts before breakage, but they have generally poor thermal and mechanical properties and thus, they are prone to break at the ejection stage. Research on SL cavities with modified interlocking stair step surfaces and draft angles resulted in lower F_E when both the layer thickness was reduced and higher draft angles were applied (Pham. and Colton., 2002, Harris et al., 2002). An investigation of laser sintered (LS) stainless steel tools found that μ between the LS cavities and the polymer were similar to that of P20 steel (Kinsella et al., 2005). Other materials such as non ferrous and non metals like polymers and silicon (Si) can also be used for producing moulding tools (Griffiths et al., 2007, Bacher et al., 1998).

In plastics injection moulding, the machining processes available for tool production can

produce cavities with different surface finishes. Then, when the tool is used during the production of parts the mould surface wears due to a number of factors such as abrasion from the melt flow, thermo-mechanical loads, and burning and corrosion caused by the diesel effect of exhaust gasses. As mentioned, part-mould forces and the associated F_E vary depending on the surface finish of the tool. Thus, the degradation of a tool surface finish over a given time period will result in a variation of F_E during the tool life.

2.9.2 Surface treatment

One method that can be used for improving the wear resistance of tool surfaces is to apply surface treatments. In particular, the wear of a surface can be reduced with traditional methods such as heat treatment and nitriding. In addition, previous research found that techniques like physical vapour deposition (PVD) and chemical vapour deposition (CVD) of titanium nitride (TiN) and chromium nitride (CrN) resulted in moulds with significantly better wear resistance (Mitterer et al., 2003, Heinze, 1998, Cunha et al., 2002). At the same time, the surface quality of the moulded parts was improved due to reduction of the part-mould forces.

In addition, nano composite coatings such as polytetrafluoroethylene (PTFE) are widely used for the reduction of part-mould forces and thus μ. Unfortunately, such coatings are not an optimum solution for mass production due to their poor wear resistance (Sawyer et al., 2003). To overcome this issue, hydrocarbon blends of PTFE within an acetone adhesive can be applied at regular intervals onto tool surfaces in spray form. However, the deposition volume could be higher than that of the feature sizes, and thus could affect the replication of micro and nano features. It was reported that by applying several coating types on cavities produced from Si substrates it was possible to reduce F_E and

demould successfully polydimethylsiloxane (PDMS) replicas (Sasaki et al., 2000, Haefliger et al., 2005). For steel moulds, (Dearnley, 1999) found that polished surfaces produced lower friction forces than spark erosion finishes, and that magnetron sputtered CrN surface treatment of P20 resulted in a smaller standard deviation of F_E compared to uncoated P20. In addition, (Navabpour et al., 2006) observed that Alumina, Dymon-iC TM and NiCr coatings also allowed a reduction of part-mould forces. Although no specific property could be identified as a single contributing factor, the surface composition and surface energy defined as the interaction between the forces of cohesion and the forces of adhesion was found to be more important than surface roughness.

In particular, low material affinity between the coating and the polymer should result in a better demoulding behaviour. However (Van Stappen et al., 2001) demonstrated that although TiN and CrN coatings had a lower surface energy than that of the polymer tested, no correlation between surface energy and F_E was found. In addition, it was noted that other parameters like injection temperature and tool roughness also play a role in explaining demoulding behaviour.

The surface treatment of tools using pulsed laser deposition (PLD) of diamond like carbon (DLC) coatings results in tools with hard surfaces of up to 70GPa. Optimisation of deposition methods can lead to the production of DLC surfaces with friction coefficients in the range of 0.05-0.2μ, an order of magnitude lower than that of ceramic coatings (Voevodin et al., 1997). Further investigations of DLC coatings where special attention was paid to the inhibiting role of gas-surface interactions, showed that duty cycles with control variables of time and speed resulted in super low friction coefficients of 0.003-0.008μ (J.A.Heimberg, 2001).

Organosilicon based coatings are an interesting alternative or complementary approach to hard wear coatings as it offers a low surface energy that is likely to minimize adhesion of moulded polymers to the inorganic mould. It can be applied as an upper layer covering a wear resistant coating (e.g. DLC), and thus to promote a "two-steps" effect, an initial low gliding contact that is followed up by a contact with an underlying hard and low friction material. To achieve this effect precursors such as hexamethyldisiloxane (HMDSO), Octamethylcyclotetrasiloxane (OMCTSO) or tetraethoxysilane (TEOS) mixed with oxidants (O_2) and/or noble gases (Ar, He) are commonly used. In particular, HMDSO is one of the most commonly used monomer for PECVD deposition of silicon oxide thin films. While HMDSO is a monomer that cannot be polymerised by applying conventional methods in its liquid state because it does not have cyclic or double bonds in its structure. On the contrary, HMDSO can be polymerised during plasma treatments by rearranging the radicals that result from their dissociation induced by the electron impact. Soft coatings of $SiO_xC_yH_z$ with high content of methylene and methyl groups can be obtained by using pure HMDSO in plasma process yields (Uddin et al., 2006). As a replacement of HMDSO, OMCTSO can also be used due to its respectively higher content of methyl groups and lower density that reduce the surface energy even further.

One problem associated with surface treatments is that of interfacial adhesion between the tool surface and the deposited material. Mechanisms for deposition adhesion include mechanical locking of irregular surfaces, physical absorption (Van Der Waals forces), chemical bonding (covalent, ionic, or hydrogen bonds) and diffusion (inter diffusion of polymer chains). If the deposition thickness exceeds 1μm, the contact pressures from the injection moulding process can cause cracking and delamination of the coating. Although

advanced Ti-DLC coatings have been developed to reduce this problem, it is still an issue for F_E and tool wear (Uddin et al., 2006).

Another role that tool coating can fulfil is to protect against undesirable polymer and tool interactions. In particular, metal tools employed to produce micro parts for medical products run the risk of releasing metal ions (Grill, 2003). For example, nickel is a common contact allergen and at the same time it is a material that is commonly used for the manufacture of micro tools (Tang et al., 2006a, Kim and Kang, 2003, Bacher et al., 1998, Yang and Kang, 2000). By coating the cavities, a barrier between the tool and the polymer can be created. Furthermore, due to the amorphous nature of DLC coatings it is possible to introduce tunable antibacterial elements and thus to counteract contamination (Hauert, 2003).

Together with high SV_R and high aspect ratio micro features, present challenges in micro injection moulding call for the decrease of part-mould forces and tool wear. Based on the findings of previous studies, it is clear that surface treatments can reduce part such force and wear factors. Most of the studies investigated refer to macro moulding applications and reports on micro moulding are less common. Therefore the effect of different surface treatments on the demoulding behaviour of parts with micro features is important. In particular experiments on the interdependence between tool surface treatments and demoulding forces in micro injection moulding require a broad range of factors relative to the understanding of this part of the process.

3.0 Summary

In the first section of this chapter, a review of the micro manufacturing and micro replication process is made. A discussion of the necessity and requirements of replication is presented, and subsequently the available micro tool manufacturing methods are presented and an analysis of their capabilities is carried out.

In the second section, the chapter continues with a general description of the state of the art in micro-injection moulding, where the main characteristics and fundamental principles such as polymer rheology are presented and critically analysed. Finally, within the context of the necessity for micro replication and the current state of the art, the third section concludes the chapter with the fundamental concepts identified for further examination in this study.

In particular, it has been shown that the runner has an influence on melt flow behaviour, and though there are some design rules for macro injection moulding these rules don't automatically apply to micro injection moulding. Consequently, an investigation into runner cross section designs in relation to the temperature, pressure and filling capabilities of micro parts is therefore necessary to prove the need for runner considerations in micro mould design.

The literature review identified polymers with a high molecular weight as having complex flow behaviour due to temperature and shear dependent viscosity, and that the influence of shear is also linked to slip at the tool wall and polymer interface. As a result interfacial instabilities such as melt fracture exist under certain macro moulding conditions, and though there is little research to be found, it is likely these conditions are

exaggerated when downscaling to micro sizes. Therefore, to further understand the relationship between the melt fill and tool surface it is proposed that micro injection moulding process factors and tools with varying surface finishes are investigated.

It has been shown that attempts were made to apply FEA models that are widely used to simulate replication processes at macro scale, for simulating injection moulding of micro parts and features. Investigations have also shown that the small features typically found in micro moulding cavities can cause shear rates to be orders of magnitude higher than those experienced in conventional injection moulding. Consequently, since correlation between actual process behaviour and simulation results is not well reported, this research proposes to investigate temperature and shear related simulation analyses with up to date techniques. The simulation analysis will be validated against physical field data and thus conclusions will be made on the simulation accuracy.

Demoulding has been identified as an important step in injection moulding. Part-mould forces that are a result of an interaction between the polymer and the mould cavities can affect the mechanical properties of the produced components. Such forces can cause a variety of defects to the produced parts, and the reduced mechanical properties and higher SV_R of micro parts makes them particularly susceptible to damage during demoulding. Based on the findings of previous studies, it is clear that surface treatments can reduce part-mould forces and tool wear. Most of the studies investigated refer to macro moulding applications and reports on micro moulding are less common. Thus, to further understand the micro moulding process this research will investigate the demoulding of a micro part together with two surface treatments of interest to the micro industry. The performance of the treatments will be evaluated by a range of process factors commonly used in micro

CHAPTER 3

THE INFLUENCE OF RUNNER SYSTEMS ON FLOW BEHAVIOUR AND MELT FILL OF MULTIPLE MICRO CAVITIES

3.1 Motivation

To increase productivity and thus reduce the unit cost, often micro moulding tools incorporate multiple cavities with the use of a runner system. The main function of the runner system is to facilitate the flow of molten material from the injection nozzle into the mould cavity. Therefore, the micro injection filling process depends on the optimum design of runner systems and this is an important pre-requisite for the production of quality parts. The research reported in this chapter is focused on the relationship between flow behaviour of the polymer melts in micro cavities and the design and dimensions size of the runner system

The chapter is organised as follows. In Section 3.2 important issues in designing runner systems for multi-cavity micro injection moulding are discussed. Then, in Section 3.3 the research method adopted to investigate experimentally the effects of runner sizes and surface to volume ratio on the flow behaviour are described. Next, Section 3.4 presents the experimental results and analyses the relationship between runner sizes and the melt fill of multiple micro cavities. Finally, Section 3.5 summarises the research carried out and gives conclusions.

3.2 The runner system

As it was stated in the previous section the runner system has an important function in facilitating the flow of molten material from the nozzle of the injection unit into the mould cavity. Its primary purpose is to provide melt to all of the cavities at the same time, and with the same pressure and temperature while avoiding an excessive reduction of the set melt temperature (T_b) (Yen et al., 2006). Some of the main factors having a considerable influence on the runner system are described below.

3.2.1 Design considerations

There are two main types of runner systems, in particular standard (Figure 3.1) and hot runners. In case of a standard runner system the melt is fed through a sprue and delivered to the part cavity via a gate. Due to the small size of micro injection moulds it is possible that the design does not include a sprue because the nozzle entry is placed directly at the parting line with the runner, and its branches lead directly to the parts' cavities. In standard runner systems, polymer solidification at the walls can be controlled by monitoring the tool temperature. In this way the temperature of the runner system can be the same as mould temperature (T_m), with the exception of some localised heating from the cyclic iso-thermal temperature changes occurring when the melt enters the cavity within each injection cycle. Alternatively, hot runner systems can be used that include heated manifolds within the mould itself. With temperatures in the range of the melt temperatures of thermoplastics, the hot runners can be considered as an extension of the nozzle up to the tool cavity (Michaeli et al., 2007). In this investigation, only the standard runner designs for filling micro cavities are investigated, and sprue and gate factors are not considered.

Several issues should be taken into account when designing runner systems for micro injection moulding. These include:

• *Polymer material.* Heat loss during the melt fill can prevent flow, so for both high and low viscosity polymers an appropriate runner size is necessary. The heat loss in the material occurs firstly at the proximity to the runner walls, where a vitrified layer of polymer acts as a secondary insulation for the higher T_b at the core of the flow. With the use of overflows to divert the melt front (Figure 3.2), the selected T_b must be maintained long enough for the cavity to be filled completely. Once the cavity has been filled with the volume required, the temperature in the core should be high enough to apply the holding pressure (P^h). This is the second stage filling section of the pressure and speed profile. The holding pressure time (t_h) packs out the material in the cavities long enough for it to solidify and counteracts any contraction during cooling.

• *Injection moulding machine.* The pressure, temperature and speed capabilities together with its minimum and maximum shot weights should be considered. The ratio of runner to part weights is important because micro part volumes with large or small runner systems can be outside the machine shot weight range. In particular, the total shot volume of a moulding as determined by part and runner dimensions should take into consideration the maximum and minimum dosing available for any given machine.

• *Mould design.* This includes part size, number of cavities and the selected layout. The choice of the runner type must be based on the available tool space and include adequate distance between the part cavities. Available technologies/methods for machining the cavities can also influence the runner design, especially the runner system size in order to minimise the tool manufacture cost. In micro injection moulding this is even a more important consideration because of the manufacturing constraints associated with micro machining and structuring technologies.

• *Part design*. The cooling time of the runner and the part depends on their dimensions. In particular, an increase in the runner size, notably its cross section, results in T_b that is less affected by wall temperature. However, there are two economic implications that are associated with large runners. The first is that the runner cooling time can exceed that of the parts, and thus lead to an increase of the cycle time. Secondly, as the runner is not part of the final product this represents an extra material cost. An optimum runner should provide flow control within a reduced working area, and ideally should be as small as possible within the part efficient filling constraints, and its cooling time equal to that of the parts.

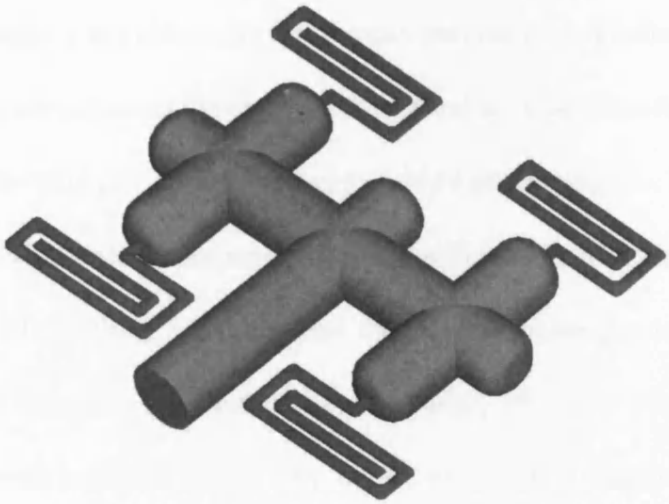

Figure 3.1 Standard runner

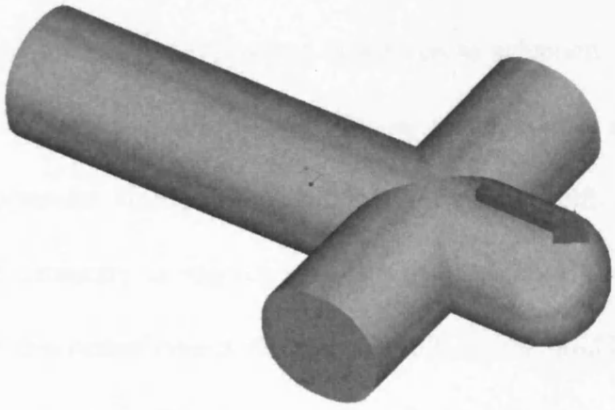

Figure 3.2 Overflow

3.2.2 Runner cross section

Three main types of runner cross sections are typically used: round, trapezoidal and parabolic (Figure 3.3). Square runners are also possible but they are rarely used due to the required draft angle on the side walls for an easier part removal. The factors mentioned in the previous section influence the cross section selection. In addition, for micro moulding surface to volume ratio (SV_R) of the runner should be considered, too. In particular, high SV_R that is typical for micro components has a significant effect on the filling behaviour (S.Yuan et al., 2003). Table 3.1 shows that the runner efficiency ratio (E_R) exhibits no difference when changing the cross sectional profiles, while it is very sensitive to any changes of the cross sectional dimensions, in particular E_R increases with the increase of the runner size (Engelmann and Dealey, 2000). SV_R is opposite to E_R, more specifically the SV_R for both cross section types decreases with the increase of the runner dimensions.

The only major difference between round and square cross sections is the increase of the material volume by more than 27% when square cross selections are used. The cross section also has an impact on the thermal losses in the runner system, and thus on ensuring that an optimum viscosity is maintained for each specific material. Due to the fact that circular geometry is regarded as the most efficient cross section, in this investigation only this runner type is studied. In multi cavity moulds, there is a need for controlled and simultaneous filling while relatively high T_b and T_m are maintained in order to replicate micro features (Sha et al., 2007a). Even though a high temperature also means that the runner requires more time to cool down to the desired ejection temperature (Zhao et al., 2005). Therefore, to ensure the selection of the most suitable moulding temperature for optimum filling and cooling cycles the size of the runner cross-sections must be chosen very carefully.

Material effects such as viscosity (η), shear stress (τ) and rate (γ), and process effects like T_m, T_b and injection speed (V_i) all relate to the part design. Thus, a good understanding of process, material and part design interactions coupled with an experimental knowledge about their combined effects is necessary in order to optimise the runner performance.

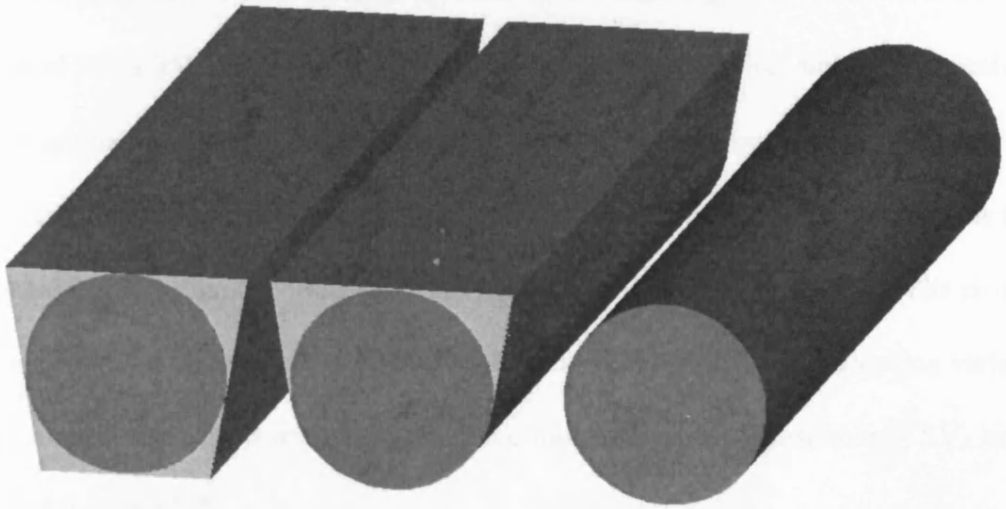

Figure 3.3 Runner cross sections

Table 3.1 SV_R and E_R comparison table.

	Type	1mm	2mm	3mm
Volume (10mm length)	Circular	7.8 mm^3	31.4 mm^3	70.7 mm^3
	Square	10.0 mm^3	40.0 mm^3	90.0 mm^3
SV_R	Circular	4	2	1.33
	Square	4	2	1.33
E_R	Circular	0.25	0.50	0.75
	Square	0.25	0.50	0.75

3.3 Experimental set-up

The following section describes the research method adopted for performing the experiments and analysing the results.

3.3.1 Part design and tool manufacture

The part used to analyse the runner size influence in the filling of micro cavities is a spiral that incorporates eight unequal sections with a total length of 29 mm and a cross-section of 500 x 250 μm (Table 3.2). Three tools with four identical and symmetrically positioned micro cavities that differed only in the size of their circular runner systems, in particular 1, 2 and 3 mm in diameter, were manufactured for replicating the spiral. Due to the symmetrical design the branches of the runner to each part are balanced and its cross section is round with an overflow for the melt front. *D* of the runner cross section varies in the range from 1 to 3 mm for these three tools and their corresponding SV_R are provided in Table 3.3.

All three tools were made from brass and the cavities were machined using micro milling. The moving and fixed halves were assembled to a primary mould tool and then inspected for parallelism and shut off of the mating faces.

Table 3.2 Spiral lengths

Section	1	2	3	4	5	6	7	8
Length mm	1	3.5	2.5	7.5	1.5	6.5	0.75	5.75
Total length mm	1	4.5	7	14.5	16	22.5	23.25	29

Table 3.3 Test part

Spiral	4 spirals + 1mm diameter runner	4 spirals + 2mm diameter runner	4 spirals + 3mm diameter runner
	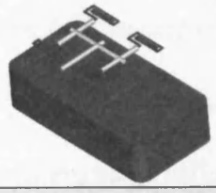		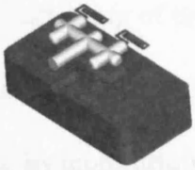
Surface area			
3.80 mm^2	86.51 mm^2	138.00 mm^2	193.00 mm^2
Volume			
3.09 mm^3	14.80 mm^3	50.20 mm^3	109.00 mm^3
SV_R			
1.22	5.84	2.74	1.77
E_R			
NA	0.25	0.50	0.75

3.3.2 Condition monitoring

Condition monitoring techniques are used in micro injection moulding to quantify natural variations that can occur within moulding cycles, and thus to identify interdependences between the resulting part quality and various tool, material and process factors. In this study, pressure (*P*) and temperature variations in the runner area were investigated using a Dynisco PCI piezoelectric force transducer and thermocouples, respectively. A National Instruments cDAQ-9172 USB data acquisition unit was utilised to analyse sensor output signals on a computer employing the National Instruments Labview 8 software. Each of the three tools had been modified to accommodate the condition monitoring sensors as it is shown in Figure 3.4.

Previous studies in which *P* in cavities was monitored had found that moulding of thin wall parts requires high injection pressures (Spina, 2004). Also, it was reported that the changes of *P* during the filling stage reflect the process condition. Thus, by monitoring P it is possible to characterise non conventional injection moulding from the point of view of describing the rheological behaviour of the polymer. Pressure sensors integrated directly in the cavity and the runner area of the cavity have been used to judge about material viscosity and the relationship between the pressure and metering size (Claveria et al., 2005, Jurischka et al., 2006).

In this research to measure *P* a measuring pin (MP), 1 mm in diameter (d), and a force transducer behind it were positioned in the centre of the runner system in the moving half of the tool as it is shown in Figure 3.5. When the transducer is subjected to a mechanical load, this results in an electrical tension that is converted into a proportional voltage using a Kistler charge amplifier. In particular, the technical specifications of the transducer and

amplifier used in this experimental study are:

- *transducer:* measuring range from 0 to 10,000 N and force sensitivity (E_f) of -4.2 pC/N;
- *amplifier:* measuring range up to 5000 pC and output range from 0 to 10V.

Ultimately, the output signal is monitored employing a National Instruments NI 9205 16-bit module.

The sensitivity, E_p, of the set-up can be expressed as follows:

$$E_p = \frac{d^2 \cdot \pi \cdot 0.1}{4} E_f \tag{16}$$

Thus, P in MPa can be expressed as:

$$P = \frac{Output(v) \times 500(pC)}{E_p} \div 10 \tag{17}$$

To monitor temperature changes during the injection moulding cycle thermocouples close to the tool-polymer interface were used in previous studies (Bendada et al., 2004). In this investigation temperature readings were taken directly from the runner area of each tool. To assess the temperature efficiency of the runners, two holes were drilled in the fixed half of the tool to accommodate 500μm diameter K type thermocouples as shown in Figure 3.4. In particular, temperature readings were taken at the entry and at the end of the runners, and the difference between them was used as an indication of the thermal efficiency of the runner. The output signal was monitored with a National Instruments NI 9211 24-bit module.

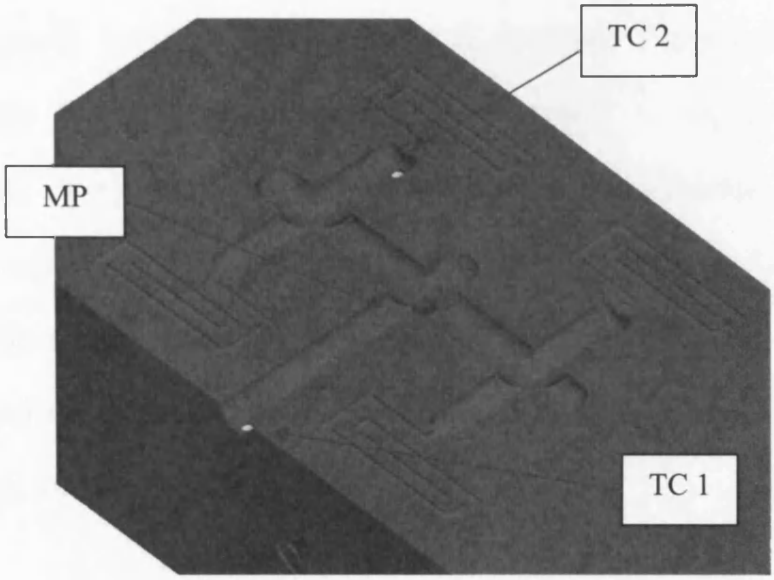

Figure 3.4 The positions of thermocouples, TC1 & TC2, and measuring pin (MP)

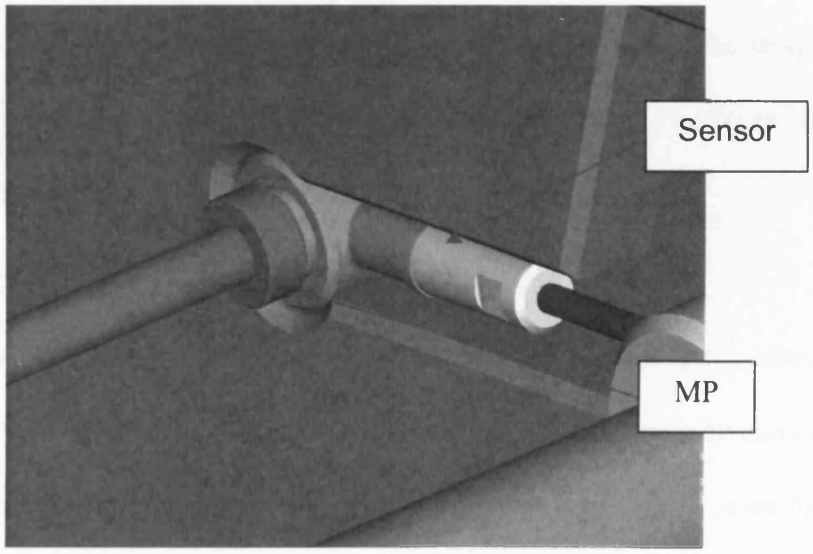

Figure 3.5 The force transducer behind MP

3.3.3 Test materials

Two commonly used materials in injection moulding, Polypropylene (PP) and Acrylonitrile Butadiene Styrene (ABS), were selected to conduct the planned experiments. Their properties are provided in Table 3.4. PP and ABS have different η and molecular weight (M_w) which is important for this study. Each polymer went through desiccant drying and dehumidifying cycles before the trials to remove any surface or absorbed moisture. The machine used to perform the micro injection moulding tests was a Battenfeld Microsystem 50.

3.3.4 Design of experiments

To study the runner size effects on the micro injection moulding process this experimental investigation was focused only on the filling stage of the process. The filling performance of micro cavities relies heavily on the speed and the temperature control during injection, therefore in addition to D the effects of T_b, T_m, V_i and holding pressure time (t_h) were investigated.

For each runner size and material used, given that four factors at three levels were considered, a Taguchi L9 orthogonal array (OA) was selected. The three levels of control for V_i and t_h were the same for all materials, while the levels for T_b and T_m were different as shown in Table 3.5. In particular, the levels of the four control parameters in this L9 experimental study were selected as follows:

- The melt temperature was controlled through T_b and was within a recommended processing window. Three levels, maximum, minimum and medium temperatures, were used for each of the polymers.

- In micro injection moulding, the polymer solidification time is much shorter than that in conventional moulding and therefore the processing requires heated tools. Therefore, T_m is raised to keep the bulk temperature of the polymer sufficiently high and thus to facilitate the melt flow during the filling stage. The T_m settings used in this research were the minimum, medium and maximum temperatures in the recommended range for each material.
- V_i has two main effects. It can help polymers to fill the cavities before the melt flow solidifies but also it can increase the shear rate of the polymer which results in shear heating. The three levels of V_i selected in this research were chosen by taking into account the capabilities of Battenfeld Microsystem 50, for which the maximum injection speed is 946.4 mm/s over a stroke distance of 84 mm.
- The three levels of t_h during which the cavity pressure is maintained were set at 0 seconds, 2 seconds and 4 seconds.

The effects of runner sizes were assessed by measuring the flow length of the mouldings, the temperature and P_{max} in the runner cavity. Given that three runner sizes and two different materials are considered, six L9 OAs were defined. In addition, ten trials were performed for each combination of controlled parameters in these six OAs. Thus, in total 10 x 9 x 6 = 540 experimental trials were carried out.

Table 3.4 Materials properties

Material	Sabic 56M10	Magnum 8434	Calibre 300
Category	Polypropylene (PP) C_3H_6	Acrylonitrile butadiene styrene (ABS) $C_{15}H_{17}N$	Polycarbonate (PC) $C_{16}H_{14}O_3$
Structure	Crystalline	Amorphous	Amorphous
n	0.3747	0.2777	0.1443
τ	1.0600E+04 Pa	7.6803E+04 Pa	1.1300E+06 Pa
D1	1.1900E+12 Pa.sec	1.7012E+14 Pa.sec	1.0600E+12 Pa.sec
D2	263.1500 K	373.1500	417.1500 K
D3	0 K	0 K	0 K
A1	23.8250	33.6060	28.9680
A2T	51.6 K	51.6 K	51.6 K
Mw	261,000	169,000	26,000
Mn	58,200	51,600	9,770
PDI	4.5	3.3	2.7
Moldflow viscosity index*	VI(210)0103	VI(240)0087	VI(300)0269
Transition temperature	150°C	90°C	170°C

Note: * - the number in the brackets refers to the material melt temperature [°C] while the other four digits signify its viscosity [Pa*sec] measured at a shear rate of 1000 [1/sec].

Table 3.5 L9 orthogonal array for PP and ABS

Trial	Holding pressure time t_h [s]		Melt temp T_b [°C]		Mould temp T_m [°C]		Injection speed V_i [mm/s]	
	PP	ABS	PP	ABS	PP	ABS	PP	ABS
1	0		220	220	20	40	200	
2			250	250	40	60	500	
3			270	280	60	80	800	
4	2		220	220	40	60	800	
5			250	250	60	80	200	
6			270	280	20	40	500	
7	4		220	220	60	80	500	
8			250	250	20	40	800	
9			270	280	40	60	200	

3.4 Analysis of the results

In this study, L9 OAs were employed to ensure that the experimental results were representative of a broad processing window. The mean value of the three response characteristics was calculated for each of the six OAs in order to analyse the results (Appendix C). In addition, by employing OAs this experimental study can be used further to optimise the process by identifying the best combination of processing parameters, and also the most significant of them in regards to the runner performance.

3.4.1 Flow length

For each trial, the runner size effects on achievable flow length were analysed. Table 3.6 and Figure 3.6 presents the flow length results obtained from all 540 trials. Given that there are four cavities the maximum and minimum average flow lengths achieved during the experiments are provided.

For the 3mm runner, the average flow length of all 9 experiments show that both PP and ABS only achieved 90% filling of the cavities. Both materials had unequal filling for the three cavities while a higher variation between the maximum and minimum lengths was observed in the case of ABS.

For the 2mm runner, PP filled completely the cavities in all 9 experiments. This shows that this runner size was more efficient than the 3mm one. For ABS, the maximum filling achieved was 90%, which was similar to that observed with the 3mm diameter runner while the minimum length was higher, 77%. Thus, for both materials the 2mm runner can be considered more efficient.

For the 1mm runner, PP filled completely the cavities in all 9 experiments. Thus, it is difficult to judge whether this runner size is more or less efficient than the 2mm one. However, it is evident that it is more efficient than the 3mm diameter runner. The maximum filling achieved in the ABS experiments was 79.5% while the minimum length was 72.4%. Although, the difference between high and low flow lengths is relatively small compared to the 2 and 3 mm runners, by looking at the maximum flow length results achieved with the three different runner sizes it is not difficult to conclude that in case of ABS the 1mm runner is the least efficient one.

The flow length results for PP indicate that the runner size had a little effect on the resulting flow length. The higher SV_R and the expected heat loss with the smaller runner could have been counteracted by the lower η at higher shear results. For ABS there is also an associated η reduction with smaller runners though in this case the reduction was not sufficient to overcome the heat loss effects of SV_r, as indicated by the lower flow length achieved with the 1 mm runner. In addition, the flow length results suggest that compared to PP η of ABS is influenced more by temperature and shear rate.

3.4.2 Temperature

For each trial, the temperature changes between TC1 and TC2 in the runner cavities was measured to judge about the size effects. Figure 3.7 presents the increase or decrease of temperatures for each runner diameter and material.

For the 3mm runner, a temperature increase between the beginning and the end of the runner system was observed for both PP and ABS, with a higher increase for PP, in particular 22 °C.

For the 2mm runner, again a temperature increase was observed for both PP and ABS, with PP being subjected to the highest increase of 36 °C.

For the 1mm runner, PP exhibited a marginal temperature increase while a decrease was observed in case of ABS. These results show clearly that the 1mm runner has the lowest deviation from the set T_b, however for increasing the flow temperature it is the least efficient of the three sizes investigated in this study.

If a temperature increase within the runner system is required in order to improve the filling, the 2mm runner can be regarded the best choice of the three sizes considered in this research.

The temperature results provide evidence of shear heating in all cases except the ABS 1 mm trials, and also support the low flow length results discussed in Section 4.1. The increase in shear with the runner size reduction leads to a lower η, while the temperature increase experienced with the 2 mm runners for both materials indicates an optimum SV_R in regards to the observed increase of the shear heating.

3.4.3 Pressure

For each trial the runner size effects on P_{max} in the runner cavities were also analysed. Figure 3.8 presents the pressure results for each runner size and material.

For the 3mm runner, ABS had a higher P_{max} than PP while the results was opposite for the 2mm one. On average, both materials were subjected to a higher P_{max} with the

decrease of the runner size. In particular, in case of PP the average P_{max} is doubled with the decrease of the runner size from 3 to 2 mm.

For the 1mm runner size, both materials experienced a higher P_{max} compared to the 3 and 2mm results. In addition, the ABS result was the highest out of all experiments.

From the carried out experiments it can be concluded that to extend the tool life it will be desirable to use a bigger size runner because of the P_{max} reduction with the increase of the runner diameter.

The 1 and 2 mm runners experienced a lower polymer flow rate compared to the 3 mm runner. One possible explanation of the flow lengths achieved in the case of the smaller diameter runners can be the beneficial effect of the P_{max} increase. Additionally, the P_{max} result could account for the variation of flow lengths within the four parts. In particular, the highest P_{max} variation between the highest and lowest flow lengths for both materials was measured in the 3 mm runner. At the same time, the increased pressure within the runner could provide a more balanced flow of material leaving the runner as it was the case with the 1 mm one.

Table 3.6 Flow length results

EX	ABS Flow Length [mm]						PP Flow Length [mm]					
	3mm runner		2 mm runner		1 mm runner		3mm runner		2 mm runner		1 mm runner	
	High	Low	High	Low	High	Low	High	Low	High	Low	High	Low
1	20	11	22	17	15.5	14.5	11	5.5	29	29	29	29
2	26.25	16	27.25	22.5	22.5	22.5	29	24.25	29	29	29	29
3	29	21	29	29	25	25	29	29	29	29	29	29
4	22	11	20	16	14.5	14.5	25.25	19	29	29	29	29
5	22.5	15	25.75	19	20.5	20.5	29	23.25	29	29	29	29
6	27.25	18	29	26.25	27.25	26.25	29	25.25	29	29	29	29
7	21	14	27.5	17	16	16	29	23.25	29	29	29	29
8	19	13	25.25	25.5	20	20	27.25	21	29	29	29	29
9	25.25	17	29	25.25	27.25	25.75	29	25.25	29	29	29	29
Ave	26.5	17	26.0	21.9	23	21	26.3	21.75	29	29	29	29
%	91.4	58.6	89.9	75.6	79.5	72.4	90.9	87.0	100	100	100	100

Note: 10 parts were measured for each combination of factors and the table includes their mean values.

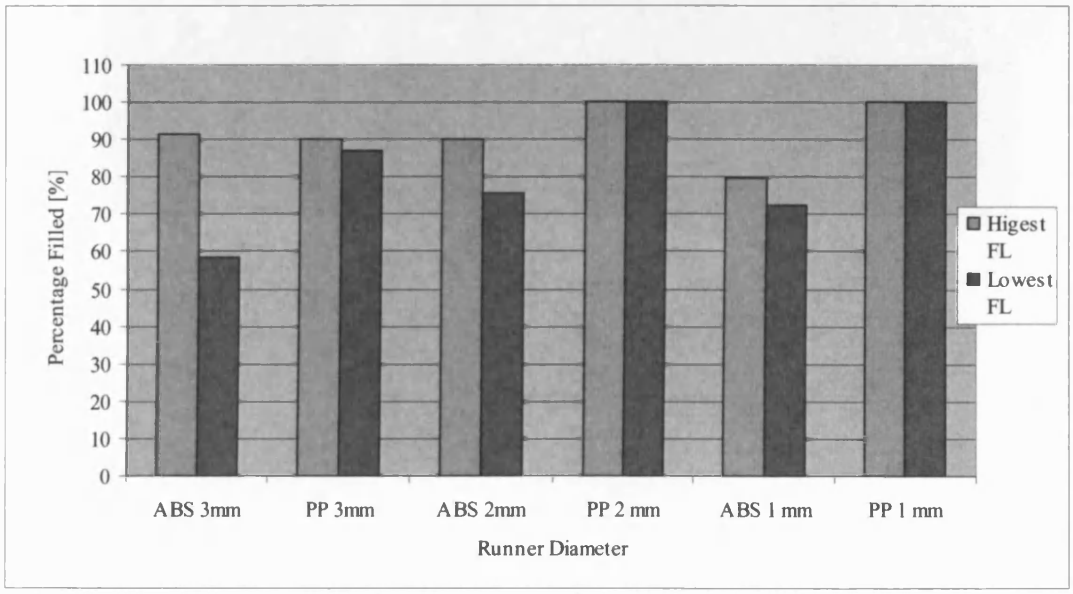

Figure 3.6 The maximum and minimum average flow lengths (FL) in percentage

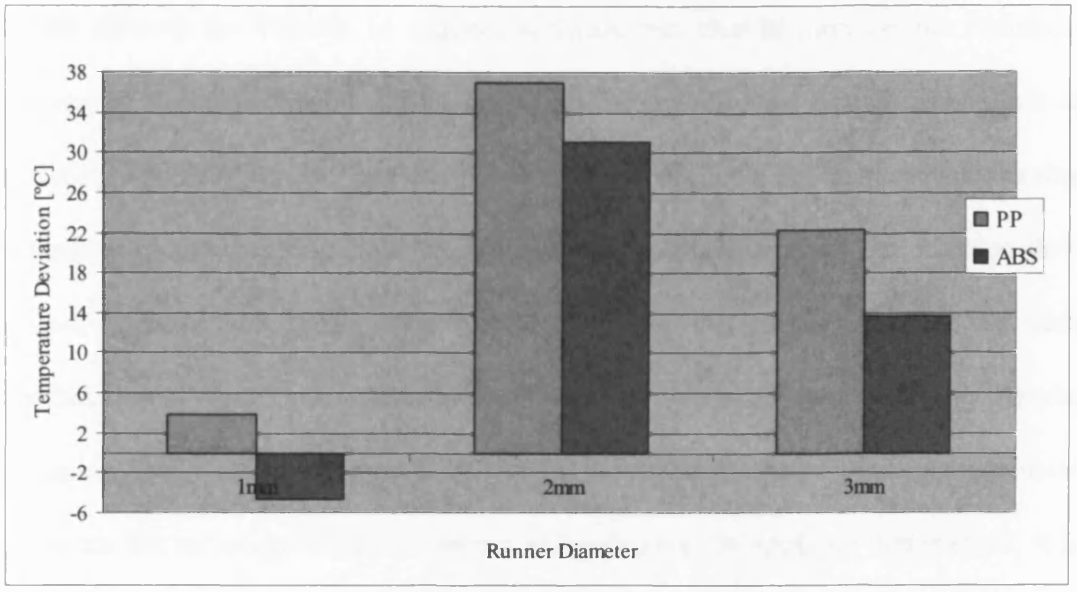

Figure 3.7 The temperature changes in the runner system

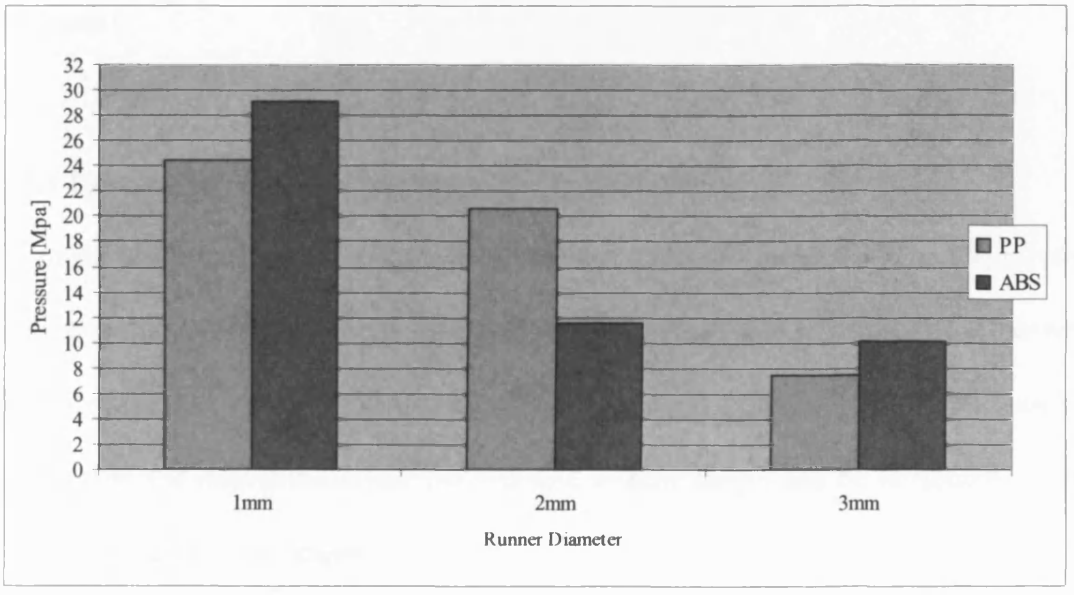

Figure 3.8 Runner cavity pressures

3.5 ANOVA analysis

In this research the Minitab 14 analysis software was used to carry out the statistical analysis of the experimental results. Based on the experimental results, an analysis of variance (ANOVA) was performed in order to assess the contribution of each processing parameter to the resulting flow length, pressure and temperature. The average flow length, pressure and temperature results based on the conducted trials for each combination of control parameters in the L9 OAs was calculated employing the Taguchi parameter design method (Roy et al. 1990) and thus to determine the optimum parameter levels for the investigated measurements and polymers. By applying this method, it is possible to identify theoretically the most influential micro injection moulding parameters within the investigated processing window with respect to flow length, temperature and pressure.

3.5.1 Parameters' contribution to runner flow length

From the conducted Taguchi analysis it can be seen that for PP and ABS T_b and V_i are the most important factors affecting the resulting flow length (Table 3.7). Also, from the two T_b is consistently the most important factor in regards to the polymer flow length. Especially, the results show that the increase in flow length can be attributed to an increase in the T_b in all cases.

3.5.2 Parameters' contribution to runner temperature

For PP and ABS T_m is the most important factor. In particular, a decrease of T_m results in an increase of runner temperature (Table 3.8). This increase in the runner temperature indicates that the T_m reduction increases the shear heating of the bulk polymer melt flow.

While for ABS, the high temperature settings result in a decrease of temperature within the runner which shows that there is less shear stress at these processing conditions.

3.5.3 Parameters' contribution to runner pressure

From the conducted Taguchi analysis it can be seen that for PP and ABS V_i and T_b are the most important factors affecting runner pressure (Table 3.9). Overall, V_i is consistently the most important factor influencing pressure in the runner. Especially, the results show that for ABS the increase of pressure in the runner system can be attributed to an increase of T_b and a decrease of V_i for all runner sizes, while for PP the results are less conclusive.

3.5.4 The theoretical best set of processing parameters

The analysis of the main effects plots for flow length, temperature and pressure (Figure 3.9, 3.10 and 3.11) provided the optimum levels for all investigated factors, and the theoretical best set of processing parameters. Table 3.10 presents the results obtained from the experiments conducted in this study, in particular it identifies the best set of processing parameters in respect to the highest flow length, pressure and temperature increase. Based on them the following conclusions can be drawn:

- Higher settings lead to an increase in the average flow length for both PP and ABS.
- Higher settings of T_m and medium to low settings of V_i result in an increase of the average pressure for both PP and ABS.
- In regards to temperature there is not a unique selection of parameter levels that can be considered optimum for both materials. The materials differ in that high to medium settings for PP generally result in a average temperature increase, while

for ABS the opposite is true where the lower settings result in a runner temperature increase.

Table 3.7 Taguchi analysis response table for runner flow length

Factors	t_h	T_b	T_m	V_i
1 mm runner				
Rank Importance	4	1	3	2
Delta [%]	0.25	5.67	0.54	1.04
2 mm runner				
Rank Importance	3	1	4	2
Delta [%]	1.17	2.92	1.0	1.58
3 mm runner				
Rank Importance	4	1	2	3
Delta [%]	1.79	6.71	4.33	4.13
1 mm, 2 mm and 3mm				
Rank Importance	4	1	3	2
Delta [%]	0.58	5.10	1.71	1.88

Table 3.8 Taguchi analysis response table for runner temperature

Factors	t_h	T_b	T_m	V_i
1 mm runner				
Rank Importance	3	2	1	4
Delta [°C]	4.437	15.538	24.537	4.327
2 mm runner				
Rank Importance	3	2	1	4
Delta [°C]	1.8	11.22	29.18	1.36
3 mm runner				
Rank Importance	1	4	2	3
Delta [°C]	13.04	1.15	12.9	9.08
1 mm, 2 mm and 3mm				
Rank Importance	3	2	1	4
Delta [°C]	5.591	9.108	22.205	2.722

Table 3.9 Taguchi analysis response table for runner pressure

Factors	t_h	T_b	T_m	V_i
1 mm runner				
Rank Importance	4	2	3	1
Delta [MPa]	0.75	2.25	2.08	2.50
2 mm runner				
Rank Importance	4	3	2	1
Delta [MPa]	0.42	0.70	0.72	1.13
3 mm runner				
Rank Importance	4	1	2	3
Delta [MPa]	0.167	0.583	0.417	0.375
1 mm, 2 mm and 3mm				
Rank Importance	4	2	3	1
Delta [MPa]	0.27	1.140	0.79	1.14

Table 3.10 Taguchi response table for the theoretical best set of processing parameters

	Flow length				**Pressure (H)**				**Temperature (H)**			
Factors	t_h	T_b	T_m	V_i	t_h	T_b	T_m	V_i	t_h	T_b	T_m	V_i
PP 3mm	3	3	3	2	3	1	3	2	3	3	1	3
PP 2mm	0	0	0	0	3	2	3	2	3	3	2	2
PP 1mm	0	0	0	0	2	1	2	2	2	3	2	2
ABS 3mm	1	3	2	2	1	3	3	1	1	1	1	1
ABS 2mm	3	3	3	2	1	3	3	1	1	1	1	3
ABS 1mm	3	3	2	2	1	3	3	1	1	1	1	3

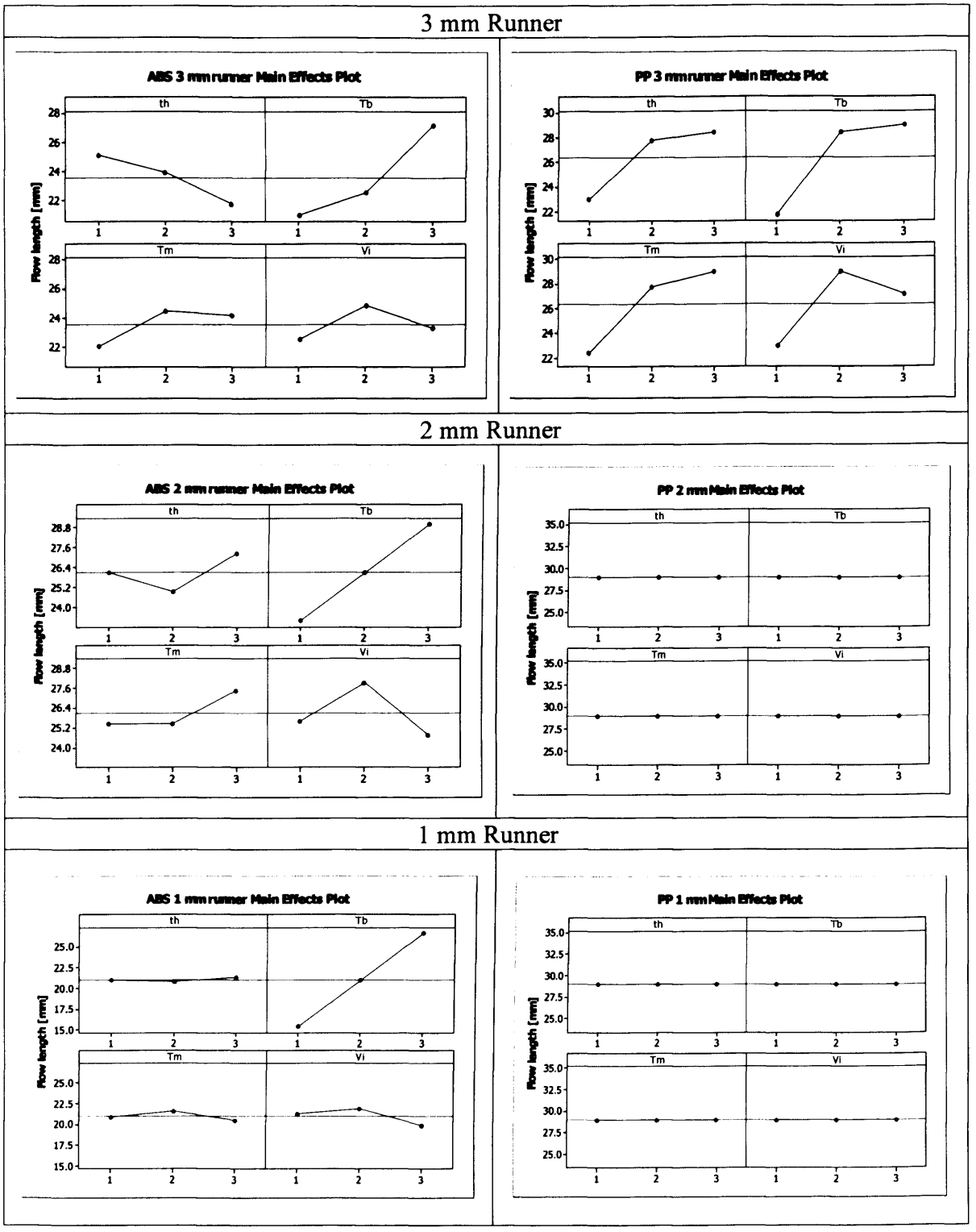

Figure 3.9 Runner flow length effects' plots

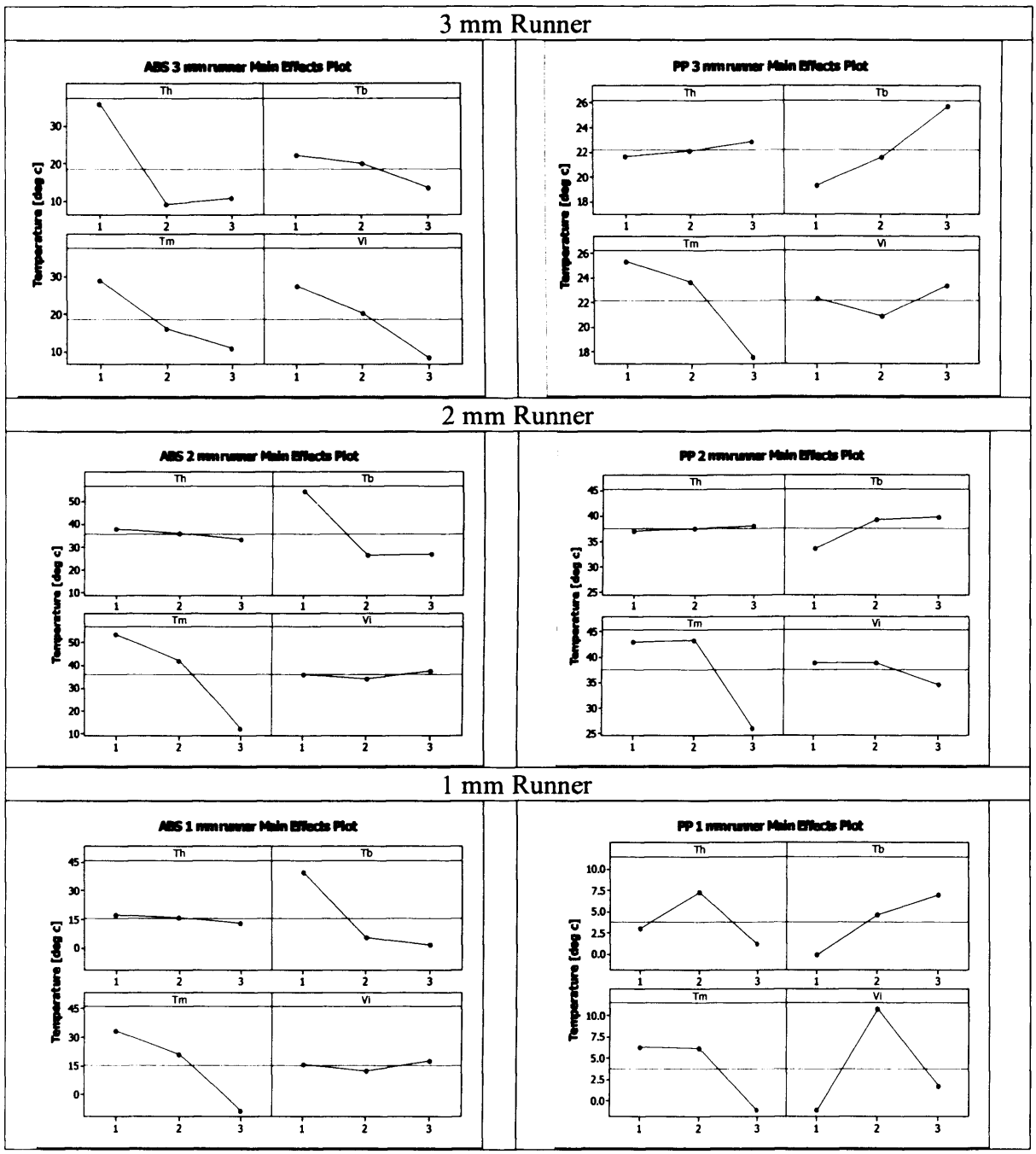

Figure 3.10 Runner temperature effects' plots

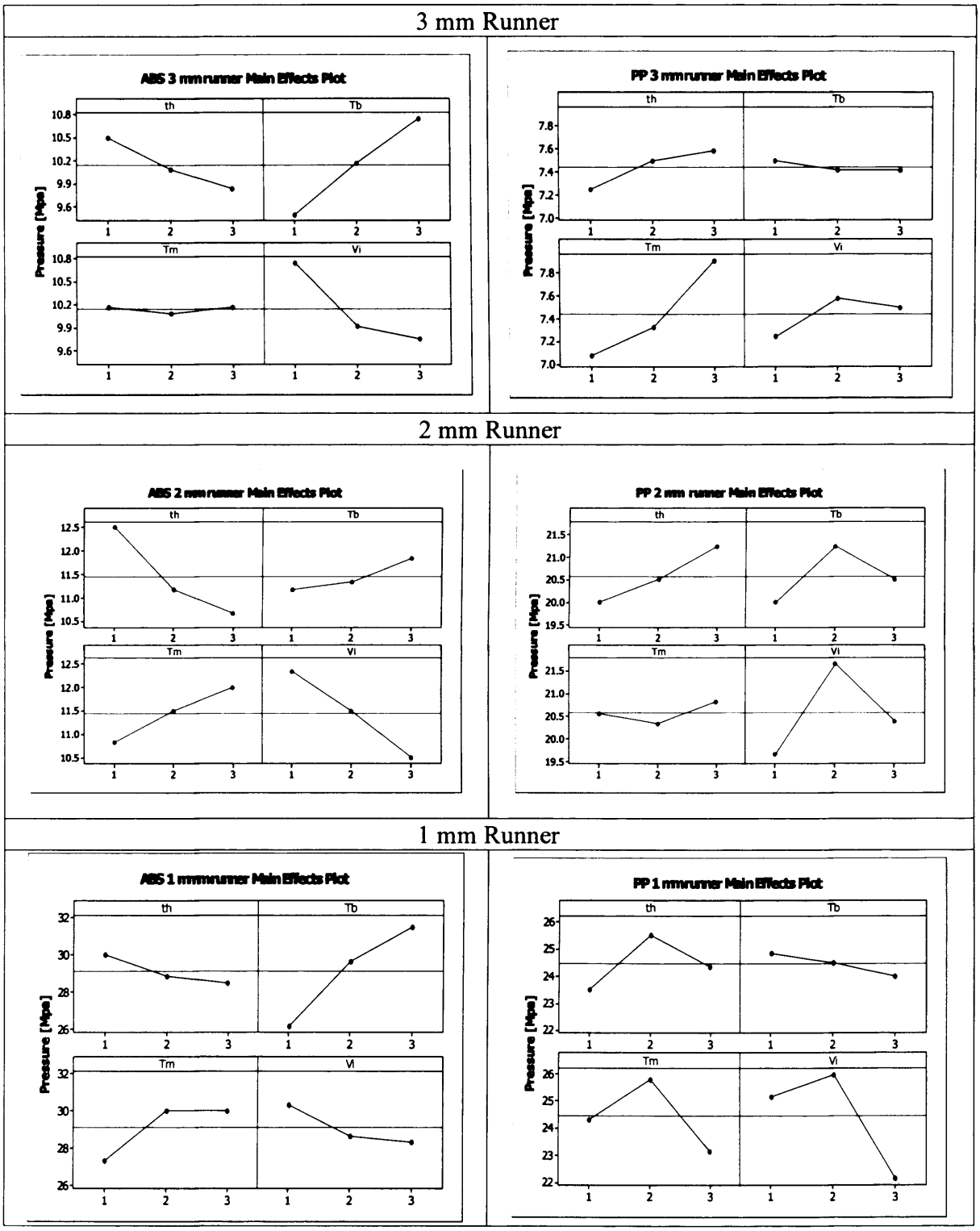

Figure 3.11 Runner pressure effects' plots

3.6 Summary and conclusions

Prior to filling a cavity the polymer material has to travel through a runner system. Therefore, it is important to understand the effects of the runner system design on the process performance in the context of micro injection moulding. Chapter 3 reports an experimental study on the flow behaviour of the polymer melts in micro cavities with a particular focus on the relationship between the filling of micro parts and the size of the runner system. In particular, to investigate the runner size effects on the micro injection moulding process the research was focused only on the filling stage of the process. The filling performance of spiral-like micro cavities was analysed as a function of runner size in combination with the four process factors, T_b, T_m, V_i and t_h,. To judge quantitatively about the process performance, the cavity temperature and pressure, and polymer flow length were measured.

A design of experiment approach was adopted to investigate the effects of the runner size together with flow properties of PP and ABS on the process performance. The results of the conducted L9 experimental studies were analysed to identify potential ways for improving the micro-injection moulding process. In particular the following conclusions can be made based on the reported research:

1. The flow length results for both PP and ABS showed that the 2mm size runner had the optimum surface to volume ratio and shear heating balance in regards to the filling performance. It is important to note that an increase of the runner dimensions did not have a positive effect because both materials failed to fill the micro cavities with the larger 3mm runner. While both materials experienced

imbalance in filling all four cavities, ABS was more prone to variations. Also, it was observed that these variations increased with the increase of the runner size.

2. A temperature increase from the set T_b was measured for both materials and all three runner sizes, except for ABS with the 1mm runner system. The use of the 2 mm runner resulted in the highest increase of the average temperature while the 1 mm runner was the least subjected to temperature variations. For PP, the temperature variations in the runner system do not seem to affect the filling performance. In particular, the micro cavities were completely filled when using the 1 mm and 2 mm runners while not with the 3 mm one in spite of the significant increase of temperature compared with the 1 mm runner system. This suggests that PP is not sensitive to temperature losses or increases due to its low viscosity characteristics. On the contrary, the results for ABS suggest that the flow temperature affects the filling performance. In particular, the highest flow length was obtained when the highest temperature increase was recorded using the 2 mm runner system. In contrast, for the 1 mm runner the decrease in temperature led to the lowest flow length.

3. For both materials, an increase in pressure with the reduction of the runner size was observed. The use of the 1 mm runner resulted in the highest pressure, with P_{max} doubled and trebled in comparison to the results obtained with the 3mm runner system for PP and ABS, respectively. However, it should be noted that by increasing the pressure in this way there are some side-effects. In particular, any increase of the pressure in the micro cavities will have a detrimental effect on the tool life and sometimes can lead to tool damage or structural damage of micro/nano features without any significant gains in the filling performance.

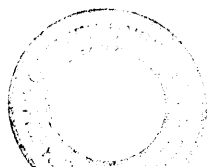

4. From the conducted Taguchi analysis it can be seen that for PP and ABS temperature is the most important factor. T_b is consistently the most important factor for the resulting polymer flow length while T_m is the most important factor in regards to runner temperature. For runner pressure V_i is consistently the most important factor.

5. The Taguchi analysis of the main effects plots for flow length, temperature and pressure provided optimum levels for each of the investigated factors. In particular, flow length increases with higher settings, and higher settings of T_m lead to an increase in pressure. For temperature, there is not a unique selection of parameter levels that can be considered optimum for both materials and considered runner sizes.

CHAPTER 4

THE EFFECTS OF TOOL SURFACE QUALITY IN MICRO INJECTION MOULDING

4.1 Motivation

The development of new micro devices is highly dependent on manufacturing systems that can reliably and economically produce micro components in large quantities. In this context micro-injection moulding of polymer materials is one of the key technologies for micro manufacturing. Currently, the replication of component micro-features is a key issue determining the reliability of the selected manufacturing route. It depends greatly on their size, aspect ratio and surface area (Webber and Ehrfeld) . Thus, it is very important to study the combined effects of process factors and tool surface quality on the replication capabilities of micro-injection moulding.

This chapter is organised as follows. In Section 4.2 factors affecting micro flow behaviour are discussed. Then, the research method adopted to investigate experimentally the effects of tool-melt flow interactions on the process performance is described in Section 4.3. Next, Section 4.4 presents the experimental results and analyses the effects of interfacial interactions on the flow length and part quality. Finally, Section 4.5 summarises the research carried out and gives conclusions.

4.2 Factors affecting micro flow behaviour

This investigation looks at the flow behaviour of the polymer melt in micro cavities with different surface roughness levels when varying process conditions/settings. There are a number of process factors that can influence the polymer flow and their interdependence has to be properly understood to achieve the desired process performance on a dedicated micro moulding machine. Also, with several alternative methods of manufacturing micro tool cavities it is important to consider the interfacial interaction between the tool and polymer.

4.2.1 Process settings

Features with high aspect and surface-to-volume ratios are typical in micro-injection moulding and therefore high melt temperature and injection speed are required to replicate them successfully (Masaki et al. 1994) In particular, this is because high surface-to-volume ratios of micro-cavities cause rapid cooling. Another reason is the temperature control for barrels, nozzles and tools that is specific and require part ejection temperatures below the polymer transition region. Also, the polymers can change their state, from a fluid to a solid, if the tool temperature is not sufficiently high, especially above the no flow temperature of the selected material. In addition, undesirable products like the burning of the polymer by compressed hot air in the cavity, called the Diesel effect, could occur due to high temperatures and injection rates (Kemmann and Weber, 2001).

To investigate the relationship between the process and the tool surface finish the following factors should be considered:

Melt Temperature (T_b). The selected T_b controls the melt temperature of the bulk material, prior to leaving the nozzle and entering the mould. An increase of T_b improves the polymer flow due to a reduction of material viscosity and shear stress. This is the case with most polymers; however, some could exhibit an increase of shear rate at a higher temperature. Selecting an appropriate temperature window is important due to its effects on the melt flow and the possibility of preventing the occurrence of material degradation. This process factor is even more important in micro-injection moulding because a relatively large volume of material is held in the machine barrel that leads to long residence time of the polymer melt (Frick et al., 2005).

Mould Temperature (T_m). The low volume of polymer required and the high surface-to-volume ratios that are typical in micro moulding mean that materials solidify much faster than in conventional moulding. By increasing the mould temperature the bulk temperature of the polymer should be kept sufficiently high to ensure the complete filling of the cavity. Previous studies in micro moulding have shown that moulds can be run continuously at temperatures even higher than the material's glass transition temperature (Hansen and Theilade, 2005). However, a balance between T_m and the transition temperature should be maintained at the injection stage in order to minimise the cycle time.

Injection Speed (V_i). The injection profile for filling a cavity has two main effects on the selected temperature of the polymer. A high V_i can facilitate the filling of micro cavities. This is because the premature freezing of polymers in thin walled sections could be alleviated by increasing injection rates. In particular, the material response is an increase

of the shear rates that leads to shear heating (Yao and Kim, 2004). This effect could decrease the material viscosity and hence help the filling process. At the same time it should be noted that such an increase of the shear rates could result also in polymer degradation and cavity gassing. Especially, the cavity gassing can have a negative effect on the tool. In extreme cases, the build up of heat pressure and volatiles could result in etching some material out of the mould (Cosma, 2001). A good balance between injection speed and shear rate can prevent the reduction of bulk temperature prior to cavity filling and prevent polymer and tool damage.

4.2.2 Polymer and tool interfacial interactions

There are several alternative methods of manufacturing cavities for micro-injection moulding. By applying each of these methods a different surface finish could be achieved. Thus, the surface finish specified at the design stage in respect to the parts and the tool cavities should take into account the manufacturing constraints introduced by these tool-making processes.

To investigate the flow of polymers in micro cavities it is important to understand interfacial interactions. (Navier, 1827) first suggested that the slip velocity at wall-fluid interfaces varies linearly with γ. The slip results from the interaction between the polymer flow and the tool surface, and also because of an entanglement of the outer layer and the bulk material. At the same time the entanglement depends on the attractions at the molecular level, γ and surface roughness.

Investigations into the flow behaviour of polymer melts and interfacial slips occurring at the tool surfaces have provided an insight into the effects of polymer molecule anchoring to solid surfaces (Leger et al., 1997) In particular, it was observed that the slip effect increases with an increase of the surface roughness. The flow of high molecular weight polymers within a contact environment, with a possible dependence of γ on the surface finish, could affect the bulk material flow and part quality in the velocity boundary area outside the bulk/wall interface (Leger, 2003). Thus, the surface finish, could result in friction levels that are beneficial for a given flow length, part design or material selection.

4.3 Experimental set-up

4.3.1 Tool design and manufacture

The design of the part used to analyse the interfacial interactions in micro-moulding is basically a series of runner sections through to a rectangular cavity as shown in Figure 4.1. The runner includes 4 unequal length sections totalling 40.8 mm. The length of the four sections is provided in Table 4.1. At the end of the runner system there is a rectangular section of 10 x 2.5 x 0.5 mm. All corners have a radius of 0.5 mm to reduce the shear effect. The runner system has a square cross section with dimensions 0.5 x 0.5 mm. Thus, the surface to volume ratio is about 30% higher in comparison to a circular cross-section. In addition, due to its square cross-section, the runner system could be easily manufactured using Wire Electro Discharge Machining (WEDM).

P20 Steel was used to produce the fixed and moving halves of the tool. The fixed half was fitted to the primary mould and the other half was fixed first to a secondary shim and then to the primary mould. Both halves were manufactured conventionally except for the cavity faces that were machined using WEDM. This was required in order to achieve an

identical surface finish on all four sides of the runner system and the part cavity. First, the fixed and moving halves of the tool inserts were machined to produce the front and back faces of the cavity as shown in Figure 4.2. Then, the shim was wire cut, see Figure 4.2b, to manufacture the side walls with the same surface finish. The 0.50 mm thickness shim was then fitted to the moving plate with screws and an epoxy adhesive, Loctite 9492 Hysol, that could maintain its mechanical properties up to 190 °C.

After the three separate parts of the tool, the two inserts and the shim, were machined they were cleaned in an ultrasonic bath of all debris from the EDM process and the remaining dielectric on the surfaces. This cleaning was essential in this research because any inclusions could affect the behaviour of the melt flow when in contact with the tool surfaces and also contaminate moulded parts with foreign bodies.

Applying the same manufacturing steps three tools were produced that differed only in their surface finish. This was achieved by machining the parts of each of them by employing different WEDM settings.

A profiling microscope, Micro-XAM, was used to measure the surface roughness of the wire cut parts. The surface roughness of the produced tools was Ra 0.07 μm, Ra 0.8 μm and Ra 1.5 μm respectively. Figure 4.3 shows measured profiles and Figure 4.4 shows the topography generated by scanning surface patches on these cavities.

Finally, the moving and fixed halves were assembled to a primary mould tool and then inspected for parallelism and shut off of the mating faces as shown in Figure 4.5.

Table 4.1 Test part design

Sections	1	2	3	4	5
Section length [mm]	5	14.5	7.3	14	15
Distance from the gate [mm]	5	19.5	26.8	40.8	55.8
Total Volume [mm^3]	55.80				
Total surface area [mm^2]	285.5				
Surface to Volume ratio	5.11				

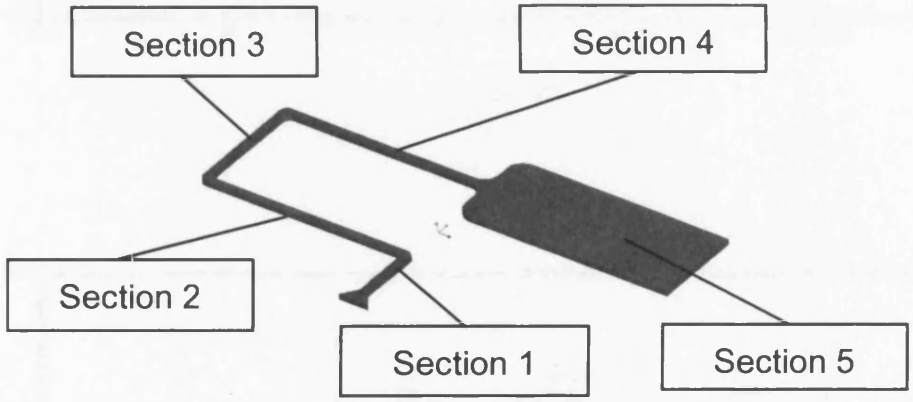

Figure 4.1 Test part

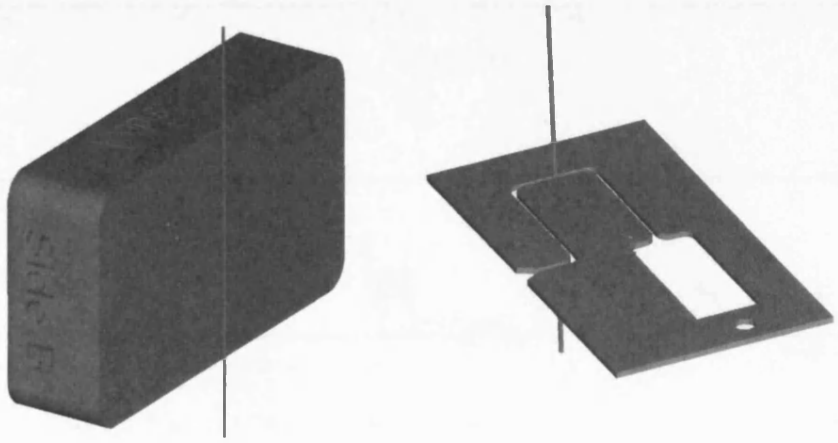

(a) (b)

Figure 4.2 The wire EDM machining of (a) the fixed and moving halves of the tool inserts and (b) the side walls of the shim.

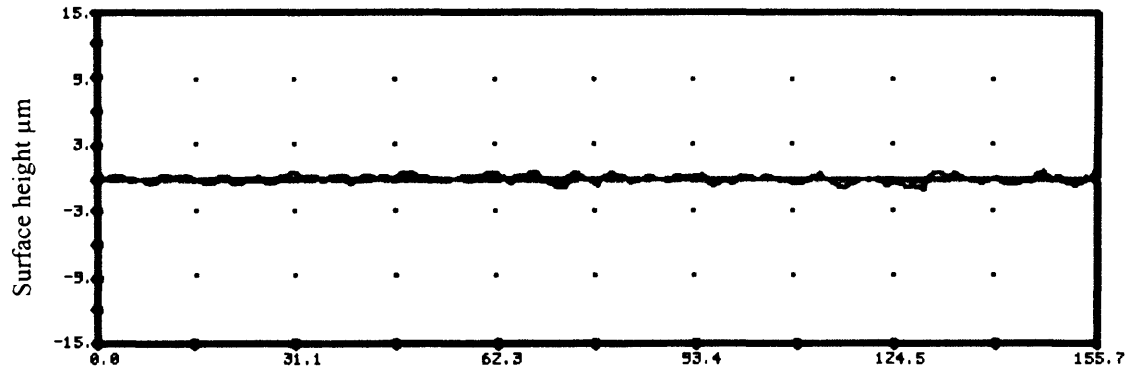

(a)

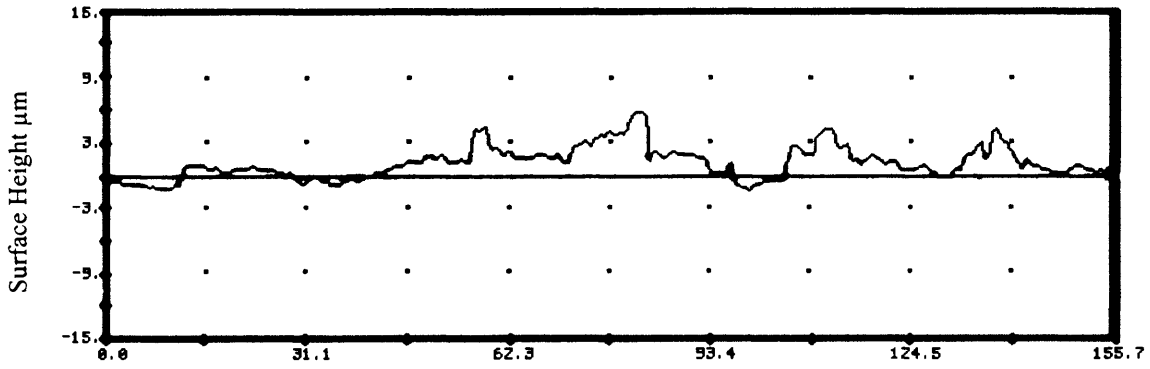

(b)

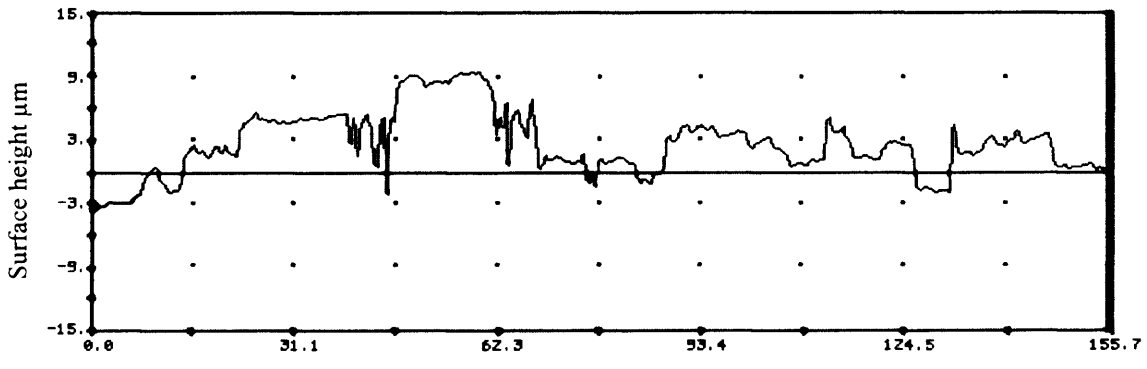

(c)

Figure 4.3 The surface roughness measurements of the three produced cavities (a) Ra 0.07 μm, (b) Ra 0.8 μm, and (c) Ra 1.5 μm

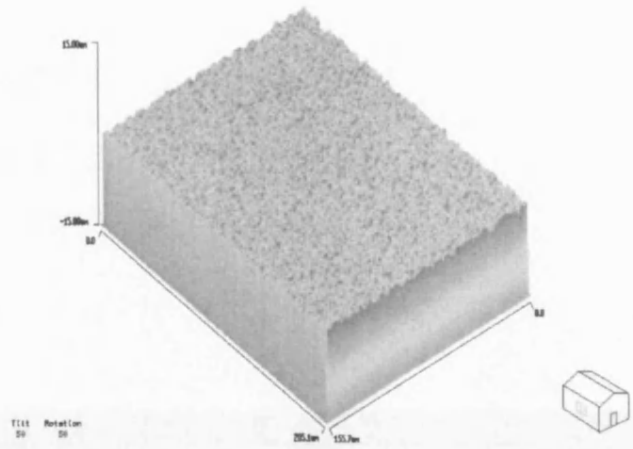

(a)

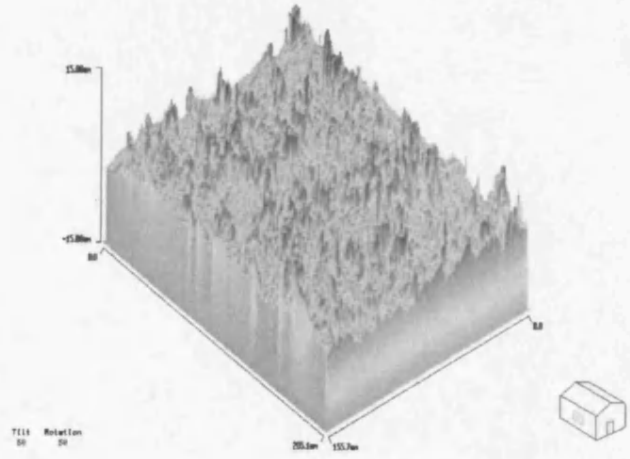

(b)

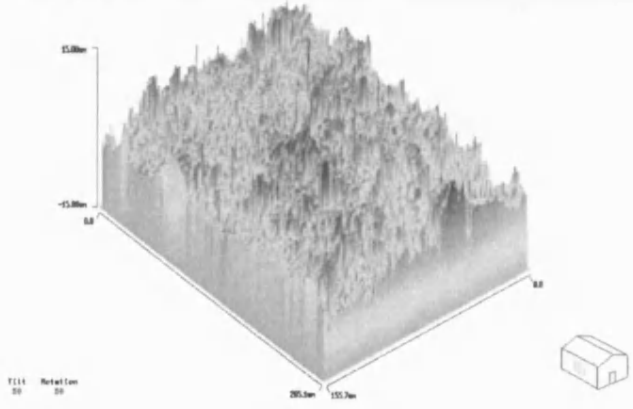

(c)

Figure 4.4 The surface roughness topography of the three produced cavities (a) Ra 0.07 μm, (b) Ra 0.8 μm, and (c) Ra 1.5 μm

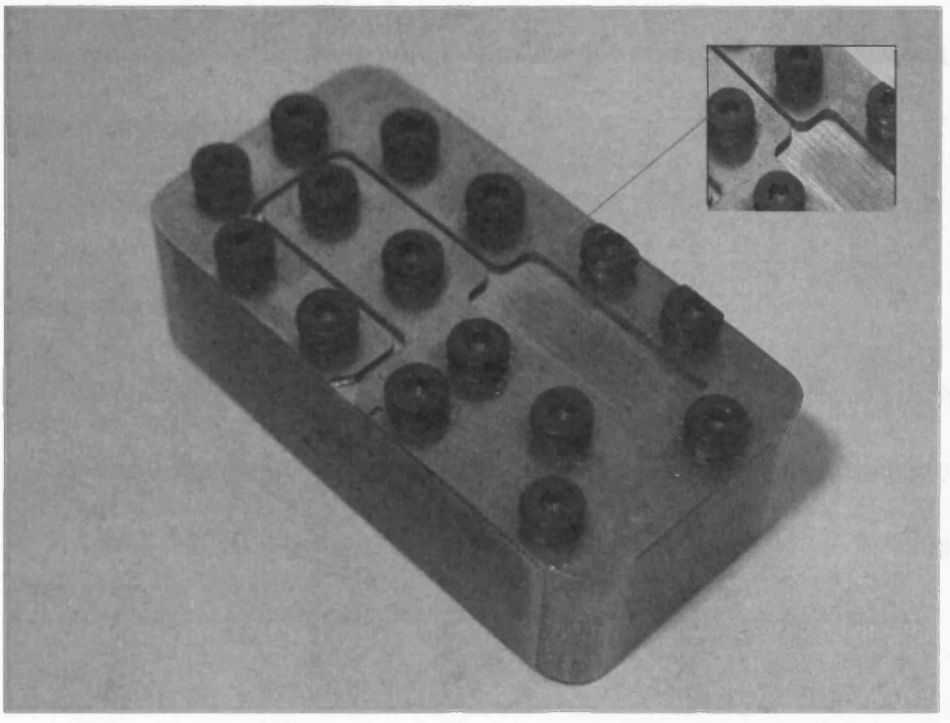

Figure 4.5 Tool assembly

4.3.2 Test materials

Three commonly used materials in injection moulding, Polypropylene (PP) Acrylonitrile Butadiene Styrene (ABS) and Polycarbonate (PC), were selected to conduct the planned experiments. Their properties are provided in Table 3.4. Each material has a different η and molecular weight (M_w) which is important for this study. The polymers went through desiccant drying and dehumidifying cycles before the trials to remove any surface or absorbed moisture. The machine used to perform the micro injection moulding tests was a Battenfeld Microsystem 50.

4.3.3 Design of experiments

The interfacial interactions affect the filling performance of micro cavities and therefore this experimental investigation was focused on the filling stage of the moulding process. Thus, in the tests carried out the process parameters affecting holding, cooling and ejection stages were set to their default values for the selected three materials.

The filling performance of micro moulds relies heavily on V_i and the temperature control during the injection, and is much less dependent on the holding pressure (Sha et al., 2007b). Therefore, the effects of T_b, T_m and V_i on the filling behaviour of cavities with different surface roughness were investigated in this study.

The Taguchi L9 orthogonal array was used to plan the experiments for each of the three materials. The selected three levels of V_i and tool surface finish were the same for all materials, while T_b and T_m levels were different for the PP, ABS and PC arrays. For each

trial 10 mouldings were measured. The three material arrays are given in Tables 4.2, 4.3 and 4.4.

The melt temperature was controlled indirectly through T_b. Each polymer has a recommended processing window. In this research the selected three levels of T_b are maximum, minimum and medium temperatures in the range for each of the polymers.

In micro moulding polymer solidification time is much shorter than that in conventional moulding and therefore the processing requires heated tools. The setting for T_m used in this research are the minimum, medium and maximum temperatures in the range for each material. By increasing T_m the bulk temperature of the polymer is kept sufficiently high to facilitate the melt flow during the filling stage. However, the effect of the T_m increase on cooling and cycle times is not analysed in this research.

The V_i has two main effects. It can help polymers to fill the cavities before the melt flow solidifies and also it can increase the shear rate of the polymer which results in shear heating. The three levels of V_i used in this research are given in Table 4.5. They were chosen taking into account the capabilities of Battenfeld Microsystem 50, especially its maximum injection speed of 946.4 mm/s over a stroke distance of 84 mm. However, it is worth noting that the high settings of V_i could lead to material degradation.

Table 4.2 L9 fractional orthogonal array for PP

Trial	Surface finish [Ra]	Melt temp T_b [°C]	Mould temp T_m [°C]	Injection speed V_i [mm/s]
1	0.07	220	20	200
2		250	40	500
3		270	60	800
4	0.8	220	40	800
5		250	60	200
6		270	20	500
7	1.5	220	60	500
8		250	20	800
9		270	40	200

Table 4.3 L9 fractional orthogonal array for ABS

Trial	Surface finish [Ra]	Melt temp T_b [°C]	Mould temp T_m [°C]	Injection speed V_i [mm/s]
1	0.07	220	40	200
2		250	60	500
3		280	80	800
4	0.8	220	60	800
5		250	80	200
6		280	40	500
7	1.5	220	80	500
8		250	40	800
9		280	60	200

Table 4.4 L9 fractional orthogonal array for PC

Trial	Surface finish [Ra]	Melt temp T_b [°C]	Mould temp T_m [°C]	Injection speed V_i [mm/s]
1	0.07	280	80	200
2		300	100	500
3		320	120	800
4	0.8	280	100	800
5		300	120	200
6		320	80	500
7	1.5	280	120	500
8		300	80	800
9		320	100	200

Table 4.5 Injection speed settings

Injection speed (V_i): 200 mm/s	Injection Volume: 55.80 mm^3 @ 0.42 s
Injection speed (V_i) 500 mm/s	Injection Volume: 55.80 mm^3 @ 0.16 s
Injection speed (V_i) 800 mm/s	Injection Volume: 55.80 mm^3 @ 0.10 s

4.4 Analysis of the results

The effects of interfacial interactions on the flow length and the resulting part quality are analysed separately.

4.4.1 Flow length

Table 4.6 presents the flow length results obtained from all 27 trials. 10 parts were measured for each combination and then the mean value was calculated (Appendix D). The combination of parameters in trial 3 of the L9 orthogonal array provided the best conditions for achieving a maximum flow length for all three materials. It should be noted that this was expected from the process point of view because all controlled parameters were set at their highest values.

The results of other trials were not conclusive in regards to the minimum flow length achieved during the experiments. Unfortunately, from the carried out tests for all three materials it was not possible to single out one process parameter as the main cause for the resulting low flow length.

PP had the highest average flow length of 51.90 mm for all 9 tests. Test 1 resulted in the lowest flow length. The variation of the length for all PP tests was 7.53 mm. This material filled the first four sections of the tool and only partially the fifth at all settings. In test 3 as it was already mentioned the highest flow length was achieved. When T_b was at its high settings the best filling results were observed, in particular tests 3, 6, and 9. At the same time the lowest filling results, tests 1, 4 and 7 were attained when T_b was at its lowest setting. Thus, it could be concluded that T_b had the greatest effect on part filling.

ABS had the second highest average flow length of 36.04 mm for all three materials. The process conditions in test 6 resulted in the lowest flow length. The difference between maximum and minimum flow lengths for all ABS tests was 15.68 mm. In all experiments the first three sections of the test tool were filled and just partially the fourth except test 3. Only in this test the melt flow reached section 5. It was not possible to identify a single factor affecting the flow filling length.

PC had the lowest average flow length of 26.34 mm for all three materials. Test 4 resulted in the lowest flow length. The difference between maximum and minimum flow lengths for all PC tests was 22.14 mm. Section 1 of the test tool was filled completely in all experiments. Only in tests 2 and 3, section 4 was filled partially. Again as it was the case with PP, T_b was the factor with the highest influence on the achieved flow length.

The experiments showed that PP was less susceptible to variations of the flow length as a result of changing process conditions. In the case of PC and ABS, the flow behaviour was much more sensitive to changes of the process parameters and tool surface quality. However, any explicit relationship between the flow length and tool surface roughness was not observed.

A dependence between the molecular weight of PP, ABS and PC, and the resulting flow length was observed. In particular, the highest flow length was achieved with PP, the materials with the highest molecular weight and visa versa the lowest for the polymer with the lowest molecular weight, PC.

Table 4.6 Flow length results

Trial	Levels				Mean value of the flow length [mm]		
	Ra	T_b	T_m	V_i	PP	ABS	PC
1	1	1	1	1	47.2	32.6	22.8
2	1	2	2	2	52.0	42.4	39.0
3	1	3	3	3	54.7	45.0	39.3
4	2	1	2	3	48.9	39.8	17.2
5	2	2	3	1	52.8	32.5	22.3
6	2	3	1	2	54.6	29.3	26.2
7	3	1	3	2	49.7	32.8	21.7
8	3	2	1	3	52.7	36.4	25.6
9	3	3	2	1	54.1	33.1	22.7

4.4.2 Optimum parameter levels

In this research the Minitab 14 analysis software was used to carry out the statistical analysis of the experimental results. Significant effects are analysed depending on the average flow length results achievable for each combination of control parameters. The average flow length based on the conducted trials for each combination of control parameters in the three L9 OAs was calculated in order to determine the optimum parameter levels for the investigated flow length and polymers employing the Taguchi parameter design method (Roy et al. 1990). The value of a given parameter is considered to be optimum, the best of the selected three levels, if its corresponding average flow length is the highest. By applying this method, it is possible to identify theoretically the best set of micro injection moulding parameters within the investigated processing window with respect to flow length. The analysis of the surface finish and flow length main effects plots (Figures 4.6-4.9) provided optimum levels for each of the factors and the theoretical best values at the optimum levels. Table 4.7 shows the results obtained for the three sets of experiments conducted in this study.

From this analysis, it is immediately apparent that there is not a unique selection of parameter levels that can be considered optimum for all three materials. However, by carrying out a systematic study for each material it is possible to identify optimum levels that lead to an increase in flow length compared to the maximum average measured. In particular, the results show that for all three materials the high temperature settings of T_b and T_m result in an increase in the overall flow length.

4.4.3 Process factor contribution to flow length

Based on the experimental results, an analysis of variance (ANOVA) was performed in order to assess the contribution of each processing parameter to the resulting flow length. From the results for the investigated materials (Table 4.8) it is apparent that there is not a unique factor that can be considered the most important for all three materials. By conducting a further ANOVA analysis of all the materials together it can be seen that for PP, ABS and PC the surface finish (Ra) and T_b are the most important factors affecting flow length. In particular, an increase in the surface quality and an increase in T_b result in an oval increase in the polymer flow length.

Table 4.7 Taguchi analysis response table for the theoretical best set of processing parameters for flow length

Factors	Ra	T_b	T_m	V_i
Material	**PP**			
Optimum levels (OL)	**3**	**3**	**3**	**2**
Predicted values at OL	55.5 (+ 1.46 %)			
Material	**ABS**			
Optimum levels (OL)	**1**	**2**	**3**	**3**
Predicted value at OL	46.3(+ 2.88 %)			
Material	**PC**			
Optimum levels (OL)	**1**	**3**	**3**	**2**
Predicted value at OL	40.9 (+ 4.07 %)			

Table 4.8 Taguchi analysis response table for the most important factors affecting flow length

Factors	Ra	T_b	T_m	V_i
Material	**PP**			
Delta [mm]	0.87	5.87	0.90	0.73
Rank Importance	**3**	**1**	**2**	**4**
Material	**ABS**			
Delta [mm]	6.13	2.03	5.67	7.67
Rank Importance	**2**	**4**	**3**	**1**
Material	**PC**			
Delta [mm]	11.80	8.83	2.90	6.37
Rank Importance	1	2	**4**	**3**
Material	**PP, ABS, PC**			
Delta [mm]	5.71	5.14	2.60	4.39
Rank Importance	1	2	**4**	**3**

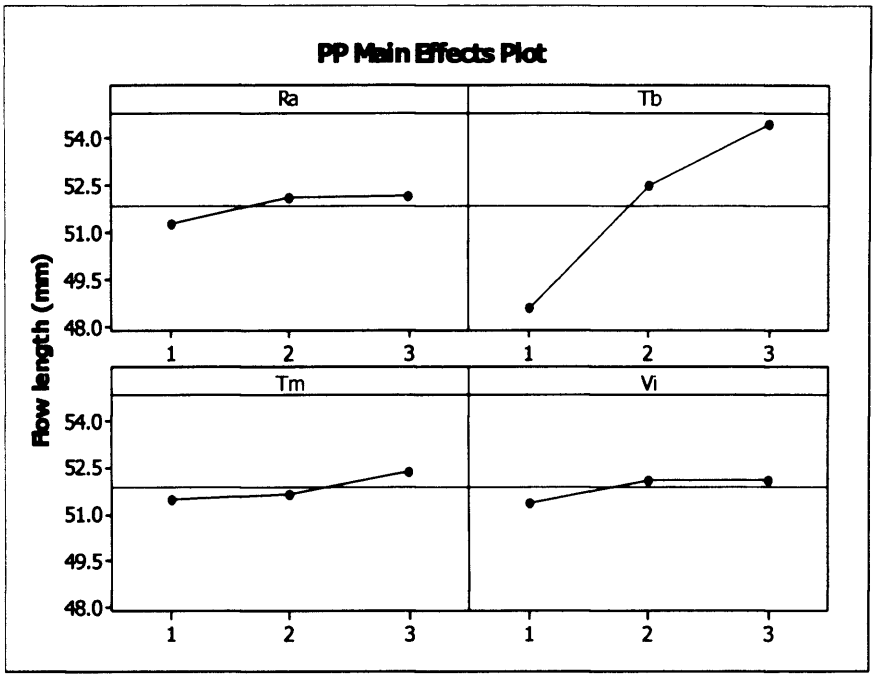

Figure 4.6 Flow length main effects plot for PP

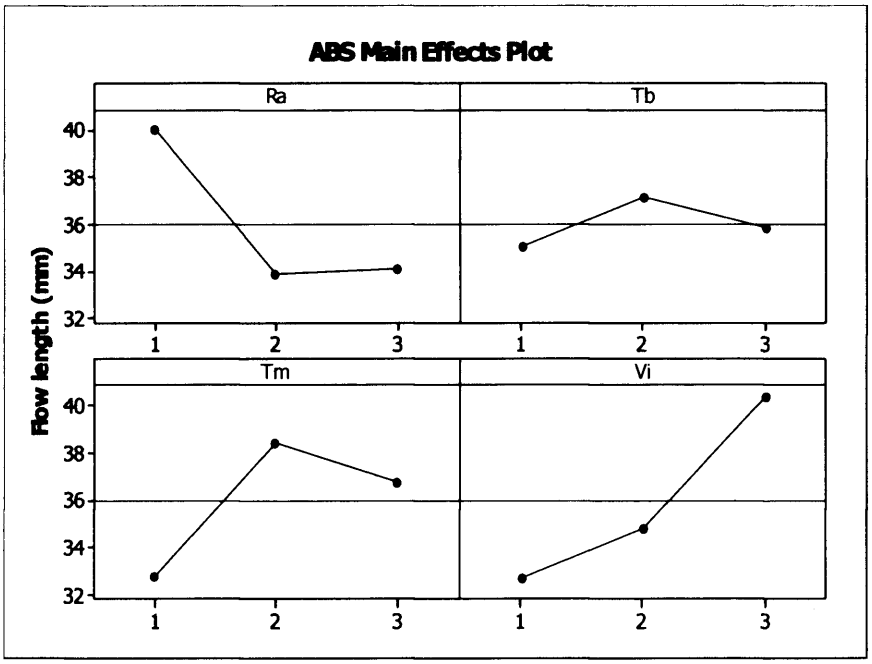

Figure 4.7 Flow length main effects plot for ABS

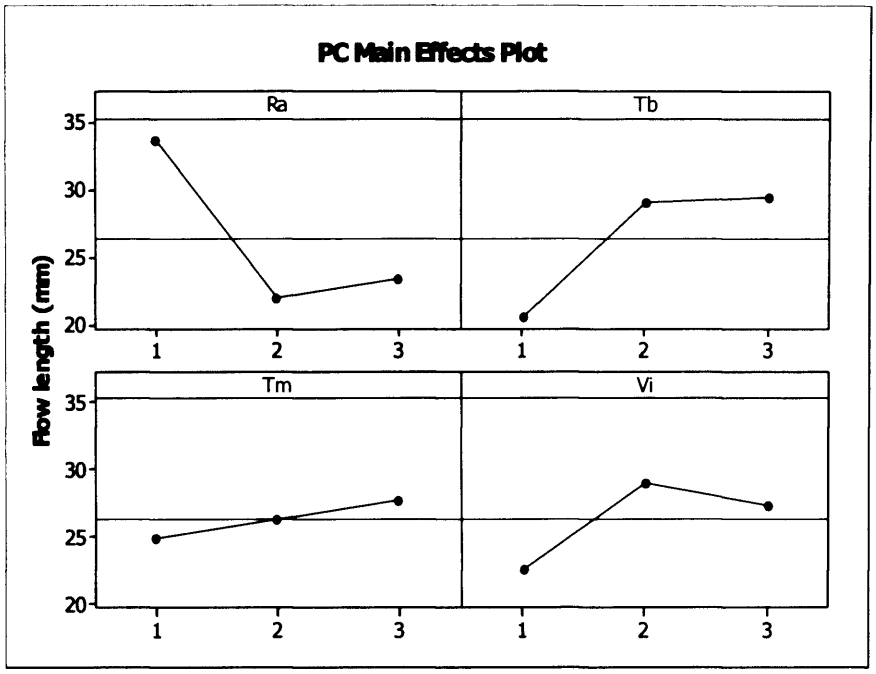

Figure 4.8 Flow length main effects plot for PC

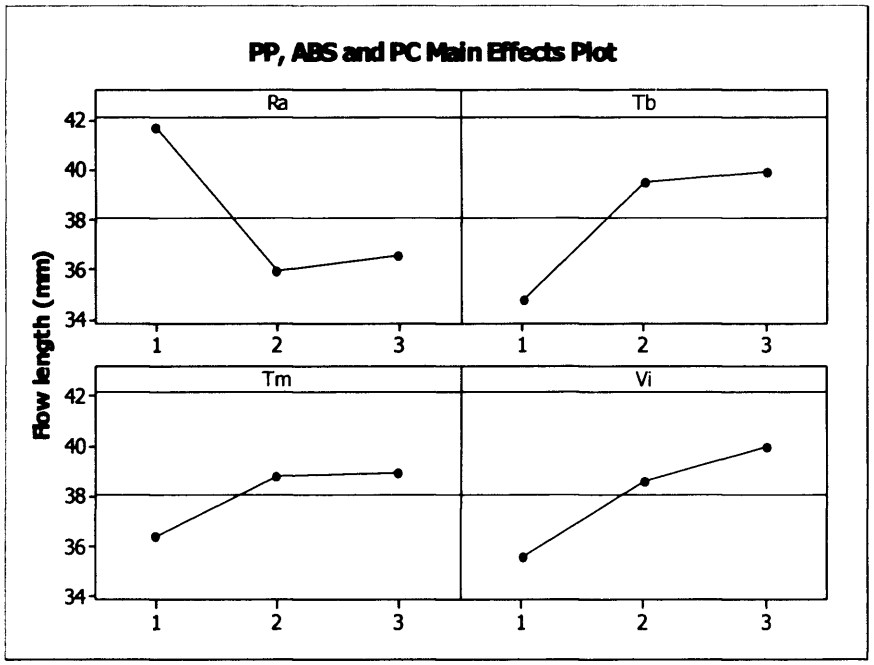

Figure 4.9 Flow length main effects plot for PP, ABS and PC

4.4.5 Part quality

Figures 4.10, 4.11 and 4.12 present pictures depicting the quality of the moulded test parts. The images were taken using an optical measuring system. Significant variations of the melt flow behaviour under the different trial settings were observed for the three investigated materials. The pictures provide a visual representation of flow directions, the existence of turbulence in the polymer flow, the presence of material phases within the part, and melt fracture.

For PP, test 1 shows a rounded flow front that should be expected for a laminar flow into a symmetric channel. All experiments with low parameter settings illustrate this effect. In addition, all tests show evidences of jetting and fountain effects when the melt flow enters section 5 of the test tool. It can be seen that the flow turbulence increases with the increase of the distance from the exit point, while the flow path show signs of randomness at the high settings. Another effect that can be detected on the pictures is that the mixing of the polymer and the master batch colour die is better for the samples produced in the two cavities with a lower surface finish. This could be considered as evidence of higher turbulence compared to the polymer flow in cavities with a higher surface finish. The importance of interfacial interactions is also evident from the trials with the highest settings of the process parameters in the cavity with the best surface finish. In particular, test 3 in Figure 4.10c shows an uneven melt front with evidence of melt fracture and gas traps. At the same time, this effect is less noticeable in the trials carried out in the other two cavities that have a lower surface finish.

The trials with ABS and PC show variations of the rounded melt front that are typical for a non Newtonian flow. The pictures of the PC samples, for example test 1 in Figure

4.12a, also depict the existence of rounded edges along the cavity walls. This is an indication of solidification of the melt flow without proper packing.

Some of the ABS and PC experiments show visual lines on the parts that are perpendicular and equally spaced to the melt flow, in particular the results from test 4 for these two materials in Figures 4.11d and 4.12d. This is an illustration of the slip stick effect during the filling stage. For both materials this occurs at low T_b and high V_i that lead to high shear stress. However, no explicit relationship between the occurrence of the slip stick effect and the tool surface finish was observed.

All materials at high T_b showed signs of degradation with some evidence of a melt fracture.

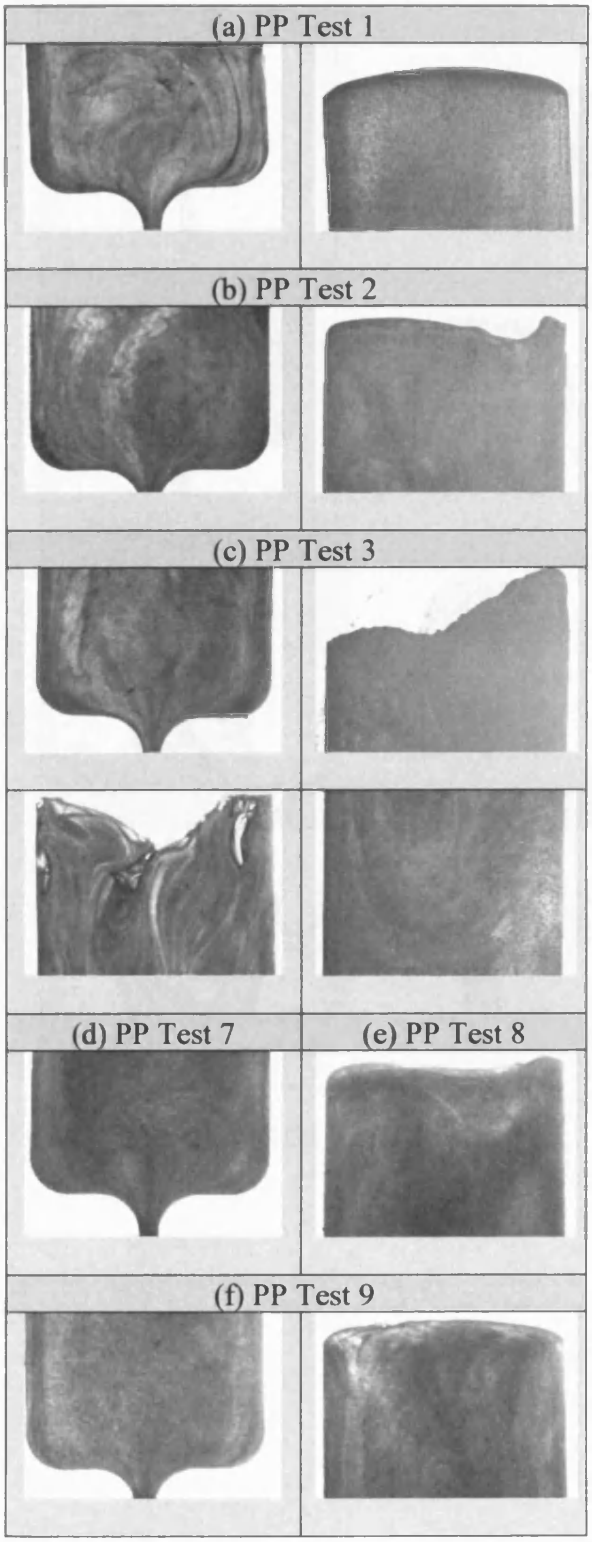

Figure 4.10 PP experiments

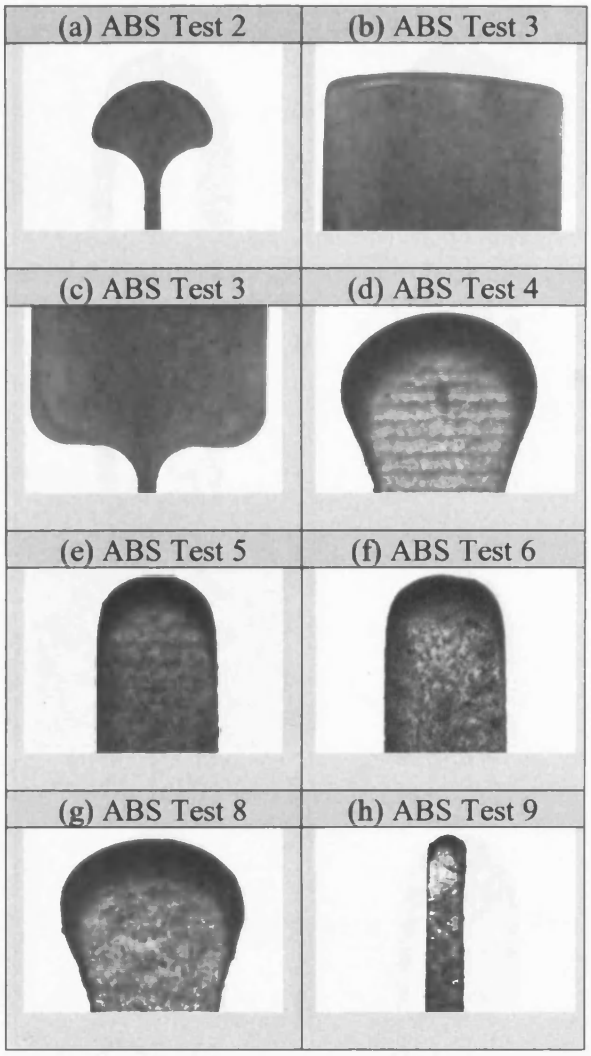

Figure 4.11 ABS experiments

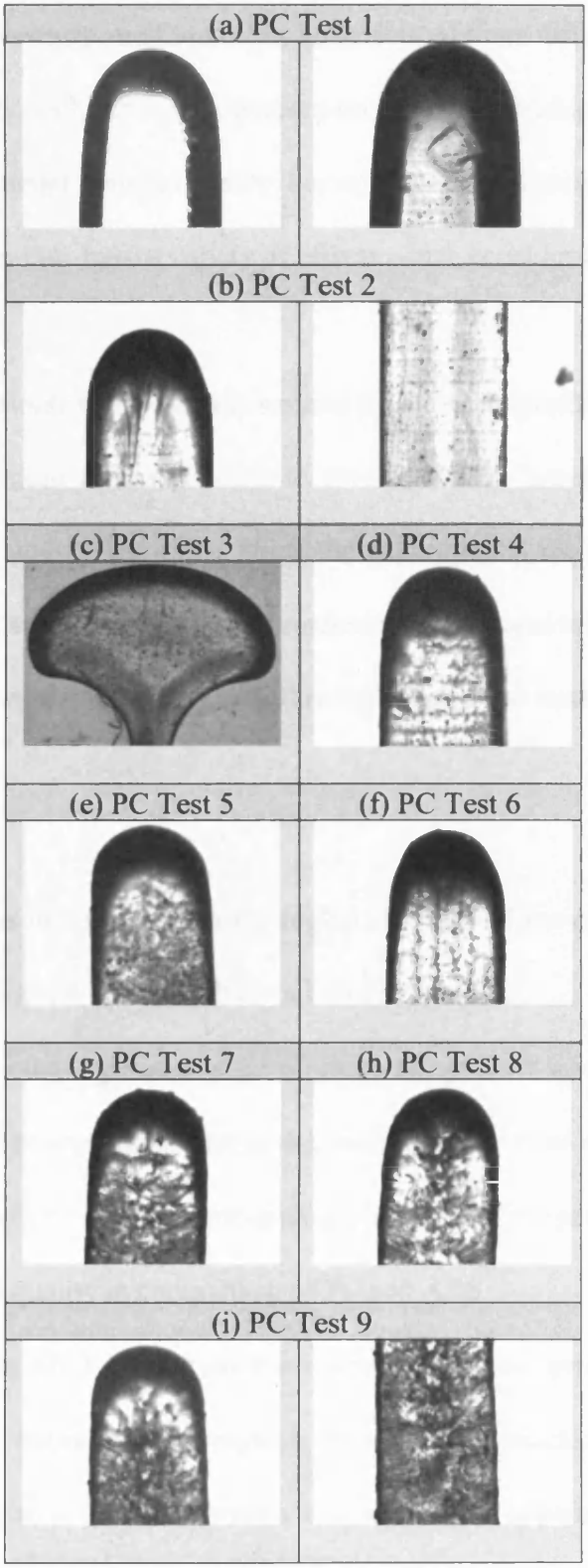

Figure 4.12 PC experiments

4.5 Summary and conclusions

Chapter 4 reports an investigation of melt flow behaviour of three different polymers at entry to the mould cavity, with particular interest paid to the relationship between the tool surface finish and flow length and part quality. For micro-injection moulding the surface finish of runners and cavities have a variety of effects worth considering.

By manufacturing three tools with a varying surface finish and subjecting each of them to different process conditions it was possible to investigate the interfacial interaction between the melt flow and cavity walls. Then, the experimental results were used to analyse the relationship and the impact of tool surface roughness and injection moulding conditions on the process performance. The following conclusions can be made based on the reported research:

- The experiments performed with the highest settings of the controlled factors resulted in the highest flow length for all three materials.
- From the conducted experiments for all three materials it was not possible to identify a single process parameter as the cause of a low flow length.
- The flow length of PP was less susceptible to changes of the process parameters and tool surface quality in comparison to PC and ABS.
- By conducting an ANOVA analysis it was possible to assess process parameters' contribution to optimum performance. From the conducted analysis, it is immediately apparent that there is not a unique selection of parameter levels that can be considered optimum for all three materials. However the results show that for all three materials the high temperature settings of T_b and T_m result in an

increase in the overall flow length. Additionally, it was shown that Ra and T_b are the most important factors that contribute to flow length. Especially, an increase in the surface quality and an increase in T_b result in an oval increase in the polymer flow length.

- There is a relationship between the tool surface finish and the level of turbulence in the melt flow. The trails for all three materials in the cavity with the highest surface finish indicate the existence of two distinctive phases in the polymer flow, while the patterns are mixed and not so clear for the other two.
- No explicit relationship between the occurrence of the slip stick effect and the tool surface finish was identified. On some of the ABS and PC samples, there are visual lines on the parts that are the result of the slip stick effect during the filling stage. For both materials this occurs at low T_b and high V_i that lead to high shear stress.

CHAPTER 5

THE FINITE ELEMENT ANALYSIS OF MELT FLOW BEHAVIOUR IN MICRO INJECTION MOULDING

5.1 Motivation

Micro injection moulding of polymer materials is one of the key technologies for micro manufacturing, and currently the successful replication of component micro-features requires an in-depth understanding of the process factors. One tool that can be used to identify potential problems and thus determine the reliability of this micro manufacturing route for serial production is that of process modelling and simulation employing Finite Element Analysis (FEA). Such simulation models can be used to assess the factors that affect the quality of injection moulded parts, e.g. shear rates and temperatures in micro cavities, that are not always easy to monitor and predict, and at the same time have a major impact on the process replication capabilities.

Although these models have been used to investigate the filling behaviour of polymers in micro channels, the results reported show significant discrepancies between the simulated process conditions and those achieved in experimental trials (McFarland and Colton, 2004). In this context, the motivation for this research is to analyse the simulation results obtained using specially developed FEA models for micro injection moulding against the experimental findings presented in Chapter 4. In this way, it will be possible to get a better insight into the melt flow behaviour in micro cavities by comparing physical field data with

the simulation results attained at identical processing conditions.

The chapter is structured in five sections. In Section 5.2 a FEA model for simulating the polymer filling behaviour in micro cavities is presented that is followed by the description of a design of experiment method employed to validate the model. In Section 5.4, the effects of a range of process variables on the melt flow behaviour are analysed by carrying out a serious of simulation runs, and the obtained results compared with the experimental findings reported in Chapter 4. Finally, conclusions are made about the accuracy and sensitivity of the proposed simulation model, and process conditions in micro cavities.

5.2 Finite element analysis of the melt flow

In this chapter the FEA model used to simulate a polymer flow in micro cavities is described. FEA models are widely used for simulating the melt fill at macro and more recently at micro scales (Su, 2004, Shen et al., 2004, Yuan et al., 2003). In particular, in this research a Finite Element Method (FEM) was employed to create a model for simulating the polymer filling behaviour in micro cavities and also to conduct a thermal analysis. By applying a Finite Difference Method (FDM) the initial mesh was generated for the geometrical model of the test part. Each element was examined using a mesh statistic tool in order to verify its accuracy within the model domain. Then, the accuracy of the imported geometric model was adjusted through node and element modifications to achieve a good reproduction of the model surface boundaries.

The CAD model of the part once imported and meshed by applying such a hybrid FEM-FDM approach, as shown in Figure 5.1, is used for dual domain analysis of laminar flow in generalised Newtonian fluids utilising the Hele-Shaw flow model. The material flow front

begins from the injection node and is then calculated throughout the model using a three node triangular mesh as illustrated in Figure 5.2. Particularly, the flow front propagates by repeatedly filling and adding further nodes. In addition, a tetrahedral element mesh was applied to the model in order to perform a complementary 3D analysis based on the Navier stokes flow model. Again, as it was the case with the orthogonal mesh, each element of the tetrahedral mesh was evaluated to verify its accuracy against the imported geometric model. Also, adjustments through node and element modifications were made to ensure an accurate reproduction.

Figure 5.1 The CAD model meshed employing the hybrid FEM-FDM approach

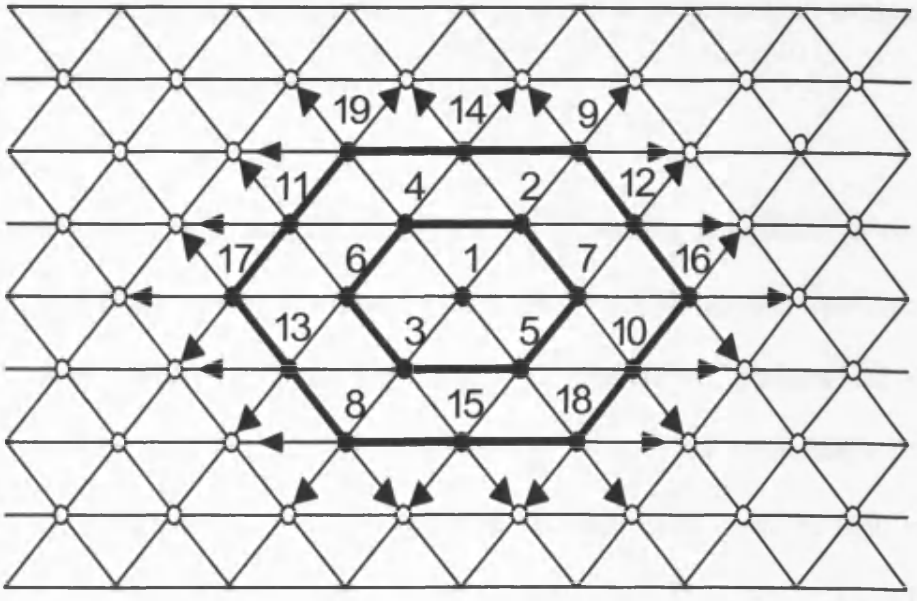

Figure 5.2 A three node triangular mesh

The filling phase of the melt flow simulation is non specific to micro injection moulding. Especially, it takes the continuity, momentum and energy equations and reduces them to perform a dimensional analysis specific to non-Newtonian fluids. The equations governing the flow of polymer melt have to be solved with the simplest of geometries, and thus by applying the finite element approach and breaking up part designs, the part complexity is reduced. The element equations are derived and assembled together with the boundary conditions, and then the solution equations are performed for each element. With each element subject to the same algebraic equation, only the values of variables change between the elements. With an appropriate mesh a numerical solution from the mathematical models is found automatically employing a simulation software.

To simulate the polymer flow behaviour the modified Cross WLF model (see equations 4 and 5) is applied. By implementing this viscosity model together with the orthogonal FDM modified dual domain and 3D meshes, it was possible to carry out both temperature and pressure related simulation analyses.

For the simulation study the melt temperature was considered uniform on entry to the mould, and the filling process involved a fountain flow with the polymer freezing on contact with the cavity walls. The model dependency on temperature, pressure and shear rate required injection time (t_i), melt temperature (T_b), and mould temperature (T_m) to be specified for each simulation run. In addition, to take into account the high surface to volume ratio in micro injection moulding, a size factor was introduced. This size factor is a global thickness multiplier (GTM) that allows any increase or decrease of the component dimensions to be taken into account when analysing the flow behaviour. Though, it should be stated that the proposed model does not allow some phenomena, e.g. surface finish or the

melt slip, to be simulated. The model created in this way was used to investigate flow length and possible flow instabilities that can lead to surface defects.

5.3 Model validation

To validate the proposed method for simulating the melt flow behaviour at micro scale the test part utilised in the experimental study reported in Chapter 4 was used to create a FEA model. The test part is shown in Figure 4.1 and the fully meshed part can be seen in Appendix D. It consists of four runners with unequal length that lead to a rectangular section. The dimensions of these five sections are given in Table 4.1. All corners have a radius of 0.5 mm. The runner system has a square cross section with dimensions 0.5 x 0.5 mm and a surface to volume ratio about 30% higher than that of a circular cross-section.

The following steps describe the procedure that should be followed to generate a Dual Domain surface mesh from a CAD model of a part (Appendix E) that is necessary to carry out FEA.

1. The part CAD model is saved into one of the file formats that are supported in the design link environment. In our case the Pro Engineer file format was selected.
2. The Pro Engineer file os translated into a Moldflow file. This is done automatically employing the Translator Wizard.
3. A mesh tool is selected to translate the Moldflow file into a matched mesh.
4. The mesh is validated using the Mesh Diagnostics function of the Moldflow software. Any issues with the mesh will be identified, e.g. overlapping elements, high aspect ratios, connectivity regions, and non-manifold edges. If problems are reported, proceed to the next step. If no serious issues are identifed, steps 5, 6 and

7 are omitted.

5. The Edit Mesh function is employed to activate mesh editing capabilities within the software and thus to correct problems such as more than one connectivity region.
6. The mesh for identified problems is reviewed and an attempt is made to fix them.
7. Once the Fix Mesh routine is completed, the Mesh Diagnostics is run again to verify whether the problems were fixed. If so, the open issues are resolved. In case additional mesh "cleanup" is required, it necessary to repeat steps 4 and 5.
8. A gate location is selected, a material is choosen, and the selected analysis is executed.
9. The results are viewed.

5.3.1. Planning of simulation experiments

The filling performance of micro moulds is highly dependent on temperature control and injection speed (V_i). To simulate their effects three commonly used materials in injection moulding, Polypropylene (PP) and Acrylonitrile Butadiene Styrene (ABS) and Polycarbonate (PC) were selected. It is important to stress that for ease of comparison these were the same three materials as those utilised in the experimental research reported in Chapter 4. However, the initial simulation runs with PC showed that it was not possible to fill completely the test cavity with all process settings, and therefore this material was excluded from the study. The material properties of the other two materials, PP and ABS, are provided in Table 3.4.

In this simulation study the effects of T_b, T_m and V_i on the filling behaviour of the test part were investigated using Taguchi Design of Experiments. In particular, maximum, minimum

and medium values of these process parameters within their recommended processing windows were utilised in the carried out simulation runs for the selected two materials. The values of T_b and T_m were identical to those used in Chapter 4. However, regarding V_i it was not possible to utilised the same values in the simulation runs, and therefore they were replaced with an injection time control parameter (t_i), in particular 0.1, 0.3 and 0.5 [s]. Also, as it was already mentioned, to take into account the high surface to volume ratio of micro parts the GTM factor was introduced. Through it an increase and decrease in the overall thickness of the parts can be modelled and thus to account for some of the scale effects in micro injection moulding. In our case, the GTM variation factor was set at 5% to make the FEA model more sensitive to nominal increases or decreases of part thickness with 25 μm. The combinations of parameters values of the considered four factors in this simulation study are provided in Table 5.1.

Table 5.1 Design of experiments factors and levels

Inputs	PP	ABS
DOE Analysis type	Taguchi then Factorial	Taguchi then Factorial
Number of factors	4	4
Injection time t_i (s)	0.10	
	0.30	
	0.50	
δV_i (%)	66.60	
Melt temperature T_b (°C)	220	
	250	
	280	
δT_b(°C)	30	
Mould temperature T_m (°C)	20	40
	40	60
	60	80
δT_m(°C)	20	
Global thickness multiplier (μm)	475	
	500	
	525	
δ GTM (%)	5	

5.3.2. Moldflow Design of Experiments

To assess the effects of T_b, T_m, t_i and GTM on the melt flow behaviour, the Moldflow software tools for conducting Design of Experiment (DoE) and factorial analysis were applied. In particular, a three-level four-factor randomised full factorial design would have required $3^4 = 81$ runs. To reduce the number of runs a Taguchi L8 screening process was used to identify the important combinations of control factors that affect part quality.

After the screening a factorial analysis was used, to investigate the interactions between the selected parameters. In particular, Faced Central Composite designs (FCC) were employed to analyse the interaction between four factors considered in the screening process. The FCC designs have the star points on the faces of the cube, and faced designs have three levels per factor (Del Vecchio, 1997). A total of 25 simulation runs (Table 5.2) were then performed to obtain results close to those of the full factorial design 81 runs.

Finally, the simulation results were analysed applying the Response Surface Methodology (RSM) (Antony, 2000). RSM creates mathematical models representing the interrelation between one or more responses of the set input parameters. Through the FCC designs multi-dimensional patterns of responses are compared by varying the levels of the selected control parameters (Figure 5.3). The results are an evaluation of the main effects of the control factors presented as criteria weightings and RSM graphs of the three most influential factors.

Table 5.2 Face centred cubic design for PP and ABS.

Trials	Factors							
	T_b (°C)		T_m (°C)		t_i (s)		GTM (μm)	
	PP	ABS	PP	ABS	PP	ABS	PP	ABS
1	220		20	40	0.10		475	
2	280		20	40	0.10		475	
3	220		60	80	0.10		475	
4	280		60	80	0.10		475	
5	220		20	40	0.50		475	
6	280		20	40	0.50		475	
7	220		60	80	0.50		475	
8	280		60	80	0.50		475	
9	220		20	40	0.10		525	
10	280		20	40	0.10		525	
11	220		60	80	0.10		525	
12	280		60	80	0.10		525	
13	220		20	40	0.50		525	
14	280		20	40	0.50		525	
15	220		60	80	0.50		525	
16	280		60	80	0.50		525	
17	220		40	60	0.30		500	
18	280		40	60	0.30		500	
19	250		20	40	0.30		500	
20	250		60	80	0.30		500	
21	250		40	60	0.10		500	
22	250		40	60	0.50		500	
23	250		40	60	0.30		500	
24	250		40	60	0.30		475	
25	250		40	60	0.30		525	

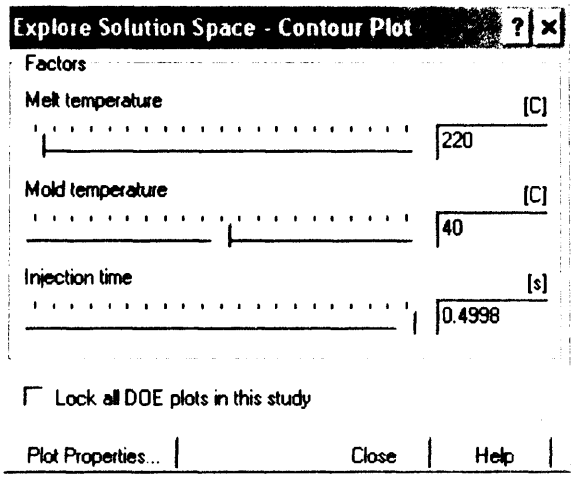

Figure 5.3 Response Surface Methodology for PP

5.3.3 Simulation of flow length

The dual domain model developed in this chapter was used to analyse the factors affecting the polymer flow length. Other researchers who have carried out 3D simulation studies employing the Navier Stokes flow model reported flow patterns that were comparable with short shots from moulding trials (Mehta and Barry, 2003). Therefore, to perform a similar study in this chapter, both the orthogonal element and tetrahedral element mesh models were used to carry out a dual domain and 3D analyses, respectively.

The simulation melt front was traced by plotting the result of the filling time against the filled volume. Also, the position and condition of the melt front was monitored visually at any specific node employing the animation viewer together with the cutting plane editor and the query result functions within Moldflow.

The actual settings that led to maximum and minimum flow length in the moulding trials in Chapter 4 are provided in Table 5.3 together with their closest ones used in this simulation study. In particular, S1 and S3 correspond to the PP and ABS minimum flow length settings respectively while S2 and S4 to the maximum flow length achieved for both PP and ABS. To judge about the sensitivity and accuracy of the proposed simulation model these results are compared with the findings reported in Chapter 4.

Table 5.3 Simulation factor settings resulting in maximum and minimum flow

	Flow Length Simulation	Actual settings				Simulation Settings			
		SF [Ra]	T_b [°C]	T_m [°C]	V_i [mm/s]	GTM [μm]	T_b [°C]	T_m [°C]	t_i [s]
S1	PP Min	0.07	220	20	200	475	220	20	0.5
S2	PP Max	0.07	270	60	800	475	270	60	0.1
S3	ABS Min	0.8	280	40	500	500	280	40	0.3
S4	ABS Max	0.07	280	80	800	475	280	80	0.1

5.4 Simulation results

5.4.1 Analysis of the DOE results

The DOE analysis uses the dual domain simulation model. The results are presented in two formats. First, in a tabular form that lists the factors in order of their rank weightings (Table 5.4). Then, in graphs (Figures 5.4 to 5.7) showing the interactions between the factors that affect shear stress (τ) and flow front temperature (T_{ff}) during the injection process. In particular, these RSM graphs depict the results of the carried out factorial comparisons of the multi-dimensional patterns of responses to varying control parameters.

The results in Table 5.4 shows the importance of the considered four factors, and control parameters, in order of their rank weightings when their effects on resulting T_{ff}, τ and overall quality are analysed. For both, PP and ABS, t_i was the most important factor based on the overall quality rank weightings, followed by T_b and T_m. However, PP showed a higher dependence on t_i while the influence of T_b and T_m was more pronounced for ABS. The GTM factor had a negligible effect when all criteria weightings were considered.

Table 5.4 Moldflow DOE Results

Criterion weightings:	Control Factors	PP	ABS
τ rank weighting [%]	t_i	83.41%	64.28%
	T_b	13.81%	17.87%
	T_m	1.79%	17.64%
	GTM	0.89%	0.17%
T_{ff} rank weighting [%]	t_i	81.59%	(3) 25.05%
	T_b	11.54%	(1) 43.65%
	T_m	6.17%	(2) 31.17%
	GTM	0.32%	(4) 0.00%
Overall quality rank weighting [%]	t_i	76.06%	46.31%
	T_b	21.05%	27.47%
	T_m	1.77%	26.05%
	GTM	1.04%	0.01%

5.4.2. Shear stress

For PP, t_i had the highest influence on τ (see Table 5.4). Figure 5.4 shows that low t_i settings result in a higher τ. The medium and high t_i led to significantly lower τ than that at low t_i. For all settings, an increase of T_b resulted in a decrease of τ except for the combination of low T_m and high t_i. In addition, these T_m-t_i settings resulted in the lowest τ achieved in all simulation runs. τ was almost constant and independent of T_b, and thus PP behaved like a Newtonian fluid. Only in the T_b range from 240°C to 260°C there was a slight decrease of τ from 0.048 to 0.046 MPa. T_m had almost no influence on τ at low t_i settings. However, at high t_i there was a small variation, in particular low T_m settings resulted in lower τ.

For ABS, again t_i had the highest influence on τ (Table 5.4). The graph in Figure 5.5 shows that low t_i results in a higher τ. At low t_i and T_b below 250°C τ exceeded its critical value for ABS. The medium and high t_i settings led to much lower τ than that at low t_i. In addition, at low and medium t_i a decrease of τ was observed with the increase of T_b. The high t_i setting led just to a small reduction of τ in the T_b range from 220°C to 250°C, while outside it τ levelled out and showed only a small increase at higher end temperatures. T_m showed almost no interactions with t_i at low t_i settings however at high t_i some variations were observed, in particular, low T_m led to lower τ.

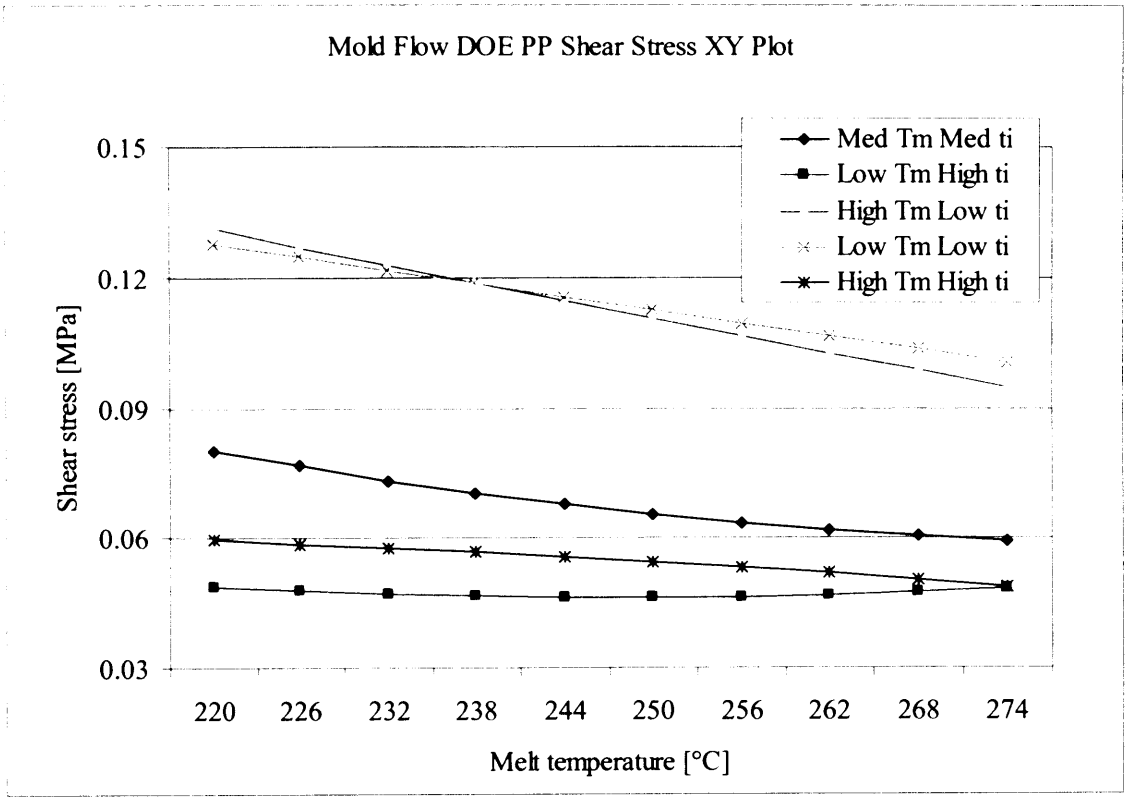

Figure 5.4 PP shear stress

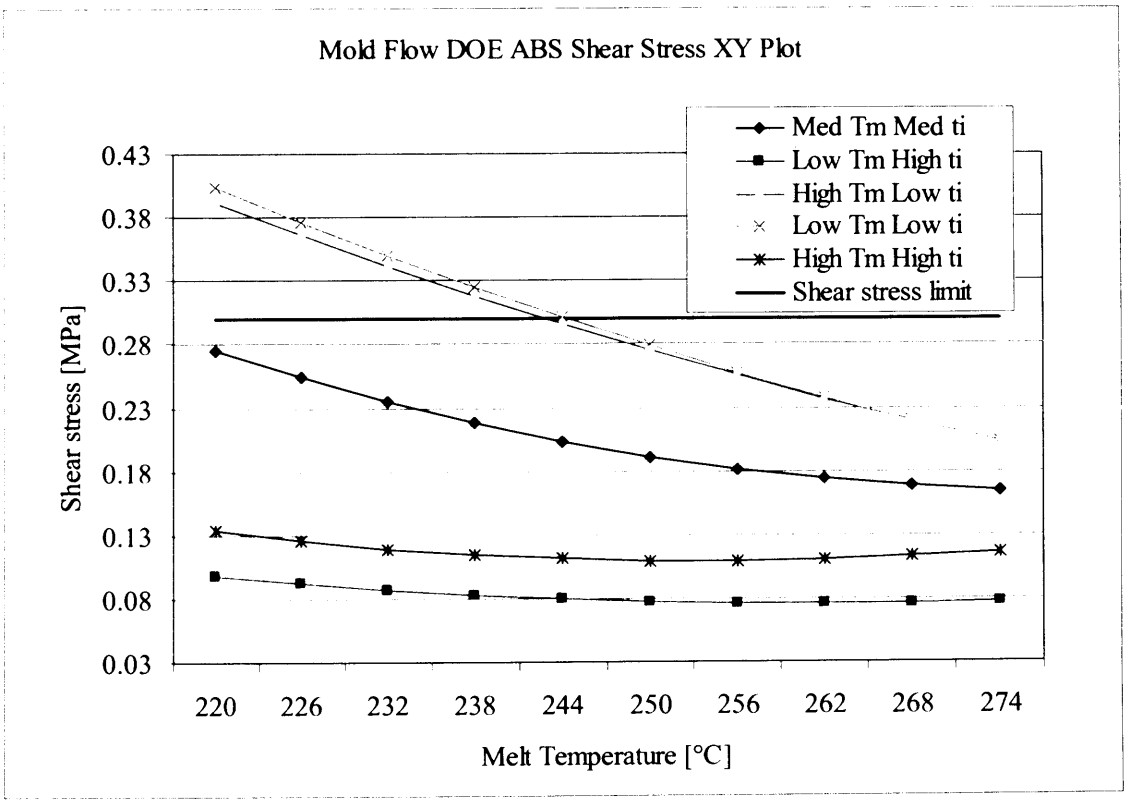

Figure 5.5 ABS shear stress

5.4.3. Flow front temperature

For PP, t_i had the highest influence on τ (see Table 5.4). The graph in Figure 5.6 shows that for all settings T_{ff} increases with the increase of T_b and this dependence is less distinct at high t_i. Low t_i settings led to a significant increase of T_{ff}, and at T_b below 260°C T_{ff} exceeded the PP melt temperature. This indicates an increase in shear heating when T_b is below 260°C. In addition, at low t_i settings T_m showed almost no interactions with t_i. However, at high t_i an increase of T_m led to a higher T_{ff}.

For ABS, T_b had the highest influence on τ (Table 5.4). The graph in Figure 5.7 shows that for all settings T_{ff} increases with the increase of T_b. At low t_i, and medium t_i and T_b below 260°C T_{ff} exceeded the ABS melt temperature. This indicates again the existence of shear heating at these settings. As it was the case with PP, at low t_i T_m did not show any interactions with T_{ff}. However, at high t_i again an increase of T_m led to a higher T_{ff}.

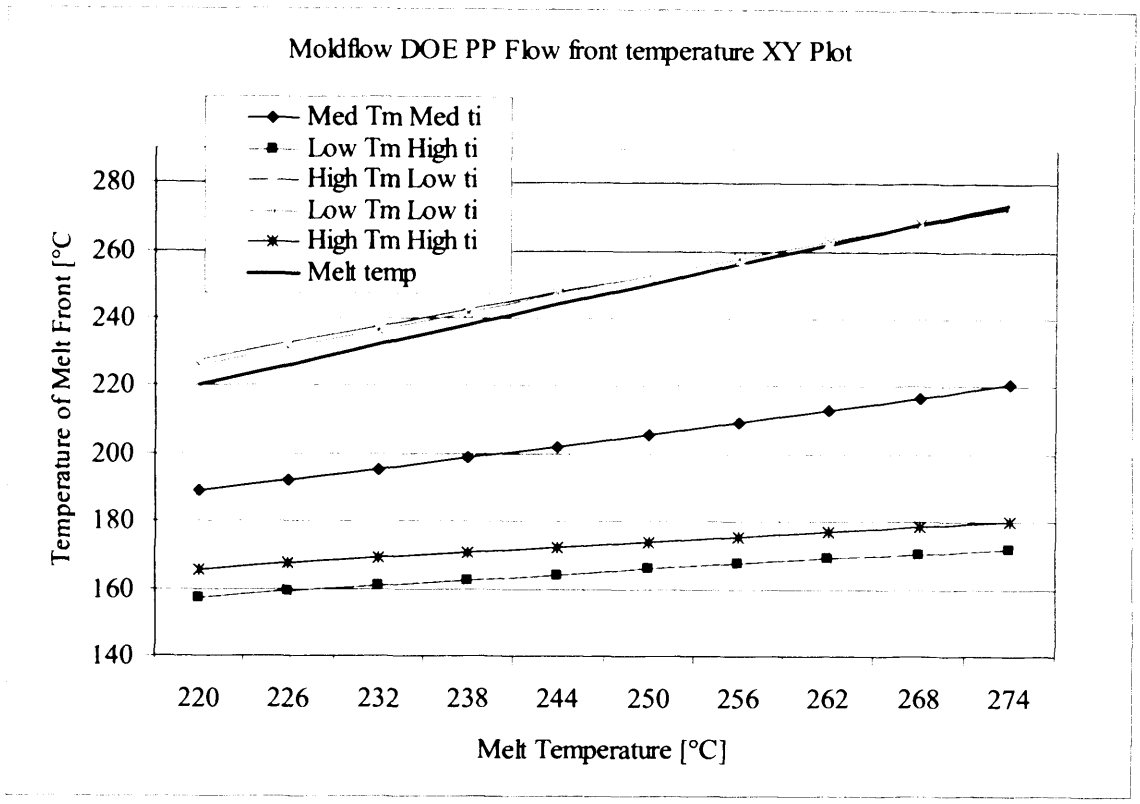

Figure 5.6 PP Flow front temperature

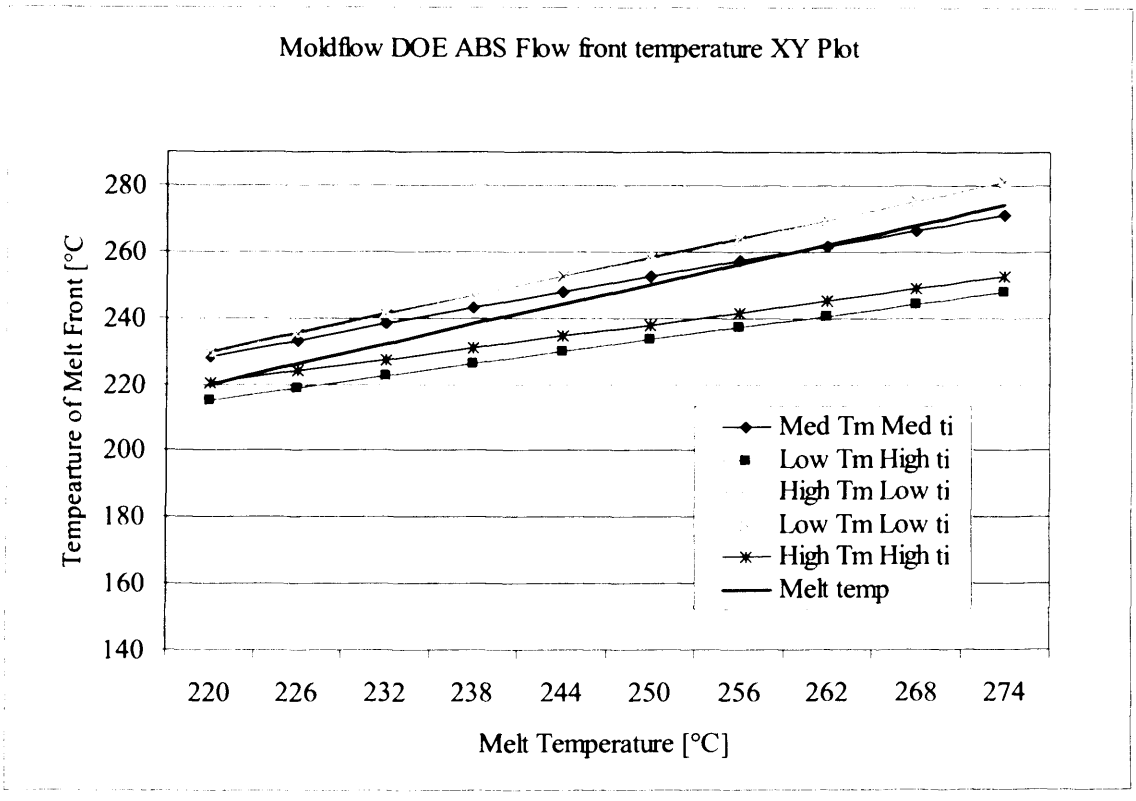

Figure 5.7 ABS Flow front temperature

5.4.4. Flow length

In Table 5.5, the experimentally obtained maximum and minimum flow lengths for both materials, PP and ABS, reported in Chapter 4, are compared with the results attained using the dual domain and 3D simulation analyses.

For PP, the parameter settings of simulation runs S1 and S2 correspond to those leading to minimum and maximum flow length in the experimental study. The dual domain results as they are depicted in Figure 5.7 shows that the mould cavity was completely filled in both simulation runs, which represented an overestimation of 15.6% and 2.1% respectively against the actual flow lengths obtained in the experiments. The temperature reduction during the filling stage, as estimated by T_{ff}, was in the range from 240 to 160 °C for T1, and between 275 and 265 °C for T3 (see Figure 5.8a, 5.8b). So, though the cavity was filled completely in both simulation runs, the difference between minimum temperatures in these two simulation runs indicates the reason for the low flow length in S1 in comparison to S2. On the contrary, the 3D simulation analysis underestimates the actual flow lengths in S1 and S2 by 13.5% and 19%, respectively. However, a correlation exists between the actual and simulation results, as the flow length for S1 is lower (see Figure 5.9a, 5.9b).

For ABS, the simulation runs corresponding to the minimum and maximum flow lengths obtained in the experimental study were S3 and S4. As it was the case with the PP dual domain results, the cavity was completely filled in both simulation runs, and thus the simulation model overestimated the flow length by 19.45% and 47.6%, respectively (see Figure 5.8c, 5.8d). However, if the temperature changes, in particular T_{ff}, during the filling stage are studied again this could explain the difference in flow lengths between S3 and S4. In the 3D simulation runs S4 resulted in an underestimation of the flow length by 10.5% as

shown in Figure 5.9c while for S3 the flow length was overestimated by 41% (see Figure 5.9d). In addition, the flow length for S3 is higher that that for S4. The closeness of the 3D S3 and S4 results suggest that some other factors that are not taken into account in this simulation study affect the flow behaviour and length, and/or that the applied models are less sensitive to low settings of T_m and t_i.

Overall, the dual domain simulation model overestimated the filling of the cavity in all tests. In particular, comparing the actual minimum and maximum flow lengths with those obtained in the simulation runs, the average overestimation for PP was 8.85% and 33.52% for ABS.

For the 3D simulation model there was an average underestimation in the filling for the PP tests of 16.5%, and though there was both an overestimation and an underestimation for ABS.

For both simulation models there were temperature variations between the trails that could explain the flow length results obtained in the experimental study.

(a) PP Low flow length result (T1)	(b) PP high flow length result (T3)
Melt Front Temperature range from 190 to 300 °C	
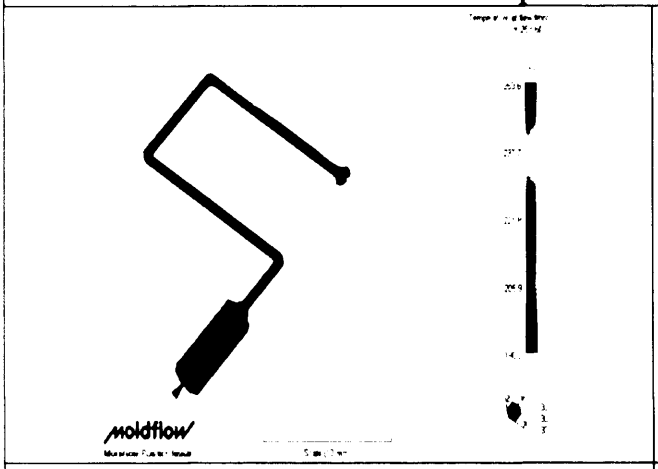	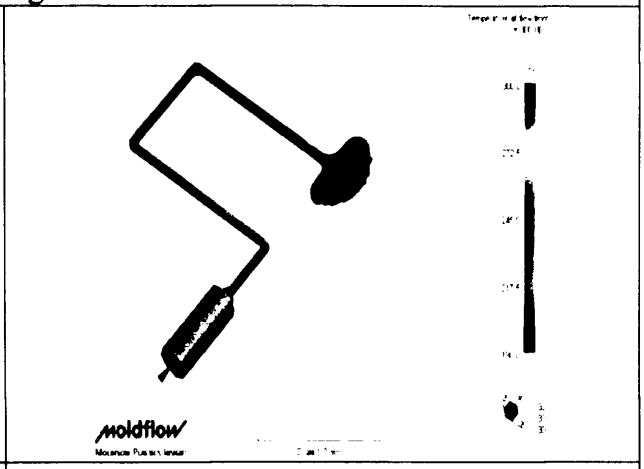
(c) ABS low flow length result (T6)	(d) ABS high flow length result (T3)
Melt front temperature range from 250 to 310 °C	
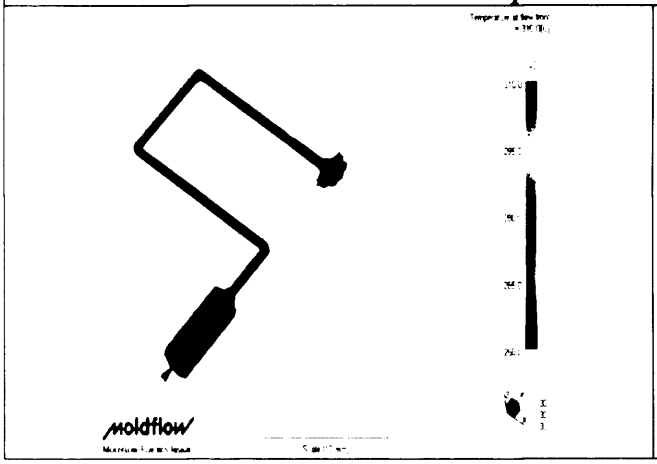	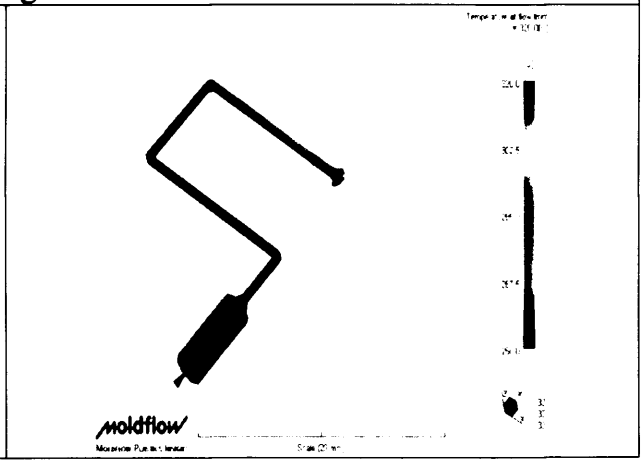

Figure 5.9 3D PP and ABS melt front temperature distribution

5.5 Summary and conclusions

In Chapter 5, by deploying and building upon the findings of Chapter 4, the conditions used to perform an empirical analysis of melt flow behaviour in micro injection moulding are applied to simulation techniques. With the use of a dedicated FEA package two models were proposed to simulate the process. Then, the effects of T_b, T_m, t_i and GTM on the filling behaviour of a test part were analysed with RSM. To validate both, the dual domain and 3D models, the simulation results were compared with the experimental findings reported in Chapter 4.

The following conclusions can be drawn from the study.

- The dual domain flow analysis overestimated the polymer flow length in all simulation runs. However, the variations of T_{ff} during the filling stage can be used to identify problems in moulding micro components.
- The 3D flow analysis underestimated the polymer flow length in PP simulation runs. However, for ABS there was both an overestimation and underestimation of the flow lengths. Overall, 3D simulations for both materials were closer to the actual results.
- It will be difficult to use the simulation model to predict surface defects. But, the analysis results can be utilised to identify process conditions leading to such defects. For example, high τ is the cause of unstable flow fronts, and excessive shear heating that leads to material degradation. In addition, inconsistent T_{ff} across a micro part indicates potential problems in filling the cavity.

- For both PP and ABS, the simulation study showed that overall t_i is the most important factor affecting part quality. In particular, low t_i results in high τ, and in the case of ABS the critical τ limit is reached at low t_i and low to medium T_b.
- The τ for ABS was highly dependent on process parameters particularly t_i. In comparison the process parameters had less effect on the PP results, as was the case in the carried out experimental trials in Chapter 4.
- The variations of T_{ff} in response to varying process parameters were much higher for PP in comparison with ABS. However, these changes in the process parameters did not have any significant effect on the flow lengths achieved in the experimental trials (Chapter 4).
- For both PP and ABS, T_{ff} at low to medium t_i resulted in an increase of T_b above its set-up level. Hence, at this processing window shear heating occurs at the melt front, and a frozen layer along the cavity walls.
- High t_i can lead to rapid melt cooling and because the T_m range is below that of T_b for PP and ABS, the polymer mobility is affected. The temperature decrease resulting from the size effects can be overcome by decreasing t_i, and T_m can be optimised for correct ejection temperatures.

CHAPTER 6

SURFACE TREATMENT EFFECTS ON PART DEMOULDING

6.1 Motivation

An important stage in micro injection moulding which can affect the accuracy and mechanical properties of the produced components is part demoulding. During this stage, part-mould forces can cause a variety of defects to micro parts, including stress marks, deformation, fracture and stretching of the polymer structures. The research reported in this chapter investigates the effects of two new tool surface treatments in combination with varying process conditions on the demoulding behaviour of parts with micro features.

The chapter is organised as follows. In Section 6.2 the important factors affecting part demoulding is discussed. Then, the experimental set-up including the method adopted for performing an empirical investigation of surface treatments' effects on the demoulding behaviour of parts with micro features is described in Section 6.3. In particular, by varying a range of micro moulding parameters within a broad processing window, the required demoulding forces for two different coatings are compared with those present in untreated tools. Next, Section 6.4 presents the experimental results and analyses the relationship between the demoulding behaviour of parts with micro features and applied coatings on micro cavities. Finally, Section 6.5 summarises the work reported in this

chapter and draws conclusions.

6.2 Factors affecting part demoulding

In order to achieve an economical and reliable production of micro parts it is important to study systematically the factors that affect the demoulding behaviour of parts with micro features. During the solidification process of the moulding cycle, the polymer melt shrinks onto the mould cavity walls and features. The part-mould adhesion forces that develop at this stage have to be overcome for subsequent part removal. To avoid yielding when breaking the bond between the polymer and the tool cavity, the maximum equivalent stress applied for part removal should not exceed the tensile yield stress of the material (Navabpour, et al. 2006). Thus, the factors that influence the demoulding process have to be studied carefully to avoid destroying parts and features and/or introducing further internal stress to a component through plastic deformation. Some of the main factors that affect demoulding are described below.

6.2.1 Part-mould forces

Part-mould forces are a result of an interaction between the polymer and the mould cavities. An ejector system that can comprise of a number of ejector pins is used to apply a release force to overcome the friction and adhesion forces. The requirement for each pin is to overcome the local friction and adhesion forces without introducing defects to the removed part.

In polymer injection moulding, predicting these friction and adhesion forces between the part and the tool is a complex task due to its dependence on part geometry and on process parameters such as the temperature and the pressure used during the process. The force

that resists the motion of one surface relative to another is defined as friction. In the injection moulding the release forces (F_R), can be characterised by the existence of imbalanced and localised part-mould forces that result from geometric and feature variations within a given part. A known process factor that has a direct impact on friction is the level to which the part is filled. A packed volume of polymer in a cavity with the optimum holding pressure (P^h) and holding time (t_h) will allow a complete fill of surface irregularities that are dependent on surface finish characteristics and surface to volume ratio of features. Alternatively, short shots or unpacked polymer volumes will lead to voids and sinks that retreat from the tool surface and thus reduce F_E.

Previous research studies on injection moulding forces and demoulding behaviour found that there are instances in which the friction effects can be difficult to explain. In particular, injection pressure, the number of ejector pins, tool surface roughness, holding pressure and tool temperature were factors that were found to influence F_E.

Together with high SV_R and high aspect ratio micro features, present challenges in micro injection moulding call for the decrease of part-mould forces and tool wear, and thus to maintain optimum mechanical and structural stability for replicating quality parts and increasing tool life.

6.2.2 Tool Coatings

In plastics injection moulding, the machining processes available for tool production can produce cavities with different surface finishes. Thus, an optimum manufacturing route has to be selected for mould manufacture. Then, when the tool is used during the production of parts the mould surface wears due to a number of factors such as abrasion

from the melt flow, thermo-mechanical loads, and burning and corrosion caused by the diesel effect of exhaust gasses. As mentioned in the previous section, part-mould forces and the associated F_E vary depending on the surface finish of the tool. Thus, the degradation of a tool surface finish over a given time period will result in a variation of F_E during the tool life.

One method that can be used for improving the wear resistance of tool surfaces is to apply surface treatments. In particular, the wear of a surface can be reduced with traditional methods such as heat treatment and nitriding. In addition applying hard coatings employing methods like chemical vapour deposition can result in moulds with significantly better wear resistance. Furthermore the moulded parts are improved due to reduction of the part-mould forces (Mitterer et al. 2003; Heinze et al; 1998; Cunha et al; 2002). Many composite coatings can be used for the reduction of part-mould forces. In particular, low material affinity between the coating and the polymer is targeted in order to achieve a better demoulding behaviour.

A problem associated with surface treatments is that of interfacial adhesion between the tool surface and the deposited material. The mechanisms of this adhesion include mechanical locking of irregular surfaces, physical absorption (Van Der Waals forces), chemical bonding (covalent, ionic, or hydrogen bonds) and diffusion (inter diffusion of polymer chains). If the deposition thickness exceeds 1 μm, the contact pressures from the injection moulding process can cause cracking and delamination of the coating. Although advanced Ti-DLC coatings have been developed to reduce this problem, it is still an issue for F_E and tool wear (Uddin et al. 2006).

Based on the findings of previous studies, it is clear that surface treatments can reduce part-mould forces and tool wear. This chapter investigates the effects that the tool coating can have on part demoulding in micro injection moulding.

6.3 Experimental set-up

6.3.1 Test materials

Two commonly used materials in injection moulding, Acrylonitrile Butadiene Styrene (ABS), and Polycarbonate (PC) were selected to conduct the planned experiments. Table 6.1 shows the material demoulding properties of ABS and PC. Each polymer was placed in desiccant drying and dehumidifying cycles before the trials to remove any surface or absorbed moisture. The machine used to perform the micro injection moulding tests was a Battenfeld Microsystem 50.

Table 6.1. Materials demoulding properties

Material	Magnum 8434	Pc Calibre 300-15
Category	Acrylonitrile butadiene styrene (ABS) $C_{15}H_{17}N$	Polycarbonate (PC) $C_{16}H_{14}O_3$
Ejection temp [°C]	85	153
Specific heat (Cp) [J/kg-C]	2032	1891
Thermal conductivity [W/m-C]	0.1520	0.185
Elastic modulus [MPa]	2240	2280
Poisson ratio	0.3920	0.417
shear modulus [MPa]	805	805
Coefficient of thermal expansion 1/C (E-05)	8.0	7.3
Moulding shrinkage [%] (ISO 294-4)	0.40-0.70	0.50-0.70
Static Coefficient of friction [μs]	0.35	0.38

6.3.2 Part design and tool manufacture

The part design used in this study is a 15mm x 20mm x 1mm micro fluidics platform (Figure 6.1). The system design includes features commonly found in micro fluidics components such as reservoirs, channels and waste compartments. The pin dimensions are 500 μm in diameter and 600 μm in height, and the cross section of the main channels is 200 x 200 μm. Table 6.2 shows some part design characteristics and compares two designs, one with the micro features and the other one without them. In particular, SV_R is 15.7% higher for the design that includes micro features.

When designing the ejection system three iterations were necessary. The first design used a single 3mm pin positioned at the centre of the part. During the carried out preliminary trials the ejector pin caused damage to the microfluidic parts, including its micro fractures, and stress marks to the PC and ABS samples respectively (Figure 6.3a, 6.3c). In the second design four 1.6mm pins were used and positioned 5mm from each corner. However, in spite of the distributed ejection force the pins caused a complete fracture of the PC parts and stress marks on the ABS parts (Figure 6.3b, 6.3d). These design iterations demonstrated how difficult it can be to define a suitable ejector system in micro IM. Finally, the third design that included four 3mm ejector pins at each corner did not cause any damage to the parts, and therefore was selected for this experimental study (Figure 6.2).

The frictional force between ejecting pins and mould were also considered. The ejector pins are a standard components (nitrided and with good surface quality) and the fit in the mould assembly was selected to ensure a smooth sliding. The temperature of the ejecting pins at the moment of ejection was also considered. In particular, it was recognised that the temperature of the mould could affect the force measurement for the

selected experimental set-up. Therefore, to minimise the tool temperature influence it was decided that only the cavity area would be heated. To localise the heating within the cavity a 5 mm thick insulating plate was incorporated in the tool design to minimise further the heat transfer to the ejector system. The ejector/cavity contact area was kept to a minimum, 75.4 mm^2 for the four pins (8.0 mm of a total 60 mm ejector stroke length).

Two identical tools were manufactured in brass. They were produced using conventional milling except for the cavity faces that were machined by micro milling. A draft angle of 1 degree was applied to each of the features, and the achieved surface finish on both tools was identical. The moving and fixed halves of the mould were assembled to a primary mould tool and then inspected for parallelism and shut off of the mating faces.

Table 6.2. Part design characteristics

Design properties	Design with micro features	Design without features
Volume	$3.10MM^3$	$3.37MM^3$
Surface area	$8.33MM^2$	$7.62\ MM^2$
SV_R	2.68	2.26

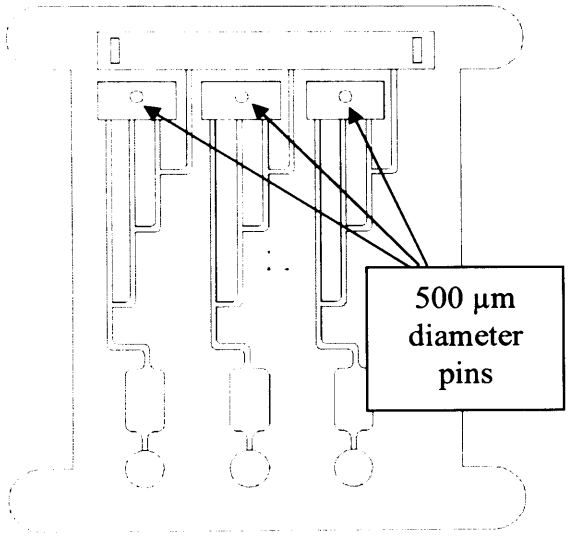

Figure 6.1 Micro fluidics platform

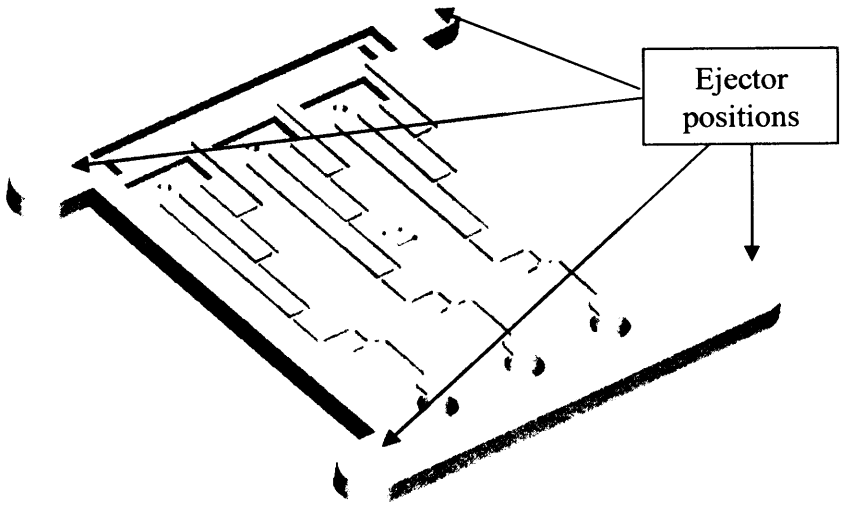

Figure 6.2 Ejector positions

PC preliminary trials	
(a) One 3 mm ejector pin	(b) Four 1.6 mm ejector pins
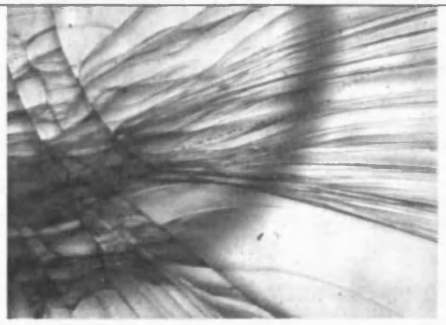	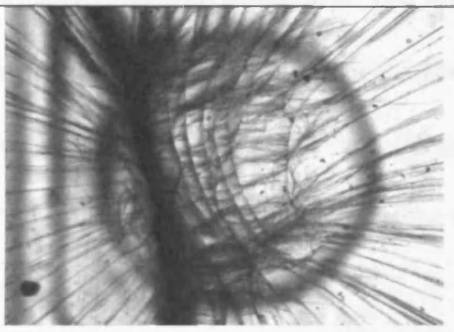
ABS preliminary trials	
(c) One 3 mm ejector pin	(d) Four 1.6 mm ejector pins
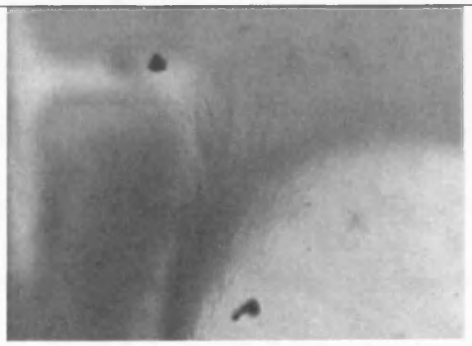	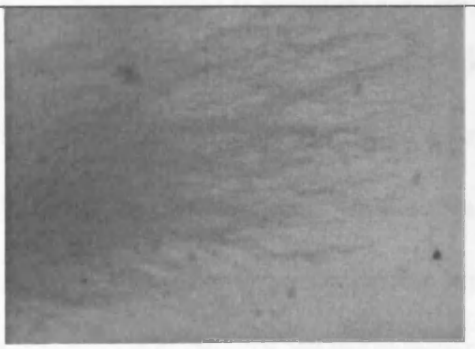

Figure 6.3 Micro injection moulding trials to select the design of the ejection system

6.4 Surface treatment

6.4.1 DLC coating

Diamond like carbon (DLC) is an amorphous carbon material that can display some of the unique properties of natural diamond. Thus, DLC applied as a coating to other materials can result in surfaces with some diamond like properties. In this investigation a DLC thin film was deposited in a Low Frequency (LF) Plasma Enhanced Chemical Vapor Deposition reactor (PECVD) at CEA as schematically shown in Figure 6.4. The lower electrode that serves as a substrate holder is powered via a 40kHz transmitter. Cyclohexane (C_6H_{12}) diluted with hydrogen was used as gas precursor. The distance between the two electrodes was kept constant at 200mm and the vacuum chamber was pumped down to a base pressure ranging from 2 to 4 10^{-4}Pa.

Prior to deposition, the substrate were cleaned first in acetone and ethanol by an ultrasonic washer, and then in a Ar + H_2 etching plasma. In order to improve the adhesion a Si-C:H intermediate layer with 0.5μm thickness, was deposited on the substrate using a plasma of tetramethylsilane (TMS) and argon. Then, a 2μm DLC film was deposited onto the Si-C:H interlayer. During the deposition the floating substrate temperature remained below 130°C. In Table 6.3 the deposition parameters used for this study are shown.
The DLC depositions were conducted by the French Atomic Energy Commission (CEA), Laboratory of Innovation for New Energy Technologies and Nanomaterials (LITEN), Grenoble, France

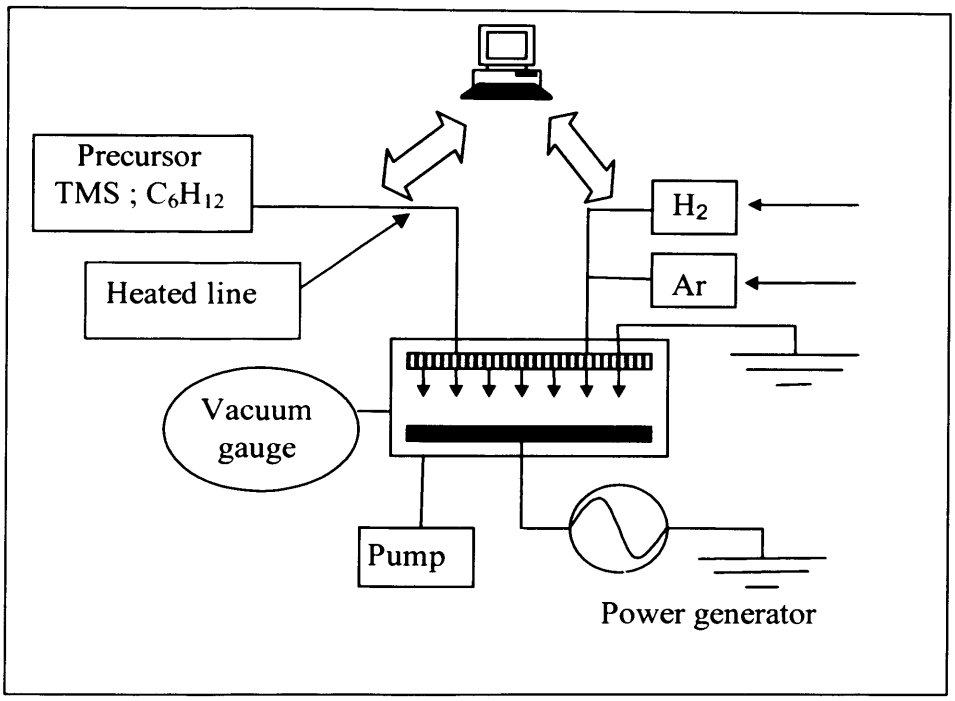

Figure 6.4. Schematic representation of the LF-PECVD reactor

Table 6.3 Deposition conditions of DLC film

Parameter	**Range**
LF Power	320 W (0.32 W/cm^2)
Vb	645 V
Working pressure	4 Pa
%H_2 in (C_6H_{12}+H_2) gas mixture	20 %

6.4.2 SiOC coating

The second tool treatment investigated in this research was an organosilicon based coating. In particular, PECVD processes developed by CEA for hydrophobic applications, and suitable for an industrial-scale deposition of high-quality and recyclable coatings were used. Plasmas are produced inside a cylindrical stainless steel vacuum chamber with a diameter of 30 cm and a parallel plate configuration. Substrates that will be coated are positioned on the lower grounded electrode. The precursors' vapour is uniformly distributed in the reactor by the upper showerhead electrode with 1 mm pinholes. The upper electrode is externally connected, through a semi-automated matching network, Dressler VM1000A, to a 13.56 MHz-RF power supply, Advanced Energy Cesar® RF, which provides a RF voltage in respect to the grounded chamber. Before the PECVD process starts and during it the chamber is evacuated to 5.10^{-3} mbar employing a rotary pump, Alcatel ADS 501.

As it was already mentioned OMCTSO can be polymerised during plasma treatments, by rearranging the radicals. Soft coatings of $SiO_xC_yH_z$ with high content of methylene and methyl groups were obtained by using OMCTSO in plasma process yields. PECVD is carried out in a reducing mixture with low plasma activation to preserve methyl groups. Deposition parameters used in this research are shown in Table 6.4. The SiOC depositions were conducted by CEA, LITEN.

6.4.3 Testing

Mechanical characterisations of the coatings were also performed and values are summarised in Table 6.5. Hardness and Young's modulus were obtained by a nanoindenteur CSEM NHT using a Berkovitch diamond tip. The values were calculated

using the Oliver and Pharr method and correspond to an average of 30 indentations with imposed penetration depths shallower than 10% of the thickness of the sample. A ball-on-disk tribo-meter was used for friction measurements. An 8mm Al_2O_3 ball was used as the mating material and a 5N load was applied on the system (Hertz pressure = 950MPa). The sliding speed was kept at 0.17m/s for a fixed number of 100,000 cycles. Tests were performed in normal atmosphere and no lubricant was used. The testing was conducted by CEA, LITEN.

Table 6.4 Deposition conditions of SiOC film

Surface treatment	Precursors	Carrier	Working pressure	Power	Process temperature	Plates spacing	Deposition rate
Hydrophobic $SiO_xC_yH_z$	OMCTSO (Partial pressure 0.15 mbar)	Reducing mixture	0.25 mbar	100 W	80 °C	30 mm	~ 1 nm/sec

Table 6.5 Mechanical properties of the coatings

Properties	**DLC**	**PDMS**
Coating Thickness	1 µm	20 nm
Hardness (GPa)	22 ±2	0.2 (On 1 µm test piece)
Young Modulus (GPa)	160 ±10	2 (On 1 µm test piece)
Friction coefficient	0.05	Not available
Wear rate ($mm^3.N^{-1}.m^{-1}$)	$5\ 10^{-7}$	Not available

6.4.4 Force measurements

In this study, variations in force during the ejection stage of the IM process were assessed using a Dynisco PCI piezoelectric force transducer. The upper range of the Dynisco PCI 4011 sensor is 10,000 N with a resolution in mN, the standard deviation of conducted force measurements, within +/- 1% for the whole range. Consultation with the sensor manufacturer was carried to better understand the sensor's functionality, and successful pre-trials were completed to validate the sensor's performance.

The sensor output signals were downloaded onto a PC using a National Instruments cDAQ-9172 USB data acquisition unit and the measured values were accessed through the National Instruments Labview 8 software. Each tool had to be modified to accommodate the force transducer.

An ejector sub assembly was manufactured to house the four pins used for part removal. This sub assembly was then fitted to the main ejector plate. 4 x 3mm holes were drilled into the moving half of the tool at each corner of the part cavity in order to guide the ejector pins (Figure 6.5a). To carry out the force measurements, the transducer was positioned in the middle of the ejector plate sub assembly (Figure 6.5b).

When the ejector assembly moves forward the part is removed from the cavity and the transducer is subjected to a mechanical load that generates an electric potential. The electric charge is then converted using a Kistler charge amplifier (type 5039A222) into a proportional voltage. The output signal is monitored with a National Instruments NI 9205 16-bit module. The measuring and output ranges of the charge amplifier are 0 to 5000 pC and 0 to 10v, respectively. With the ejector pins acting on the transducer, the resulting

force (F) from the measured output voltage can be calculated using the following equation:

$$F = \frac{Output(v) \times 500(pC)}{E_f} \qquad (2)$$

where: E_f is force sensitivity, -4.2 pC/N.

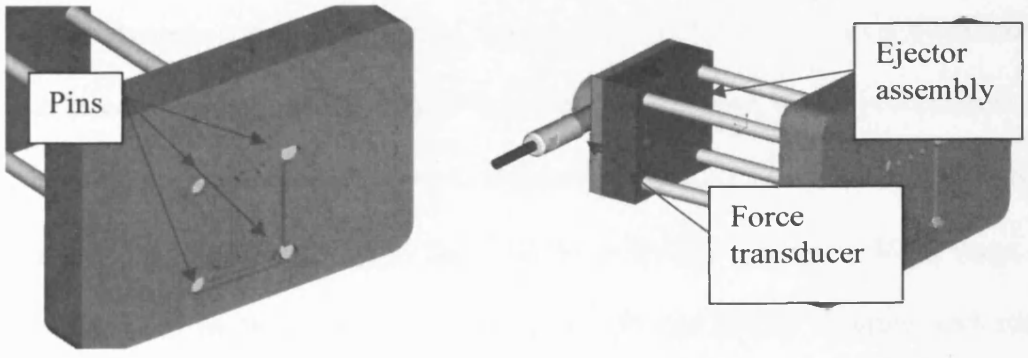

Figure 6.5 (a) Ejector positions (b) Force transducer and ejector assembly

6.5 Design of experiments

Due to the fact that the filling performance of micro moulds relies heavily on the temperature control during injection, the effects of barrel temperature (T_b) and mould temperature (T_m) were also investigated. In addition, the cooling time after part filling (t_c) and the use of a delay for controlling the ejection time (t_e) were also taken into account. Thus, given that four factors at three levels each were considered, a Taguchi L9 orthogonal array (OA) was selected for each combination of tool and polymer material. The three levels of control for t_c and t_e were the same for the two materials, while the levels for T_b and T_m were different for each material (see Table 6.6 and 6.7).

Within a recommended processing window the melt temperature was controlled through T_b. Three levels, maximum, minimum and medium temperatures, were selected for each of the polymers. In micro moulding, the polymer solidification time is much shorter than that in conventional moulding and therefore the processing requires external heating. Therefore the tools were heated to increase T_m and thus to keep the bulk temperature of the polymer sufficiently high to facilitate the melt flow during the filling stage. The T_m settings used in this research were again the minimum, medium and maximum temperatures in the recommended range for each material.

During part cooling the polymer elasticity modulus increases with the temperature decrease. Thus, after filling it is necessary the temperature to be sufficiently low to facilitate the demoulding without introducing any part deformation. To increase the rate of thermal diffusivity two process factors are considered, t_c and t_e. The main difference between them is that t_c is the set time for the polymer to cool down before the

demoulding stage starts. The effect of cooling is further investigated by the use of t_e, during which the mould opens and it is partially exposed to ambient temperature. For t_c the three levels were set at 1 second, 5 seconds and 10 seconds. While the time delay option available on the Battenfeld Microsystem 50 was used to set t_e to 0, 5 and 10 seconds.

The parameters were selected carefully considering polymers' thermal properties and the necessary cooling for successful part de-moulding. In regards to ejection forces Menges & Moren (1993) concluded that the cooling time had a higher importance than holding pressure/time and therefore t_c and t_e were selected in stead of holding parameters in this experimental study. Holding time/pressure is certainly important for macro injection moulding, however in micro injection moulding the polymer solidification time is significantly shorter, and thus the application of post injection pressure to the part is less effective, hence the holding parameters can be consider to some extend redundant for this research. Also, the additional cooling to t_e was specifically selected above the holding parameters to ensure that the melt/tool temperature parameters did not counteract the influence of cooling time.

The response of each tool surface treatment to each set of control parameters was analysed by measuring F_E during the part ejection. Given that three tool surfaces, untreated, DLC and SiOC treated, and two materials, PC and ABS, are investigated, six L9 OAs were defined. In addition each experiment was repeated ten times. Thus, a total of 540 trials (10 x 9 x 6) were carried out.

Table 6.6 L9 fractional orthogonal array for ABS

Trial	T_b [°C]		T_m [°C]		t_c [s]		t_e [s]	
	Level	Value	Level	Value	Level	Value	Level	Value
1	A1	220	B1	40	C1	1	D1	0
2	A1	220	B2	60	C2	5	D2	5
3	A1	220	B3	80	C3	10	D3	10
4	A2	250	B1	40	C2	5	D3	10
5	A2	250	B2	60	C3	10	D1	0
6	A2	250	B3	80	C1	1	D2	5
7	A3	280	B1	40	C3	10	D2	5
8	A3	280	B2	60	C1	1	D3	10
9	A3	280	B3	80	C2	5	D1	0

Table 6.7 L9 fractional orthogonal array for PC

Trial	T_b [°C]		T_m [°C]		t_c [s]		t_e [s]	
	Level	Value	Level	Value	Level	Value	Level	Value
1	A1	280	B1	80	C1	1	D1	0
2	A1	280	B2	100	C2	5	D2	5
3	A1	280	B3	120	C3	10	D3	10
4	A2	300	B1	80	C2	5	D3	10
5	A2	300	B2	100	C3	10	D1	0
6	A2	300	B3	120	C1	1	D2	5
7	A3	320	B1	80	C3	10	D2	5
8	A3	320	B2	100	C1	1	D3	10
9	A3	320	B3	120	C2	5	D1	0

6.6 Analysis of the results

6.6.1 Average Force results

In this study, L9 OAs were employed to ensure that the experimental results were representative of the considered processing window. For each trial, the effects of the applied surface treatments on F_E were investigated and then based on the conducted 540 trials the F_E mean values were calculated for each of the six OAs as shown in Figure 6.6 and Appendix F.

For the untreated tool on average both ABS and PC results were subjected to the highest demoulding forces of all six groups of experiments. ABS had a higher average than PC. For the untreated surface, ABS has a higher average than PC. ABS has a coefficient of friction of 0.35 while PC has a higher coefficient of 0.38 as shown in Table 6.1. This result is due to the part shrinkage. From the ABS and PC PVT data (Appendix B) it can be seen that under increased pressure and temperature the ABS specific volume increases more than that of the PC material. Thus, when the ABS part temperature drops the volume decreases more than that for PC. The reason for the higher ejection forces for ABS than those for PC, in spite of the material higher coefficient of friction, is that the part shrinkage onto the mould features has a higher influence/impact on the ejection forces than the material coefficient of friction.

For the two tools with the DLC and SiOC coatings, both materials experienced a reduced demoulding force compared to the untreated tool. The average ABS results with the DLC coating were the lowest of all experiments, and compared to the untreated tool results there were a F_E reduction of 16.2% and 41.6% for the SiOC and DLC treated tools, respectively. In case of PC, the reduction of F_E for both coatings was much more modest,

in particular by 8.09% and 10.68%.

6.6.2 Optimum parameters levels

The average demoulding force based on the 10 trials conducted for each combination of control parameters in the six L9 OAs was calculated in order to determine the optimum parameter levels for the investigated surface treatments and polymers employing the Taguchi parameter design method (Roy et al. 1990). The value of a given parameter is considered to be optimum, the best of the selected three levels, if its corresponding average F_E is the lowest. Figure 6.7 shows the results obtained for the six sets of experiments conducted in this study.

By applying this method, it is possible to identify theoretically the best set of micro IM parameters within the investigated processing window with respect to F_E. In particular, for the six combinations of surface treatments and polymers, the theoretical best set of processing parameters is provided in Table 6.8.

From this analysis, it is immediately apparent that there is not a unique selection of parameter levels that can be considered optimum for surface treatments or polymers investigated in this research. Thus, if another polymer is used it will not be possible to judge what combination of processing parameters will be optimum. Therefore, systematic experimental studies should be carried out every time when new combinations of tools and polymers are considered.

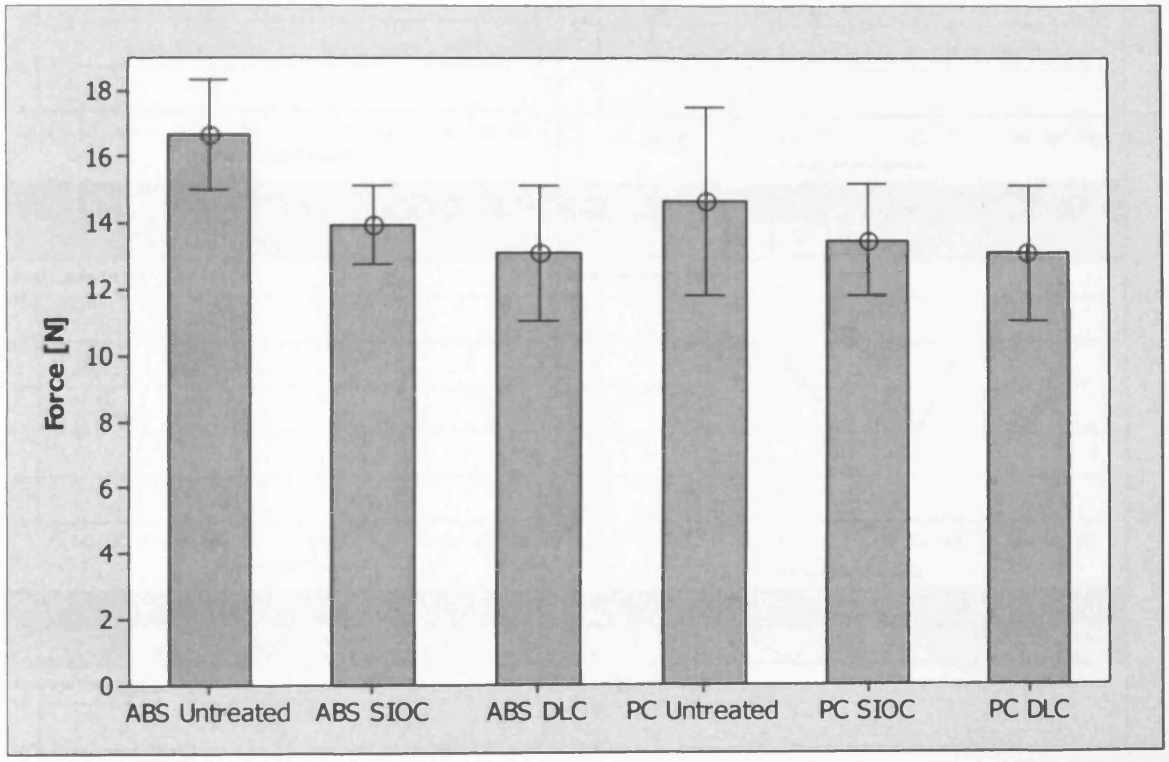

Figure 6.6 The average demoulding force for the six OAs

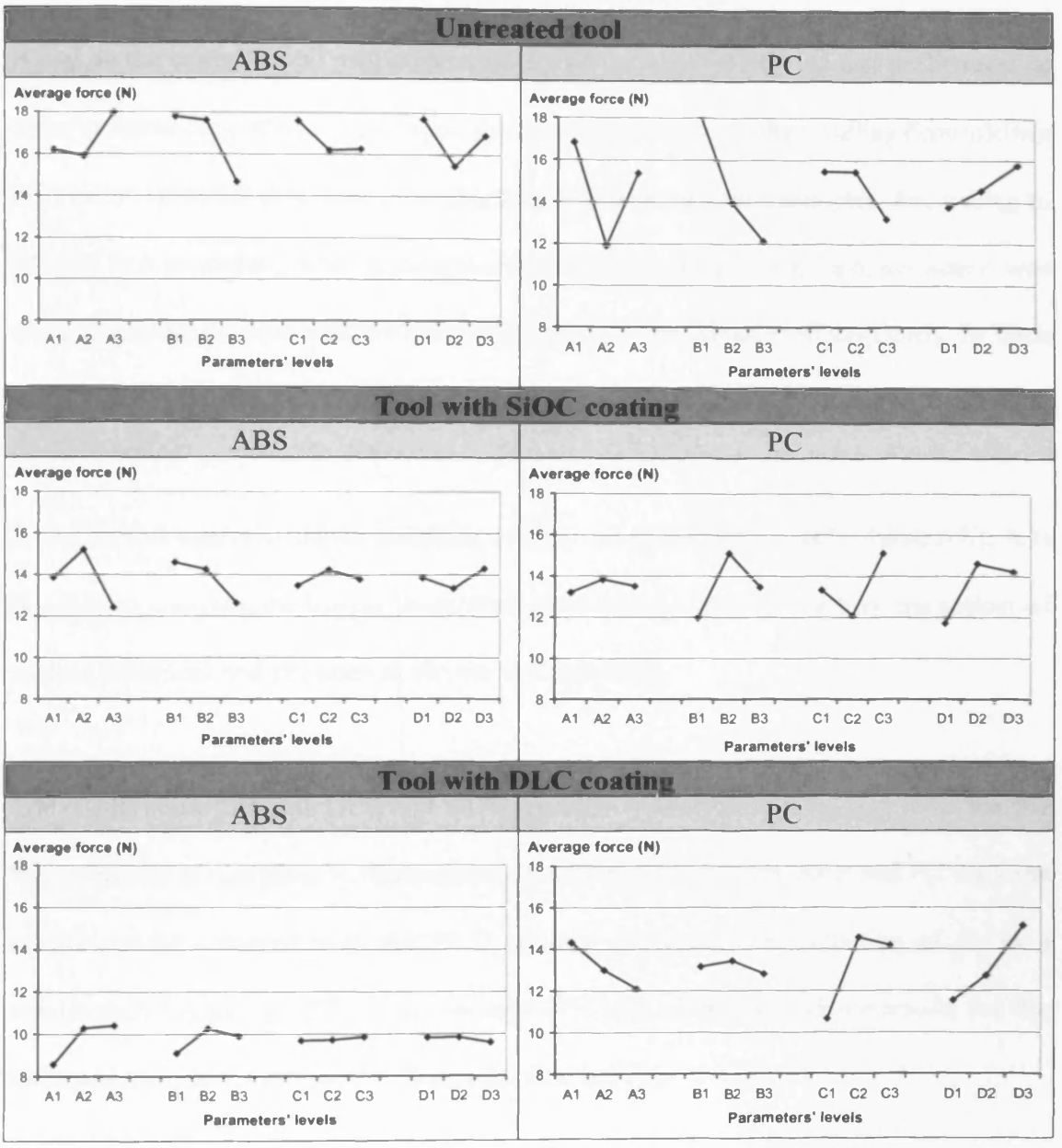

Figure 6.7 Main effects for each combination of surface treatments and polymers

Table 6.8 The theoretical best set of processing parameters

	T_b [°C]	T_m [°C]	t_c [s]	t_e [s]
Untreated & ABS	250	80	5	5
Untreated & PC	300	120	10	0
SiOC & ABS	280	80	1	5
SiOC & PC	280	80	5	0
DLC & ABS	220	40	1	10
DLC & PC	320	120	1	0

6.6.3 Parameters' contribution to optimum performance

Based on the experimental results, an analysis of variance (ANOVA) was performed in order to assess the contribution of each processing parameter to the resulting demoulding behaviour. Table 6.9 shows the percentage contribution of each parameter. According to the ANOVA procedure, when a particular factor was not significant, its contribution was disregarded and the contribution of the other factors were adjusted subsequently. In such cases, the percentage contributions of the process factors are not included in Table 6.9.

Based on this analysis and the selection of the best parameters' levels (Table 6.8), it is possible to compute the lowest theoretical demoulding force for each combination of surface treatment and polymer as shown in Table 6.10.

The results show that both DLC and SiOC coatings reduce the demoulding force for the two polymers investigated in this research. Furthermore, for both ABS and PC the best results can be achieved with the DLC coating. However, the reduction of F_E is a significantly higher for ABS, approximately 40% in comparison with the results for the untreated tool. In the case of PC, this reduction is 15%.

Table 6.9 Percentage contribution of each parameter

	Untreated tool		SiOC coating		DLC coating	
	ABS	PC	ABS	PC	ABS	PC
T_b	10.3	27.7	51.1	-	72.9	12.4
T_m	38.8	42.3	26.7	32.4	23.3	-
t_c	-	-	-	29.9	-	48.2
t_e	11.1	-	-	32.4	-	35.0

Table 6.10 The lowest theoretical demoulding force

	Untreated tool		SiOC coating		DLC coating	
	ABS	PC	ABS	PC	ABS	PC
F_E [N]	12.62	9.33	11.22	8.74	7.90	7.99

6.7 Summary and conclusions

The chapter reports an experimental study that investigates part demoulding behaviour in micro IM, with a particular focus on the effects of surface treatments on the demoulding forces. In particular, the demoulding performance of a representative microfluidics part was studied as a function of tool surface treatment in combination with four process parameters, T_b, T_m, t_c and t_c, employing the design of experiment approach. In addition, the results obtained using different combinations of process parameters were analysed to identify the best processing conditions in regards to demoulding behaviour of micro parts in the context of the surface treatments and polymer materials investigated in this research

The following conclusions can be made based on the reported research:

1. The average demoulding forces measured for both PC and ABS showed clearly that surface treatments reduce significantly F_E in comparison with untreated tools. The DLC coating resulted in a 40% reduction of F_E when using ABS while for PC it was more moderate, 16%. It is important to note that the part quality improved with the use of surface treated tools.

2. From the conducted six sets of experiments, it is immediately apparent that there is not a unique selection of parameter levels as far as the demoulding behaviour is concerned that can be considered optimum for the surface treatments or polymers investigated in this research. Thus, it is not possible to draw any conclusions about an optimum set of process parameters or generic rules that can apply to other polymers, too. Therefore, systematic experimental studies should

be carried out every time new combinations of tool treatments and polymers are considered.

3. By conducting an ANOVA analysis it was possible to assess process parameters' contribution to optimum performance. The lowest theoretical demoulding forces computed for each combination of tool treatment and polymer showed again that DLC and SiOC coatings reduce significantly the demoulding forces for the polymers considered in this research. Furthermore, by performing a Taguchi analysis it was possible to determine the best set of process parameters in regard to the demoulding forces for each of the investigated combinations of surface treatments and polymers.

Finally, it is important to stress that in micro IM the polymer properties become an even more important factor in selecting surface treatments. Experimental studies and simulations of demoulding behaviour should precede the tool manufacture.

CHAPTER 7

CONTRIBUTIONS, CONCLUSIONS AND FUTURE WORK

This chapter summarises the main contributions and the conclusions reached in this work. It also provides suggestions for future work.

7.1 Contributions

The overall aim of this research was to investigate the factors affecting the performance of micro-injection moulding technology. To carry out this research the following micro-injection moulding process concerns were investigated:

- The influence of runner size on the process performance;
- Tool surface finish effects on the process;
- Tool surface treatment effects on part de-moulding;
- Factors affecting the polymer flow length in micro cavities.

The main research finding and contributions to existing knowledge in micro injection moulding are presented below.

7.1.1 Runner system

The investigations into the relationship between the runner cross section and achievable flow length showed that the 2 mm size runner had the optimum surface to volume ratio and shear heating balance in regards to the filling performance. An increase of the runner

dimensions did not have a positive effect. Also, it was observed that imbalance in filling multiple micro cavities simultaneously increases with the increase of the runner size.

There is an optimal runner size for filling multi cavity micro tools and any further size reduction can lead to a temperature decrease from the set melt temperature. The use of a runner with an optimum dimensions results in an increase of the average temperature however the melt flow can be subjected to temperature variations. Such temperature variations affect the filling performance; in particular, the melt temperature is consistently the most important factor for improving polymer flow length. However, the results are not conclusive for low flow lengths.

The pre filling capabilities of multi cavity micro tools show that the reduction of the runner size and injection speed leads to a pressure increase. However, it should be noted that by increasing the pressure in this way there will not be significant gains in the filling performance.

7.1.2 Surface finish effects

The analysis of the filling of micro cavities with varying surface finish reveals that high settings of controlled process parameters, such as melt temperature, mould temperature, injection speed and tool surface roughness lead to high flow lengths. In particular, it was shown that surface finish and polymer temperature are the most important factors that affect to flow length. Also, the investigation shows that some polymers are less susceptible to changes of the process parameters and tool surface finish.

At some process settings that lead to high shear stress, in particular low melt temperature

and high injection speed, there are visual lines on the parts. These lines are an evidence of the slip stick effect during the filling stage. However, the carried our research did not identify any explicit relationship between the occurrence of the slip stick effect and the tool surface finish.

7.1.3 Process modelling and simulation

The use of existing FEA simulation models for predicting the flow behaviour in micro injection moulding show that they underestimate the polymer flow length in most of the cases. Based on the curried out simulation studies it can be stated that the 3D flow analysis provides a more accurate information about the filling of micro mould cavities than the dual domain flow analysis. In addition, it will be difficult to use the existing FEA tools to predict surface defects however they can be utilised to identify process conditions leading to defects such as unstable flow fronts, and excessive shear heating that leads to material degradation. The simulation studies showed that the overall injection time is the most important factor affecting part quality. In particular, low injection time is the main cause of the high shear stress in micro melt flows.

The simulation experiments revealed that the variations of flow front temperature in response to varying process parameters differ for different polymers. However, these changes in the process parameters do not have any significant effect on the flow lengths achieved in the experimental trials. At low to medium injection time the increase of the flow front temperature translates in an increase of the melt temperature above its set-up level. Hence, at these processing conditions shear heating occurs at the melt front, and a frozen layer along the cavity walls. At the same time setting high injection times in the simulation runs leads to rapid melt cooling, and thus due to the difference between mould

and barrel temperatures the polymer mobility is affected. Therefore, the temperature decrease resulting from the size effects in micro injection moulding can be compensated by reducing the injection time, and simultaneously the desired ejection temperature can be achieved by optimising the mould temperature.

7.1.4. Surface treatment effects

The investigation of part de-moulding from micro mould cavities revealed that surface treatments reduce significantly the de-moulding forces in comparison with untreated tools. Additionally, by using surface treated tools it is possible to improve part quality. From the conducted empirical studies of both the effects of process factors and the de-moulding behaviour, it is apparent that there is not a unique selection of process settings in regards to part de-moulding that can be considered optimum for different types of surface treatments or polymers investigated in this research. Therefore, systematic experimental studies should be carried out every time new combinations of tool treatments and polymers are considered. In addition, it is important to stress that in micro injection moulding the polymer properties become an even more important factor in selecting surface treatments.

7.2 Conclusions

Based on the carried our research the following generic conclusions can be made:

- The measurement of flow length in micro moulding is indicative of how well a part can fill, and thus replicate. Single and multiple cavity parts normally require a runner system to deliver the polymer to mould cavities, and its performance has a direct impact on the achievable flow lengths and part filling. The investigation

of runner size effects together with other process factors revealed that an optimum runner surface to volume ratio exists in regards to the filling performance. It was found that the variation of the polymer temperature and the speed with which it is injected has a direct effect on the filling performance of the runner. Additionally, it was shown that runner size can affect considerably the pressure and temperature of the polymer during the moulding process. Therefore, it is very important to select an appropriate runner system when designing micro moulding tools.

- The investigation into the potential influence of tool surface finish on achievable flow lengths identified that high process settings in particular the polymer temperature and high surface finish improve the filling of micro cavities. Similar to conventional moulding, at some processing conditions the interactions between the polymer and the tool surface can lead to slip stick effects. Though it was shown that tool surface finish contributes to the filling performance, no explicit relationship between the occurrence of the slip stick effect and the tool surface finish was found.
- In spite of the limitations of existing FEA simulation models for analysing the polymer flow in micro cavities, they can be applied successfully for identifying processing conditions that are difficult to predict by performing only empirical studies. In particular, process factors that influence melt flow temperature, pressure and shear conditions can be readily identified. Therefore, such FEA tools can be used to determine the optimum level of process parameters, and also to identify processing conditions that can lead to part defects and mould damage.
- Part de-moulding is a critical stage in the micro injection moulding, and any failures can lead to part and/or mould damage. By optimising process parameters and by applying surface treatments on tool cavities it is possible to reduce

significantly the adhesion and friction forces, and ultimately the de-moulding forces in order to eliminate and if not possible at least to reduce any detrimental effects on part quality during the ejection stage. The proposed experimental method for determining the best processing parameters for a given combination of a polymer and a surface treatment can be used to minimise the de-moulding forces.

7.3 Future work

The filling process in micro injection moulding involves the transportation of a polymer mass from the machine barrel to the cavity via a runner. This transfer is possible by applying a force and by displacing the air within the cavity. Having shown that the injection speed is an important factor affecting the moulding process, it follows that by varying this speed, the compression forces and the volume of air evacuated from the cavity will also vary. Therefore, it is necessary to study the effects of air evacuation and permissible venting during the micro moulding process. Such research should investigate the air displacement factors, temperature, rate and volume, with a particular focus on the localised heating and degradation of the polymer at the air/tool/polymer flow front interface. Additionally, the potential variation of air temperature and pressure in micro cavities could result in thermodynamic effects that increase the possibility of gas occurrence in the cavity that is polymer dependent. Such gas outputs resulting from the process have the potential to increase the toxicity of the moulded polymer, and corrode chemically the tool cavity or its surface treatment. This could result in premature aging and wear of the tool, and therefore a scientific investigation of the process thermodynamics is very important.

The effects of polymer flow and varying tool surface finish have been investigated in this study. The cavities with varying surface finish used in this research cover a wide range of sizes, however the nature of the machining processes applied to fabricate them results in a random surface topography. With the advances in tool-making processes it will be possible to produce micro and nano features in cavities with controlled surface topographies, and consequently the flow behaviour in such tools could be adversely or inversely affected. In this context, it is important to investigate the moulding of parts with micron and sub micron features of varying geometry, aspect ratio and direction to polymer flow. A series of specially designed test tools can be used to understand the polymer behaviour over a given range of tool structures, surfaces and materials. Consequently, these studies can provide an insight into process phenomena such as slip stick effects in micro injection moulding.

The experiments on de-moulding behaviour identified that surface treatments have the potential to reduce ejection forces and thus improve manufacturability. One area that requires further investigation is that of the operational life of the selected treatments. Lifecycle tests could be performed in a way similar to that of the conducted experimental study on de-moulding forces, whereby measurement of the ejection forces over time allows the optimum service life of the tool and its surface treatment to be predicted. Additionally, such experiments could be performed employing tools with different surface finish, resulting from pre- and post-surface treatments, and tools with structured nano features. The information gained through such studies could also be of use in understanding the tool - surface treatment wear mechanisms, and thus to perform planned re-treatment of moulding surfaces to prevent their damage.

Further advances in micro injection moulding process are expected to come from the machine tool development, new tool-making technologies and the use of specialised polymers. Machines that provide injection speeds exceeding those currently available are under development. At the same time major advances in tool-making technologies are required in regards to achievable surface quality and their integration in process chains for machining cavities that incorporate meso, micro and nano features, simultaneously. This should be complemented by advances in polymer materials and additives, and respective surface treatments for reducing tool wear and polymer-cavity adhesion and friction forces.

Such advances are just a pre-requisite, and should be supported by the development of new simulation models for more accurate prediction of melt flow behaviour at micro and even nano scale. Also, it is important to stress that all these technology and process developments should be underpinned by the advances in characterisation and inspection techniques and their standardisation in order to broaden the application area of the micro injection moulding process, and ultimately increase its take up by industry.

APPENDIX A

Viscosity and shear rate result differences between PP and ABS polymers

Table A.1 PP and ABS viscosity data

PP 220[C]	PP 236.7[C]	PP 253.3[C]	PP 270[C]	ABS 220[C]	ABS 240[C]	ABS 260[C]	ABS 280[C]
2697.12	2226.54	1867.65	1589.25	8543.26	3316.3	1478.14	745.329
2554.85	2119.77	1785.77	1525.2	8255.16	3257.15	1463.13	740.663
2408.16	2008.54	1699.72	1457.38	7939	3189.97	1445.78	735.228
2258.4	1893.77	1610.11	1386.19	7595.47	3114.11	1425.82	728.911
2107.07	1776.54	1517.71	1312.16	7226.2	3029.05	1402.94	721.59
1955.73	1658.01	1423.38	1235.94	6833.85	2934.39	1376.85	713.131
1805.94	1539.4	1328.05	1158.24	6422.07	2829.95	1347.27	703.393
1659.17	1421.93	1232.71	1079.85	5995.44	2715.81	1313.93	692.23
1516.82	1306.76	1138.33	1001.56	5559.3	2592.33	1276.62	679.496
1380.07	1194.99	1045.86	924.174	5119.49	2460.23	1235.2	665.048
1249.93	1087.56	956.152	848.469	4682.07	2320.58	1189.62	648.758
1127.18	985.263	869.979	775.14	4252.93	2174.8	1139.94	630.518
1012.36	888.727	787.966	704.794	3837.56	2024.59	1086.37	610.257
905.809	798.386	710.603	637.935	3440.71	1871.92	1029.24	587.946
807.637	714.508	638.237	574.947	3066.25	1718.84	969.066	563.611
717.795	637.197	571.074	516.097	2717.05	1567.47	906.478	537.347
636.08	566.418	509.192	461.539	2394.94	1419.81	842.239	509.318
562.17	502.019	452.559	411.324	2100.83	1277.68	777.196	479.765
495.657	443.754	401.046	365.411	1834.74	1142.59	712.24	448.997
436.074	391.305	354.452	323.685	1596.01	1015.77	648.258	417.387
382.915	344.307	312.52	285.972	1383.44	898.053	586.082	385.349
335.66	302.368	274.956	252.058	1195.41	789.943	526.452	353.321
293.79	265.079	241.441	221.694	1030.08	691.619	469.983	321.742
256.796	232.032	211.647	194.62	885.457	602.986	417.143	291.024
224.194	202.83	185.248	170.563	759.525	523.724	368.249	261.536
195.526	177.091	161.923	149.257	650.303	453.35	323.474	233.586
170.368	154.456	141.367	130.44	555.899	391.262	282.859	207.409
148.327	134.589	123.291	113.862	474.544	336.791	246.333	183.169
129.046	117.182	107.428	99.2887	404.616	289.238	213.738	160.954
112.203	101.954	93.5301	86.5027	344.64	247.902	184.853	140.789
97.5052	88.6495	81.3728	75.3037	293.299	212.105	159.412	122.644
84.6931	77.0396	70.752	65.5092	249.42	181.205	137.125	106.443
73.5345	66.9184	61.4844	56.9541	211.97	154.606	117.693	92.0788
63.8233	58.103	53.4055	49.4902	180.045	131.764	100.821	79.4218
55.3774	50.4307	46.3693	42.9846	152.857	112.19	86.2231	68.3298
48.0362	43.7578	40.2457	37.3192	129.724	95.4459	73.6331	58.6558
41.6585	37.9576	34.9199	32.3892	110.055	81.1439	62.8034	50.2536
36.1202	32.9184	30.2908	28.1019	93.3414	68.9439	53.5095	42.9825
31.3126	28.5424	26.2692	24.3757	79.1469	58.5483	45.5493	36.7099
27.1408	24.7437	22.7768	21.1387	67.0972	49.6987	38.7429	31.3134
23.5217	21.4472	19.7453	18.3279	56.872	42.1712	32.9316	26.6815
20.3828	18.5875	17.1146	15.8882	48.198	35.7725	27.976	22.7137
17.661	16.1071	14.8324	13.7711	40.8417	30.3367	23.7546	19.3206

15.3014	13.9564	12.8531	11.9346	34.6046	25.7211	20.1618	16.4234
13.256	12.0917	11.1368	10.3418	29.3173	21.8035	17.1064	13.9525
11.4833	10.4754	9.64884	8.96069	24.8359	18.4796	14.5097	11.8475
9.94704	9.0746	8.35905	7.76338	21.0382	15.6602	12.304	10.0559
8.61592	7.86063	7.2412	6.72555	17.8202	13.2695	10.4314	8.53223
7.46261	6.80873	6.27248	5.8261	15.0938	11.2426	8.84217	7.23721
6.46344	5.89734	5.43309	5.04665	12.784	9.52446	7.49388	6.13716

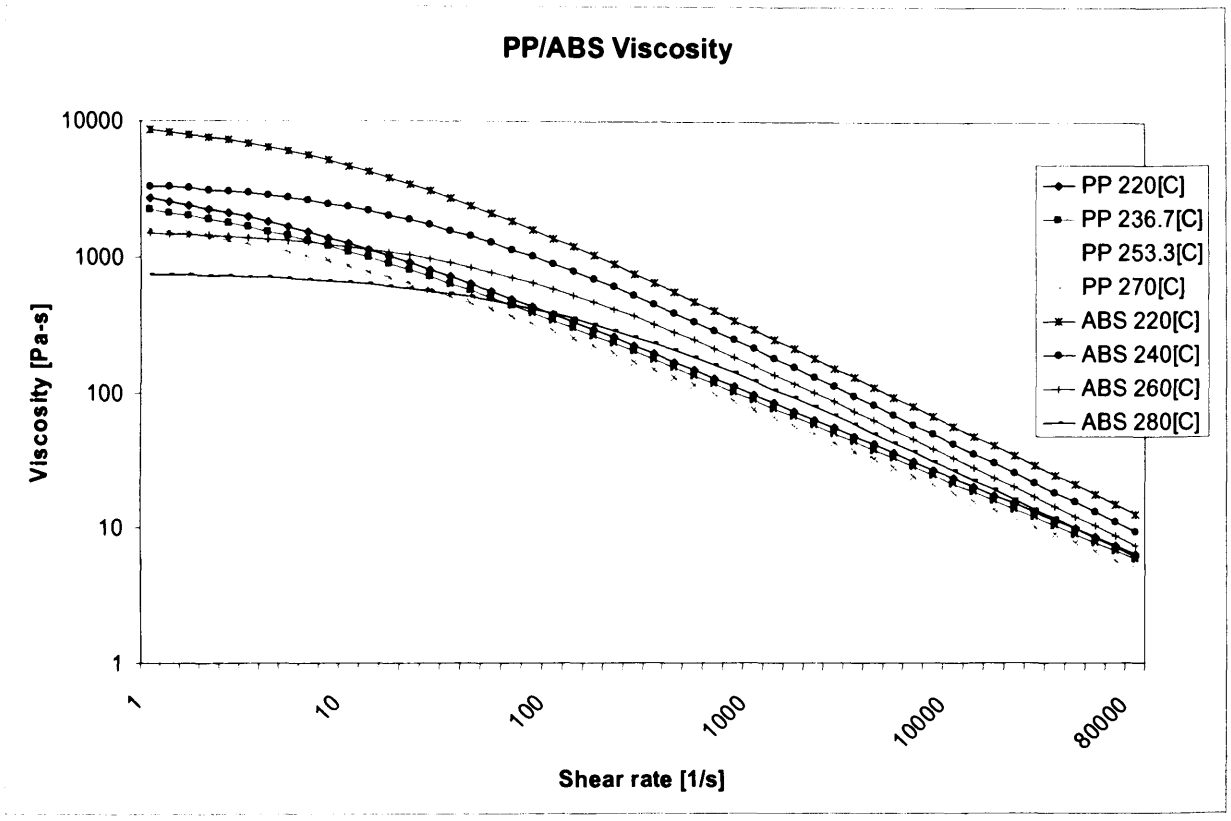

Figure A.1 PP and ABS viscosity curve

APPENDIX B

Pressure Volume and Temperature (PVT) for ABS and PC polymers

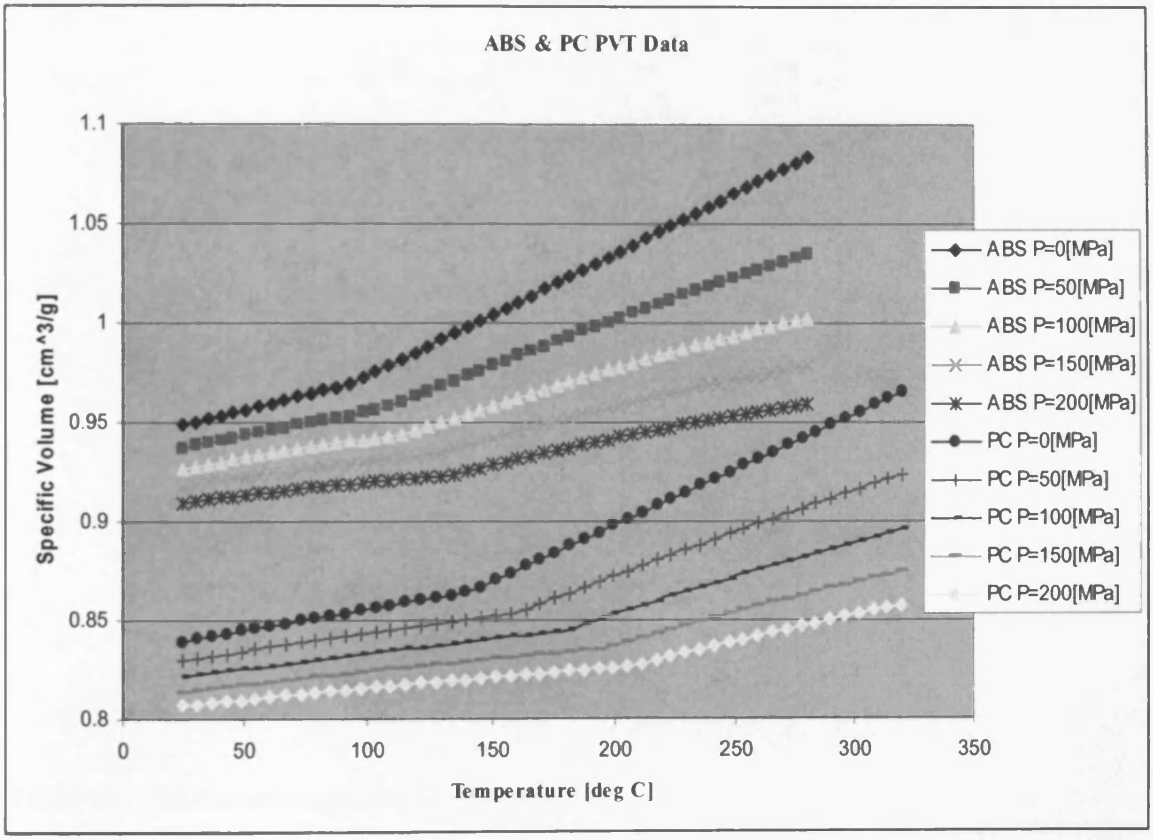

Figure B.1 ABS and PC PVT data

APPENDIX C

Conditioning monitoring average results for the runner experiments

Table C.1 Runner average cavity pressure results

ABS	3 mm	2 mm	1 mm
1	10.5	12.5	26.5
2	10.25	12.5	31
3	10.75	12.5	32.5
4	9	10	26
5	10.75	12.5	31.5
6	10.5	11	29
7	9	11	26
8	9.5	9	26.5
9	11	12	33
PP	3 mm	2 mm	1 mm
1	6.75	18.5	24.5
2	7.25	21.5	26.5
3	7.75	20	19.5
4	7.5	19.5	25
5	7.75	20.5	25
6	7.25	21.5	26.5
7	8.25	22	25
8	7.25	21.7	22
9	7.25	20	26

Table C.2 Runner average flow length results

	3 mm		2 mm		1 mm	
ABS	H	L	H	L	H	L
1	20	11	22	17	15.5	14.5
2	26.25	16	27.25	22.5	22.5	22.5
3	29	21	29	29	25	25
4	22	11	20	16	14.5	14.5
5	22.5	15	25.75	19	20.5	20.5
6	27.25	18	29	26.25	27.25	26.25
7	21	14	27.5	17	16	16
8	19	13	25.25	25.5	20	20
9	25.25	17	29	25.25	27.75	25.25
PP	H	L	H	L	H	L
1	11	5.5	29	29	29	29
2	29	24.25	29	29	29	29
3	29	29	29	29	29	29
4	25.25	19	29	29	29	29
5	29	23.25	29	29	29	29
6	29	25.25	29	29	29	29
7	29	23.25	29	29	29	29
8	27.25	21	29	29	29	29
9	29	25.25	29	29	29	29

Table C.3 Runner average temperature results

ABS	3 mm	2 mm	1 mm
1	58.45	74.22	59.72
2	36.16	33.13	10.63
3	12.77	6.83	-18.16
4	-0.22	62.32	47.82
5	11.85	2.84	-17.65
6	15.99	43.04	16.79
7	8.21	26.47	10.47
8	12.27	43.07	23.07
9	12.18	30.52	5.27
PP	3 mm	2 mm	1 mm
1	22	40	-3.22
2	21.19	46.02	13.06
3	21.66	24.81	-0.95
4	21.94	36.66	3.7
5	16.96	29.13	-1.66
6	27.49	46.71	19.89
7	13.95	24.25	-0.66
8	26.58	42.38	2.36
9	28.01	47.53	1.76

APPENDIX D

Average Flow length results for PP, ABS and PC

Table D.1 Average flow length results

PP Experiments								
1	2	3	4	5	6	7	8	9
48.82	52.33	54.17	47.6	51.94	54.28	51.62	53.67	52.54
47.43	53.31	55.3	50	55.28	52.74	48.5	51.67	54.13
47.3	50.8	55.3	46.54	51.43	54.05	49.8	53.89	55.07
46.11	52.4	55.07	49.37	51.69	55.5	49.7	51.72	55.3
46.24	52.8	55.49	48.53	50.58	55.42	50.48	53.9	53.78
48.46	52.11	52.82	51.21	54.43	55.52	48.75	53.05	53.39
46.82	51.9	55.49	48.9	49.58	55.6	49.09	50.88	54.69
48.8	50.55	55.35	47.94	54.89	55.5	51	51.26	54.1
44.69	52.71	55.49	51	55.21	55.29	49.7	53.9	54
48	51.8	52.53	48.42	53.93	53.04	49.3	54.04	54
47.267	52.071	54.701	48.951	52.896	54.694	49.794	52.798	54.1
ABS Experiments								
1	2	3	4	5	6	7	8	9
32.52	42.19	46.22	40.98	32.79	30.6	33.15	36.57	31.76
31.95	42.22	43.96	37.49	40.88	30.18	29.82	32.49	33.46
33.5	41.98	45.77	38.44	30.79	33.51	34.78	35.82	31.43
32.25	42.8	46.44	41.6	31.19	31.94	30.22	40.86	27.8
32.09	42.75	44.59	38.09	31.63	31.18	35.06	38.76	33.65
31.65	42.61	43.98	41.31	31.49	27	32.96	34.41	29.61
32.53	43.03	45.64	39.89	30.5	26	36.9	40.39	30.47
32.23	41.8	46.75	38.88	29.9	27.8	33.75	34.07	36.96
33.31	42.52	44.14	39.96	35.43	27.8	30.98	35.27	33.71
34.49	42.69	43.3	41.4	31.38	27.3	30.92	35.38	43.01
32.652	42.459	45.079	39.804	32.598	29.331	32.854	36.402	33.186
PC Experiments								
1	2	3	4	5	6	7	8	9
22.7	41.6	37.67	14.48	22.86	26.43	20	27.2	21.97
22.06	35.04	35.7	13.85	21.7	24.05	21.86	25.1	22.15
21.56	40.65	41.09	18.73	22	25.45	21.56	24.07	23.58
23.66	40.8	36.6	18.07	22.4	25.58	22.52	28.33	22.15
21.99	38.92	35.14	18.72	22.26	26.8	22.58	26.91	24.76
23.21	41.01	43.04	14.61	21.89	28.8	22.3	23.04	22.61
23.79	36.37	42.56	18.25	22.3	26.78	21.66	24.69	22.49
23.01	40.49	39.05	19.24	21.82	26.8	22.84	26.8	22.88
22.88	37.3	39.25	19.7	23.61	26.9	21.81	26.8	21.94
23.28	38	43.6	16.55	22.29	25.25	20	23.5	23.07
22.814	39.018	39.37	17.22	22.313	26.284	21.713	25.644	22.76

APPENDIX E

Fully meshed part for simulation experiments

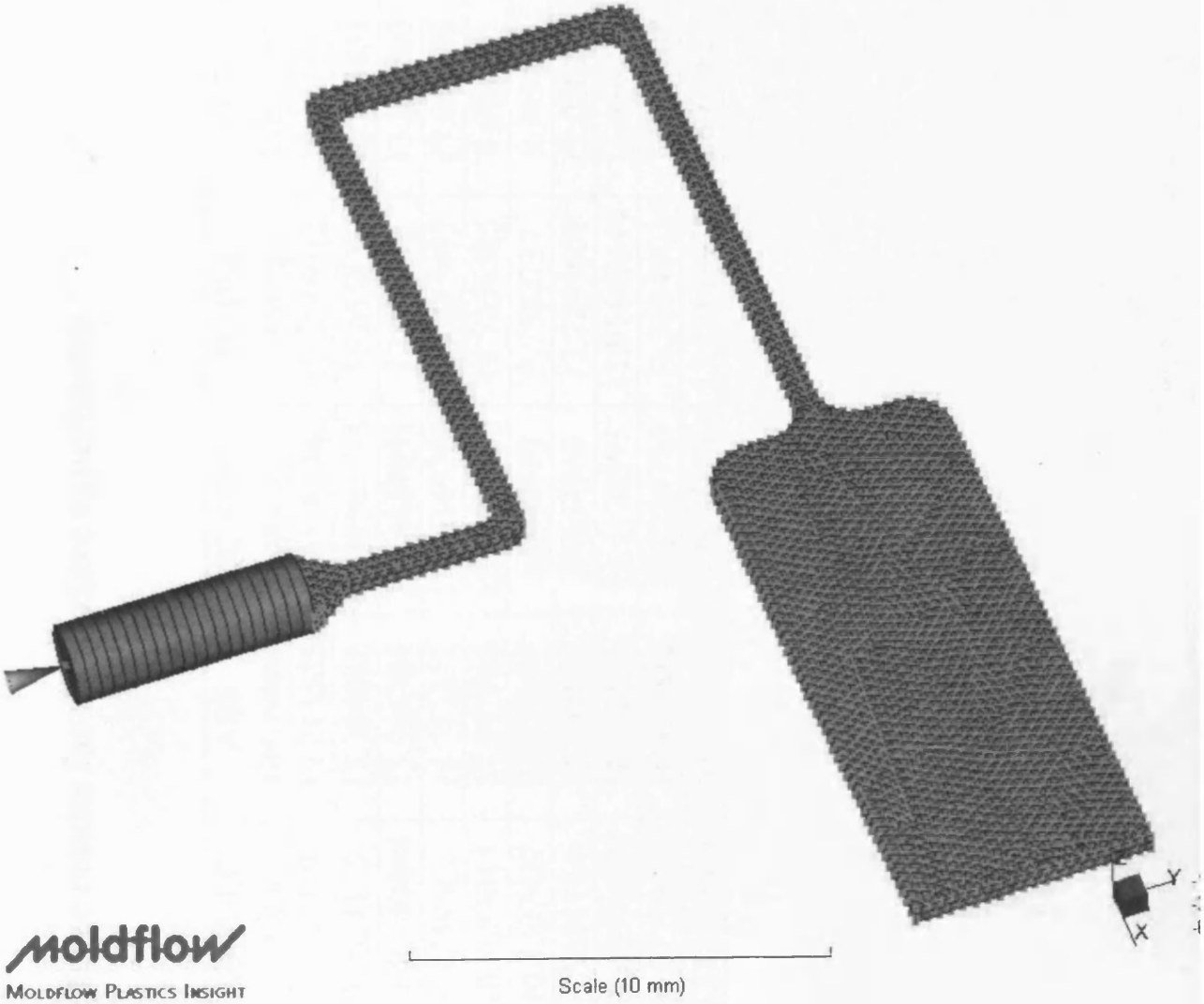

Figure E.1 Meshed part

APPENDIX F

Condition monitoring average force results for the surface experiments

Table F.1 Average Force results

L9 test	ABS SIOC coating	ABS DLC coating	ABS Untreated	PC SIOC coating	PC DLC coating	PC Untreated
T1	14.28349067	7.9149399	19.215525	9.661161462	10.2548012	19.977839
T2	14.21128291	9.1014175	15.384082	14.49561718	15.655878	16.713431
T3	13.06225978	8.640140444	13.996304	15.44459891	17.039848	13.820303
T4	16.8404516	9.4259662	16.713312	11.56169382	16.4475493	17.045679
T5	15.59264933	10.9683014	17.397562	15.22286675	12.7236585	8.698781
T6	13.15351956	10.4307427	13.527087	14.690193	9.7582737	9.949828
T7	14.03969933	9.9381184	17.397562	14.654969	12.7295609	17.026163
T8	12.9563035	10.68399189	20.036506	15.6128595	11.91549644	16.439731
T9	11.6544078	10.57756622	16.478882	10.2254796	11.5684303	12.608288
Average	13.97711828	9.742353851	16.68298022	13.50771547	13.12149959	14.69778256

REFERENCES

(2005) *The dictionary of science*, OUP Oxford; 5 edition

ALAM, K. & KAMAL, M. R. (2005) A robust optimization of injection molding runner balancing. *Computers & Chemical Engineering,* 29, 1934-1944.

ANDERSON, J. D. (1995) *Computational Fluid Dynamics: The Basics with Applications*, McGraw-Hill.

ANTONY, J. (2000) Multi-Response optimization in industrial experiments using Taguchi's quality loss function and principal components analysis. *Journal of Quality and Reliability Engineering,* 16, 3-8.

AZCARATE, S., URIARTE, L., BIGOT, S., BOLT, P., STAEMMLER, L., TOSELLO, G., ROTH, S., SCHOTH, A., WOLFGANG, M., STEFAN, D. & BERTRAND, F. (2006) Hybrid tooling: A review of process chains for tooling microfabrication within 4M. *4M 2006 - Second International Conference on Multi-Material Micro Manufacture.* Oxford, Elsevier.

BACHER, W., BADE, K., MATTHIS, B., SAUMER, M. & SCHWARZ, R. (1998) Fabrication of LIGA mold inserts. *Microsystem Technologies,* 4, 117-119.

BATAINEH, O. M. & KLAMECKI, B. E. (2005) Prediction of local part-mold and

ejection force in injection molding. *Journal of Manufacturing Science and Engineering-Transactions of the Asme,* 127, 598-604.

BELOFSKY, H. (1995) *Plastics:Product Design and Process Engineering* Hanser Publishers, Munich Vienna New York.

BENDADA, A., DERDOURI, A., LAMONTAGNE, M. & SIMARD, Y. (2004) Analysis of thermal contact resistance between polymer and mold in injection molding. *Applied Thermal Engineering,* 24, 2029-2040.

BIRD, R.B., ARMSTRONG, R.C., HASSAGER, O., Dynamics of Polymeric Liquids, Vol 1, John Wiley & Sons, 1987.

BILLMAYER, F. W. (1971) *Textbook of polymer science. Second edition*, John Wiley and Sons, NY.

BINET, C., HEANEY, D. F., SPINA, R. & TRICARICO, L. (2005) Experimental and numerical analysis of metal injection molded products. *Journal of Materials Processing Technology,* 164-165, 1160-1166.

BONACCURSO, E., BUTT, H.-J. & CRAIG, V. S. J. (2003) Surface Roughness and Hydrodynamic Boundary Slip of a Newtonian Fluid in a Completely Wetting System. *Physical Review Letters,* 90, 144501.

BOURDON, R. & SCHNEIDER, W. (2002) A Systematic Approach to Microinjection Moulding. *Business Briefing:Medical Device Manufacture & Technology.*

BRALLA, J. G. (1999) *Design for Manufacturability Handbook*, McGraw-Hill.

BROCHARD-WYART, F., DE GENNES, P. G. & PINCUS, P. (1992) *C.R Acad.Sci.*, 314-873.

CHANG, R., Y. & YANG W, H. (2001) A novel three dimensional analysis of polymer injection molding. *ANTEC 2001 Conference Proceedings.*

CHANG, R. Y., CHEN, C. H. & SU, K. S. (1996) Modifying the Tait equation with cooling-rate effects to predict the pressure-volume-temperature behaviors of amorphous polymers: modeling and experiments *Polymer Engineering and Science (USA),* 36, 1789-1795.

CHANG, R.Y. & YANG W.H Numerical simulation of mold filling in injection molding using a three-dimensional finite volume approach *International Journal for Numerical Methods in fluids Int. J. Numer. Meth. Fluids* 2001; 37: 125–148 (DOI: 10.1002/fld.166).

CLAVERIA, I., JAVIERRE, C. & PONZ, L. (2005) Method for generation of rheological model to characterize non-conventional injection molding by means of spiral mold. *Journal of Materials Processing Technology,* 162-163, 477-483.

COATES, P. D., WHITESIDE, B. R., MARTYN, M. T., SPARES, R., GOUGH, T., WOLFGANG, M., STEFAN, D. & BERTRAND, F. (2006) Micromoulding -- precision processing for controlled products. *4M 2006 - Second International Conference on Multi-Material Micro Manufacture.* Oxford, Elsevier.

COSMA, L. (2001) *Thin wall processing of engineering resins. Specialised molding techniques*, William Andrew Inc.

CUNHA, L., ANDRITSCHKY, M., PISCHOW, K., WANG, Z., ZARYCHTA, A., MIRANDA, A. S. & CUNHA, A. M. (2002) Performance of chromium nitride and titanium nitride coatings during plastic injection moulding. *Surface and Coatings Technology,* 153, 160-165.

DAWKINS, R. (2006) *The God Delusion* Bantam Press.

DEARNLEY, P. A. (1999) Low friction surfaces for plastic injection moulding dies--an experimental case study. *Wear,* 225-229, 1109-1113.

DEL VECCHIO, R. J. (1997) *Understanding Design of experiments: A Primer for Technologists*, Hanser/Gardner Publications.

DIMOV, S. (2005) 4M Network of excellence: An Instrument for Integration of European research in Multi-Material Micro Manufacture IN UK, E. (Ed.) *First international conference on Multi-Material Micro Manufacture.*

DIMOV, S., PHAM, D., IVANOV, A., POPOV, K. & FANSEN, K. (2004) Micromilling strategies: optimization issues. *Proceedings of the Institution of Mechanical Engineers, Part B: Journal of Engineering Manufacture,* 218, 731-736.

DIMOV, S. S., MATTHEWS, C. W., GLANDFIELD, A., DORRINGTON, P., WOLFGANG, M., STEFAN, D. & BERTRAND, F. (2006) A roadmapping study in Multi-Material Micro Manufacture. *4M 2006 - Second International Conference on Multi-Material Micro Manufacture.* Oxford, Elsevier.

DOBREV, T., PHAM, D. T. & DIMOV, S. S. (2005) A simulation model for crater formation in Laser milling. IN MENZ, W. & DIMOV, S. (Eds.) *Proceedings of First International Conference on Multi-Material Micro Manufacture.* Kurstruhe, Germany, Elsevier (Oxford).

DRDA, P., P, WANG.S. (1995) Slip Stick transition at polymer Melt/Solid Interfaces. *Physical review letters of the American Physical society,* 75, 2698-2701.

DRDA, P. P. & WANG, S.-Q. (1995) Stick-Slip Transition at Polymer Melt/Solid Interfaces. *Physical Review Letters,* 75, 2698.

EHMANN, K. F. (2007) A Synopsis of U.S. Micro-Manufacturing Research and Development Activities and Trends. *4M 2007 Proceedings of the 3rd International Conference on Multi-material Micro Manufacture.* Whittles publishing.

ENGELMANN, P. & DEALEY, R. (2000) Injection mold design guidelines: Maximizing performance using copper alloys. *Modern Mold and Tooling*, 49-52.

FAN, B., KAZMER, D. & NAGERI, R. (2006) An Analytical Non-Newtonian and Nonisothermal Viscous Flow Simulation. *Polymer-Plastics Technology and Engineering*, 45, 429-438.

FRICK, A., STERN, C. & BERGER, U. (2005) Manufacturing of high quality micro prototypes by injection moulding using hybrid mould technology. *4M 2005 - First International Conference on Multi-Material Micro Manufacture.* Oxford, Elsevier.

GANDARIAS, E., DIMOV, S., PHAM, D., IVANOV, A., POPOV, K., LIZARRALDE, R. & ARRAZOLA, P. (2006) New Methods for Tool Failure Detection in Micromilling. *Proceedings of the Institution of Mechanical Engineers, Part B: Journal of Engineering Manufacture,* 220, 137-144.

GOWER, M. (2000) industrial applications of laser micromachining. *Optics Express,* 7, 56-67.

GREENE, J. P. (1997) Numerical Analysis of injection moulding of glass fiber reinforced thermoplastics Part 1 Injection flow and pressure. *Journal of Polymer Engineering and Science,* 37, 590-602.

GRIFFITHS, C., BIGOT, S., BROUSSEAU, E., WORGULL, M., HECKELE, M., NESTLER, J. & AUERSWALD, J. (2007) Polymer inserts tooling for prototyping of micro fluidic components in micro injection moulding. *4M 2007 Proceedings of the 3rd International Conference on Multi-material Micro Manufacture.* Whittles publishing.

GRIFFITHS, C. A., DIMOV, S. S., PHAM, D. T., WOLFGANG, M., STEFAN, D. & BERTRAND, F. (2006) Micro injection moulding: The effects of tool surface finish on melt flow behaviour. *4M 2006 - Second International Conference on Multi-Material Micro Manufacture.* Oxford, Elsevier.

GRILL, A. (2003) Diamond-like carbon coatings as biocompatible materials-an overview. *Diamond and Related Materials,* 12, 166-170.

GRILLET, A. M., BOGAERDS, A. C. B., PETERS, G. W. M. & BAAIJENS, F. P. T. (2002) Numerical analysis of flow mark surface defects in injection moulding flow. *The Journal of Rheology,* 46, 651-669.

HAEFLIGER, D., NORDSTROM, M., RASMUSSEN, P. A. & BOISEN, A. (2005) Dry release of all-polymer structures. *Microelectronic Engineering,* 78-79, 88-92.

HANSEN, H. N. & THEILADE, U. A. (2005) Surface microstructure replication in injection moulding. *Proceedings of First International Conference on Multi-Material Micro Manufacture.*

HARMANDARIS, V. A., MAVANTZAS, V. G., THEODOROU, D. N., KROGER, M., RAMIREZ, J., OTTINGER, H. C. & D. VLASSOPOULOS, D. (2003) Cross over from the Rouse to the entangled polymer melt regime: Signals from long detailed atomistic molecular dynamics simulations supported by rheological experiments. *American Chemical Society Macromolecules,* 36, 1376-1387

HARRIS, R., NEWLYN, H. & DICKENS, P. (2002) Selection of mould design variables in direct stereolithography injection mould tooling. *Proceedings of the Institution of Mechanical Engineers, Part B: Journal of Engineering Manufacture,* 216, 499-505.

HAUERT, R. (2003) A review of modified DLC coatings for biological applications. *Diamond and Related Materials,* 12, 583-589.

HEINZE, M. (1998) Wear resistance of hard coatings in plastics processing. *Surface and Coatings Technology,* 105, 38-44.

HELLELOID, G. T. (2001) On the computation of viscosity shear rate temperature master curves for polymetric liquids. *ournal of Applicable Mathematics,* 1, 1-11.

HEYDERMAN, L. J., SCHIFT, H., DAVID, C., GOBRECHT, J. & SCHWEIZER, T. (2000) Flow behaviour of thin polymer films used for hot embossing lithography. *Microelectronic Engineering,* 54, 229-245.

HIEBER, C. A. & SHEN, S. F. (1995) A finite-element/finite-difference simulation of the

injection molding filling process. *Journal of Non-Newtonian Fluid Mechanics,* 56, 361-361.

HOPKINSON, N. & DICKENS, P. (1999) Study of ejection forces in the AIMTM process. *Materials & Design,* 20, 99-105.

HTTP://BRAD.AC.UK/ACAD/UKMIG/MEMBERS/HIGHSHEAR.HTM.

HTTP://EN.WIKIPEDIA.ORG/WIKI/MOORES_LAW.

HTTP://WWW.DEVICELINK.COM/EMDM/ARCHIVE/99/03/REPORT.HTML.

HTTP://WWW.DSM.COM/EN_US/HTML/DEP/COLDRUNNERSYSTEMS.HTM.

HTTP://WWW.IMMNET.COM/ARTICLES?ARTICLE=665.

INN, Y. & WANG, S. (1996) Hydrodynamic Slip: polymer adsorption and desorption at melt/solid interfaces. *Physical review letters of the American Physical Society,* 76, 467-470

J.A.HEIMBERG, K. J. W., I.L.SINGER (2001) Superlow friction behaviour of diamond like carbon coatings:Time and speed effects. *Applied Physics letters* 78.

JAVIERRE, C., FERNANDEZ, A., AISA, J. & CLAVERIA, I. (2006) Criteria on

feeding system design: Conventional and sequential injection moulding. *Journal of Materials Processing Technology,* 171, 373-384.

JOHANNABER, F. (1994) *Injection moulding machines A users Guide*, Carl hanser publishers Munich Vienna new York.

JURISCHKA, R., A.SCHOTH, MULLER, C., THIEBAUD, D., GALLERA, R. & H.REINECKE (2006) Hard Tooling by μEDM - milling for Injection Moulding. *Proceedings of second International Conference on Multi-Material Micro Manufacture (4M)*, 199-202.

KEMMANN, O. & WEBER, L. (2001) *Simulation of the Micro Injection Molding Process. Specialised molding techniques*, William Andrew Inc.

KENNEDY, P. (1993) *Flow Analysis Reference Manual* Victoria. Austrailia, Moldflow Pty ltd.

KIM, S. M. & KANG, S. (2003) Replication qualities and optical properties of UV-moulded microlens arrays. *Journal of Physics D: Applied Physics,* 36, 2451-2456.

KIM, Y., BAE, J., KIM, H. & KANG, S. (2004) Modelling of passive heating for replication of sub-micron patterns in optical disk substrates. *Journal of Physics D, Applied Physics,* 37, 1319-1326.

KINSELLA, M. E., LILLY, B., GARDNER, B. E. & JACOBS, N. J. (2005) Experimental determination of friction coefficients between thermoplastics and rapid tooled injection mold materials *Rapid Prototyping Journal* 11 167 - 173

KNOWLES, M., RUTTERFORD, G., KARNAKIS, D. & FERGUSON, A. (2007) Micro-machining of metals, ceramics and polymers using nanosecond lasers. *The International Journal of Advanced Manufacturing Technology,* 33, 95-102.

KUKLA, C., LOIBL, H., DETTER, H. & HANNENHEIM, W. (1998) Micro injection moulding – The aims of a project partnership. *Kunstoffe Plast. Europe, 6.*

KUSSUL, E. M., RACHKOVSKIJ, D. A., BAIDYK, T. N. & TALAYEV, S. A. (1996) Micromechanical engineering: a basis for the low cost manufacturing of mechanical microdevices using micro equipment. *J.Micromech.Microeng,* 6, 410-425.

KWAK, S., KIM, T., PARK, S. & LEE, K. (2003) Layout and sizing of ejector pins for injection mould desian using the wavelet transform. *Proceedings of the Institution of Mechanical Engineers, Part B: Journal of Engineering Manufacture,* 217, 463-473.

LAUGA, E., BRENNER, M. P. & STONE, H. A. (2005) Handbook of Experimental Fluid Dynamics. IN EDS FOSS, J., TROPEA,C., AND YARIN, A (Ed.) *Microfluidics: the no slip boundary condition.* Springer, NY.

LEE, H. S. (1997) Finite element analysis for the flow characteristics along the thickness

direction in injection molding. *Polymer Engineering & Science,* 37, 559-567.

LEGER, L. (2003) Friction mechanisms and interfacial slip at fluid solid interfaces. *J.Phys Condens. Matter,* 15.

LEGER, L., HERVET, H., MASSEY, G. & DURLIAT, E. (1997) Wall slip in polymer melts. *J.Phys Condens. Matter,* 9, 7719-7740.

LI, C. S. & SHEN, Y. K. (1995) Optimum design of runner system balancing in injection molding. *International Communications in Heat and Mass Transfer,* 22, 179-188.

LOESCHNER, H., STENGL, G., BUSCHBECK, H., CHALUPKA, A., LAMMER, G., PLATZGUMMER, E. & VONACH, H. (2003) Large-field particle beam optics for projection and proximity printing and for maskless lithography. *Journal of Microlithography, Microfabrication, and Microsystems* 2, 34-48.

MADOU, M. J. (2001) *Fundamentals of microfabrication,* CRC Press.

MADOU, M. J., LEE, L. J., DAUNERT, S., LAI, S. & SHIH, C.-H. (2001) Design and Fabrication of CD-like Microfluidic Platforms for Diagnostics: Microfluidic Functions. *Biomedical Microdevices,* 3, 245-254.

MASUZAWA, T. (2000) State of the art of micromachining. *Annals of the CIRP,* 49, 473-488.

MASUZAWA, T. (2001) Micro-EDM, Proceedings of the 13th International Symposium for Electromachining ISEM XIII.

MASUZAWA, T., FUJINO, M. & KOBAYASHI, K. (1985) Wire electro-discharge grinding for micro-machining. *Annals of the CIRP,* 34, 431-434.

MCFARLAND, A. W. & COLTON, J. S. (2004) Production and analysis of injection molded micro-optic components. *Society of Plastics Engineers Polymer Engineering and Science,* 44, 564-579.

MEEUSEN, W. (2003) Micro-Electro-Discharge: Technology, computer-aided design & manufacturing and applications. *Department of Mechanical Engineering* Leuven.

MEHTA, N. M. & BARRY, C. (2003) Validation of flow simulation for micro moulded parts. *Proceedings of the ANTEC International Conference.*

MEIJER, J., DU, K., GILLNER, A., HOFFMANN, D., KOVALENKO, V. S., MASUZAWA, T., OSTENDORF, A., POPRAWE, R. & SCHULZ, W. (2002) Laser Machining by short and ultrashort pulses, state of the art and new opportunities in the age of the photons. *CIRP Annals - Manufacturing Technology,* 51, 531-550.

MENGES, G. & MOHREN, P. (Eds.) (1993) *How to Make Injection Molds* Hanser Gardner

MICHAELI, W., OPFERMANN, D. & KAMPS, T. (2007) Advances in micro assembly injection moulding for use in medical systems. *The International Journal of Advanced Manufacturing Technology,* Volume 33, 206-201.

MITTERER, C., HOLLER, F., REITBERGER, D., BADISCH, E., STOIBER, M., LUGMAIR, C., NOBAUER, R., MULLER, T. & KULLMER, R. (2003) Industrial applications of PACVD hard coatings. *Surface and Coatings Technology,* 163-164, 716-722.

MÖNKKÖNEN, K., PAKKANEN, T. T., HIETALA, J., PÄÄKKÖNEN, E. J., PÄÄKKÖNEN, P., JÄÄSKELÄINEN, T. & KAIKURANTA, T. (2002) Replication of sub-micron features using amorphous thermoplastics. *Polymer Engineering & Science,* 42, 1600-1608.

MUCCIO, E., A (1994) *Plastics Processing technology* ASM International.

NAMSEOK, L., YOUNG-KYN, K. & SHINILL, K. (2004) Temperature dependence of anti-adehesion between a stamper with sub-micron patterns and the polymer in nano-moulding processes. *Journal of physics D: Appl.Phys,* 35, 1624-1629.

NAVABPOUR, P., TEER, D. G., HITT, D. J. & GILBERT, M. (2006) Evaluation of non-stick properties of magnetron-sputtered coatings for moulds used for the processing of polymers. *Surface and Coatings Technology,* 201, 3802-3809.

NAVIER, C. L. M. H. (1827) Mem. Acad. Sci Inst. Fr 6, 839 (1827).

NETO, C., EVANS, D. R., E. BONACCURSO, E., BUTT, H. J. & CRAIG, V. S. J. (2005) Boundary slip of Newtonian liquids: A review of experimental studies *Rep. Prog. Phys.*, 68, 2859-2897.

NICHETTI, D. & MANAS-ZLOCZOWER, I. (1998) Viscosity model for polydisperse polymer melts. *The Journal of Rheology,* 42, 951-969.

NICOUD, J. D. (1995) Microengineering:when is small too small? Nanoengineering:when is large too small. *IEEE Sixth International Symposium on Micro machine and Human Science*

OCHIAI, Y., MANAKO, S., FUJITA, J. & NOMURA, E. (1999) High resolution organic resists for charged particle lithography. *Journal of Vacuum Science & Technology B,* 17, 933-938.

OZCELIK, B. & ERZURUMLU, T. (2006) Comparison of the warpage optimization in the plastic injection molding using ANOVA, neural network model and genetic algorithm. *Journal of Materials Processing Technology,* 171, 437-445.

PEARSON, J. R. A. (1976) Instability in Non-Newtonian Flow. *Annual Review of Fluid Mechanics* 8, 163-181.

PHAM, D., DIMOV, S., JI, C., PETKOV, P. & DOBREV, T. (2004) Laser milling as a 'rapid' micromanufacturing process. *Proceedings of the Institution of Mechanical Engineers, Part B: Journal of Engineering Manufacture,* 218, 1-7.

PHAM, D., DIMOV, S., PETKOV, P. & PETKOV, S. (2002) Laser milling. *Proceedings of the Institution of Mechanical Engineers, Part B: Journal of Engineering Manufacture,* 216, 657-667.

PHAM., G. T. & COLTON., J. S. (2002) Ejection force modeling for stereolithography injection molding tools. *Polymer Engineering & Science,* 42, 681-693.

PIOTTER, V., MUELLER, K., PLEWA, K., RUPRECHT, R. & HAUSSELT, J. (2002) Performance and simulation of thermoplastic micro injection molding. *Microsystem Technologies,* 8, 387-390.

PLATZGUMMER, E., BIEDERMANN, A., LANGFISCHER, H., EDER-KAPL, S., KUEMMEL, M., CERNUSCA, S., LOESCHNER, H., LEHRER, C., FREY, L., LUGSTEIN, A. & BERTAGNOLLI, E. (2006) Simulation of ion beam direct structuring for 3D nanoimprint template fabrication. *Microelectronic Engineering,* 83, 936-939.

PONTES, A. J. & POUZADA, A. S. (2004) Ejection force in tubular injection moldings. Part I: Effect of processing conditions. *Polymer Engineering and Science,* 44, 891-897.

PONTES, A. J., POUZADA, A. S., PANTANI, R. & TITOMANLIO, G. (2005) Ejection force of tubular injection moldings. Part II: A prediction model. *Polymer Engineering & Science,* 45, 325-332.

POPOV, K., DIMOV, S., PHAM, D. & IVANOV, A. (2006) Micromilling strategies for machining thin features. *Proceedings of the Institution of Mechanical Engineers, Part C: Journal of Mechanical Engineering Science,* 220, 1677-1684.

POSLINSKI, A. J. (Ed.) (2001) *Effects of processing conditions and material models on the injection pressure and flow length in thin wall parts,* NY, William Andrew Publishing.

POTOCNIK, J. (2007) The Future of Science & Technology in Europe. Lisbon Portugal.

POUZADA, A. S., FERREIRA, E. C. & PONTES, A. J. (2006) Friction properties of moulding thermoplastics. *Polymer Testing,* 25, 1017-1023.

PRIEZJEV, N. V. & TROIAN, S. M. (2004) Molecular Origin and Dynamic Behavior of Slip in Sheared Polymer Films. *Physical Review Letters,* 92, 018302.

CRAWFORD, R.J. (Ed.) (1987) *Plastics Engineering 2nd Edition* Pergamon Press.

REES, A., DIMOV, S., IVANOV, A., HERRERO, A. & URIARTE, L. (2007) Micro-electrode discharge machining: factors affecting the quality of electrodes produced on the

machine through the process of wire electro-discharge machining. *Proceedings of the Institution of Mechanical Engineers, Part B: Journal of Engineering Manufacture,* 221, 409-418.

RICE, J.G. & SCHNIPKE, R.J. An Equal-Order Velocity-Pressure Formulation That Does Not Exhibit Spurious Pressure Modes, *Comp. Meth. Appl. Mech. Eng., 58* (1986) 1315-149

Roy, R., ed. A primer on the Taguchi method. 1990, Van Nostrand Reinhold,New York.

BIGOT, S,. IVANOV, ANATAS., POPOV, K. (2005) A study of the micro EDM electrode wear. *4M 2005 - First International Conference on Multi-Material Micro Manufacture*
Oxford, Elsevier.

YUAN, S,. HUNG, N. P., NGOI, B. K. A. & ALI., M. Y. (2003) Development of microreplication process-Micromoulding. *Materials and manufacturing processes* 18, 731-751.

SAITO, T., SATOH, I. & KUROSAKI, Y. (2002) A new concept of active temperature control for an injection molding process using infrared radiation heating. *Polymer Engineering & Science,* 42, 2418-2429.

SASAKI, T., KOGA, N., SHIRAI, K., KOBAYASHI, Y. & TOYOSHIMA, A. (2000) An experimental study on ejection forces of injection molding. *Precision Engineering,* 24, 270-273.

SAWYER, W. G., FREUDENBERG, K. D., BHIMARAJ, P. & SCHADLER, L. S. (2003) A study on the friction and wear behavior of PTFE filled with alumina nanoparticles. *Wear,* 254, 573-580.

SHA, B., DIMOV, S., GRIFFITHS, C. & PACKIANATHER, M. S. (2007a) Investigation of micro-injection moulding: Factors affecting the replication quality. *Journal of Materials Processing Technology,* 183, 284-296.

SHA, B., DIMOV, S., GRIFFITHS, C. & PACKIANATHER, M. S. (2007b) Micro-injection moulding: Factors affecting the achievable aspect ratios. *The International Journal of Advanced Manufacturing Technology,* Volume 33.

SHAMES, I. H. (1992) *Mechanics of Fluids* NY, McGraw Hill.

SHEN, Y. K., SHIE, Y. J. & WU, W. Y. (2004) Extension method and numerical simulation of micro injection moulding. *International Communications in Heat and Mass Transfer,* 31, 795-804.

SHEN, Y. K. & WU, W. Y. (2002) An Analysis of the three-dimensional micro-injection molding. *International Communications in Heat and Mass Transfer,* 29, 423-431.

SHEN, Y. K., YEH, S. L. & CHEN, S. H. (2002) THREE-DIMENSIONAL NON-NEWTONIAN COMPUTATIONS OF MICRO-INJECTION MOLDING WITH THE FINITE ELEMENT METHOD. *International Communications in Heat and Mass Transfer,* 29, 643-652.

SMIALEK, C. D. & SIMPSON, C. L. (2001) *Flow instabilities in thin walled moulding of thermoplastic Polyurethane.* , NY, William Andrew Publishing.

SPINA, R. (2004) Injection moulding of automotive components: comparison between hot runner systems for a case study. *Journal of Materials Processing Technology,* 155-156, 1497-1504.

SU, Y. C., SHAH, J., AND LIN, L. (2004) Implementation and analysis of polymetric microstructure replication by micro injection moulding. *Journal of Micromechanics and Microengineering,* 14, 415-422.

TADMOR, Z. & GOGOS, C. (1973) *Principles of polymer processing*, John Wiley and Sons, NY.

TANG, P. T., FUGL, J., URIARTE, U., BISSACCO, G. & HANSEN, H. N. (2006a) Indirect tooling based on micromilling, electroforming and selective etching. *4M 2006 - Second International Conference on Multi-Material Micro Manufacture.*

TANG, S. H., KONG, Y. M., SAPUAN, S. M., SAMIN, R. & SULAIMAN, S. (2006b) Design and thermal analysis of plastic injection mould. *Journal of Materials Processing Technology,* 171, 259-267.

TAYLOR, J. B., KANDLIKAR, S. G. & CARRANO, A. L. (2005) Characterisation of the effect of surface roughness and texture on fluid flow past present and future. *Proceedings of ICMM2005 3rd International Conference on Microchannels and Minichannels.*

TERAMACHI, S., HASEGAWA, A., AKATSUKA, M. & YAMASHITA, A. (1978) Molecular Weight Distribution and Correlation between Chemical Composition and Molecular Weight in a high conversion copolymer of styrene-methyl acrylate. *American Chemical Society Macromolecules*, 1206.

THEILADE, U. R. O. (2004) Surface micro topography replication in injection moulding. *DTU Department of Manufacturing Engineering and Management,* . Technical University of Denmark.

THRONE, J. L. (1979) *Plastic Process Engineering*, Marcel Dekker INC New York and Basel.

TOSELLO, G., FILLON, B., AZCARATE, S., SCHOTH, A., MATTSSON, L., GRIFFITHS, C., STAEMMLER, L. & BOLT, P. J. (2007) Application of different process chains for polymer microfluidics fabrication including hybrid tooling

technolgies,standardization and replication: a benchmark investigation within 4M Polymer Division. *Proceedings of third International Conference on Multi-Material Micro Manufacture (4M)*, 77-80.

UDDIN, M., HO, W., CHOW, C. & CHAN, H. (2006) Interfacial adhesion of spin-coated thin adhesive film on silicon substrate for the fabrication of polymer optical waveguide. *Journal of Electronic Materials,* 35, 1558-1565.

URIARTE, L., HERRERO, A., IVANOV, A., OOSTERLING, H., STAEMMLER, L., TANG, P. & ALLEN, D. (2006) Comparison between microfabrication technologies for metal tooling. *Proceedings of the Institution of Mechanical Engineers, Part C: Journal of Mechanical Engineering Science,* 220, 1665-1676.

VAN STAPPEN, M., VANDIERENDONCK, K., MOL, C., BEECKMAN, E. & DE CLERCQ, E. (2001) Practice vs. laboratory tests for plastic injection moulding. *Surface and Coatings Technology,* 142-144, 143-145.

VOEVODIN, A. A., DONLEY, M. S. & ZABINSKI, J. S. (1997) Pulsed laser deposition of diamond-like carbon wear protective coatings: a review. *Surface and Coatings Technology,* 92, 42-49.

WEBBER, L. & EHRFELD, W. Micromoulding Market Position and Development Kunststoffe 89(10) (1999) pp 192-102.

WELTY, J. R., WICKS, C. E. & WILSON, R. E. (1984) *Fundamentals of Momentum, Heat, and Mass transfer,* NY, Wiley.

WIMBERGER-FRIEDL, R. (Ed.) (2001) *Injection Molding of Sub-μm Grating Optical Elements* NY, William Andrew Publishing.

YANG, H. & KANG, S.-W. (2000) Improvement of thickness uniformity in nickel electroforming for the LIGA process. *International Journal of Machine Tools and Manufacture,* 40, 1065-1072.

YAO, D. & KIM, B. (2004) Scaling issues in miniaturization of injection molded parts. *Journal of Manufacturing Science and Engineering,* 126, 733-739.

YEN, C., LIN, J. C., LI, W. & HUANG, M. F. (2006) An abductive neural network approach to the design of runner dimensions for the minimization of warpage in injection mouldings. *Journal of Materials Processing Technology,* 174, 22-28.

YOSHII, M. & KURAMOTO, H. (1994) Experimental study of transcription of minute width grooves in injection moulding. *Polymer Engineering and Science,* 34, 1215.

YOUNG, W. (2005) Effect of process parameters on injection compression molding of pickup lens. *Applied Mathematical Modelling,* 29, 955-971.

YU, L., LEE, L. J. & KOELLING, K. W. (2004) Flow and heat transfer simulation of

injection molding with microstructures. *Polymer Engineering and Science,* 44, 1866-1876.

YUAN, S., HUNG, N. P., NGOI, B. K. A. & ALI, M. Y. (2003) Development of micro replication process. *Journal of Materials and Manufacturing Processes,* 18, 731-751.

ZHAO, J., LU, X., CHEN, Y., CHOW, L. K., CHEN, G., ZHAO, W. & SAMPER, V. (2005) A new liquid crystalline polymer based processing aid and its effects on micro-molding process. *Journal of Materials Processing Technology,* 168, 308-315.

ZHAO, J., MAYES, R. H., CHEN, G., XIE, H. & CHAN, P. S. (2003) Effects of process parameters on the micro molding process. *Polymer Engineering & Science,* 43, 1542-1554.

ZHAO, R. & MACOSKO, C. W. (2002) Slip at Molten Polymer Polymer Interfaces. *Journal of Rheology* 46, 145-167

ZUYUAN, Y., TAKAHISA, M. & MASATOSHI, F. (1998) 3-D Micro-EDM with Simple Shaped Electrode. *Annals of the CIRP,* 47, 169 – 172.